The role of innate lymphoid cells in liver disease

Identification of a hepatic IL-13-producing ILC3-like population potentially involved in liver fibrosis

Doctoral thesis

to obtain a doctorate (PhD)

from the Faculty of Medicine

of the University of Bonn

Jan Raabe

from Mannheim, Germany

2022

Written with authorization of

the Faculty of Medicine of the University of Bonn

First reviewer: Prof. Dr. Jacob Nattermann

Second reviewer: Prof. Dr. Michael Hölzel

Day of oral examination: 02.05.2022

From the Clinic and Policlinic for Internal Medicine I

Director: Prof. Dr. Christian P. Strassburg

Table of Contents

List of abbreviations

AhR:	Aryl hydrocarbon receptor
ANOVA:	Analysis of variance
AREG:	Amphiregulin
BFA:	Brefeldin A
CLD:	Chronic liver disease
CLP:	Common lymphoid progenitor
CTL:	Cytotoxic T lymphocyte
DGE:	Differential gene expression
DMSO:	Dimethylsulfoxid
DTT:	Dithiothreitol
ECM:	Extracellular Matrix
EDTA:	Ethylenediaminetetraacetic acid
FBS:	Fetal bovine serum
FDR:	False discovery rate
FICZ:	6-Formylindolo[3,2-b]carbazole
HBSS:	Hanks' balanced salt solution
HSA:	Human serum albumin
HSC:	Hepatic stellate cell
IFNγ:	Interferon-gamma
IHL:	Intrahepatic lymphocyte
ILC:	Innate lymphoid cell
ILCP:	Innate lymphoid cell precursor

LSEC: Liver sinusoidal endothelial cell

LTi cell: Lymphoid tissue-inducer cell

MELD: Model for End-Stage liver disease

MFI: Mean fluorescent intensity

NAC: N-acetylcysteine

NCR: Natural cytotoxicity receptor

NK cell: Natural killer cell

P/S: Penicillin-Streptomycin

PBC: Primary biliary cholangitis

PBMC: Peripheral blood mononuclear cells

PBS: Phosphate-buffered saline

PMA: Phorbol 12-myristate 13-acetate

PSC: Primary sclerosing cholangitis

scRNA-seq: Single-cell RNA sequencing

SD: Standard deviation

TGFβ: Tumor growth factor-beta

Th cell: T helper cell

TSLP: Thymic stromal lymphopoietin

tSNE: T-distributed stochastic neighbor embedding

UMAP: Uniform manifold approximation and projection

1. Introduction

1.1 The liver as immunological organ

The liver is the largest internal organ of the human body and traditionally appreciated for its indispensable roles in metabolism, detoxification and protein synthesis. To perform its tasks as a central part of the digestive system, the liver is supported by a dual blood supply, receiving both oxygenated blood via the hepatic artery as well as nutrient-rich blood drained from the gastrointestinal tract via the portal vein. As a consequence, the liver is constantly exposed to a plethora of exogenous agents, which are passed on from the intestinal organs, such as microbial products, environmental toxins and food antigens (Kubes and Jenne, 2018).

Due to this prominent localization, the liver also functions as an important immunological barrier tasked with the detection and clearance of invading pathogens, especially when the intestinal epithelium is compromised. For this purpose, the hepatic compartment relies on a highly specialized immune system, which is so essential to host defense that it has shaped the perception of the liver as an immunological organ (Mackay, 2002; Racanelli and Rehermann, 2006).

The unique immune system of the human liver comprises a complex network of structures, cells and molecules, designed to continuously monitor the incoming bloodstream for foreign substances (Ficht and Iannacone, 2020; Nemeth et al., 2009). Blood arriving from the hepatic tributaries flows through capillary-like vessels, called liver sinusoids, where it is scanned by tissue-resident immune cells. Here, a fine balance between the immunological tolerance of dietary or commensal microbial products and the initiation of rapid and robust immune responses against harmful pathogens is vital to maintain the physiological functions of the liver. The mediation of this balance is closely related to the hepatic immune cell repertoire, which is characterized by an exceptionally pronounced share of innate immune cells (Gao et al., 2007; Robinson et al., 2016). Besides specialized myeloid cells, such as Kupffer cells or dendritic cells, this also includes intrahepatic lymphocytes (IHL) with innate-like properties such as γδ T cells, natural killer T cells as well as the most recently identified lymphoid cell type: the innate lymphoid cells (ILC).

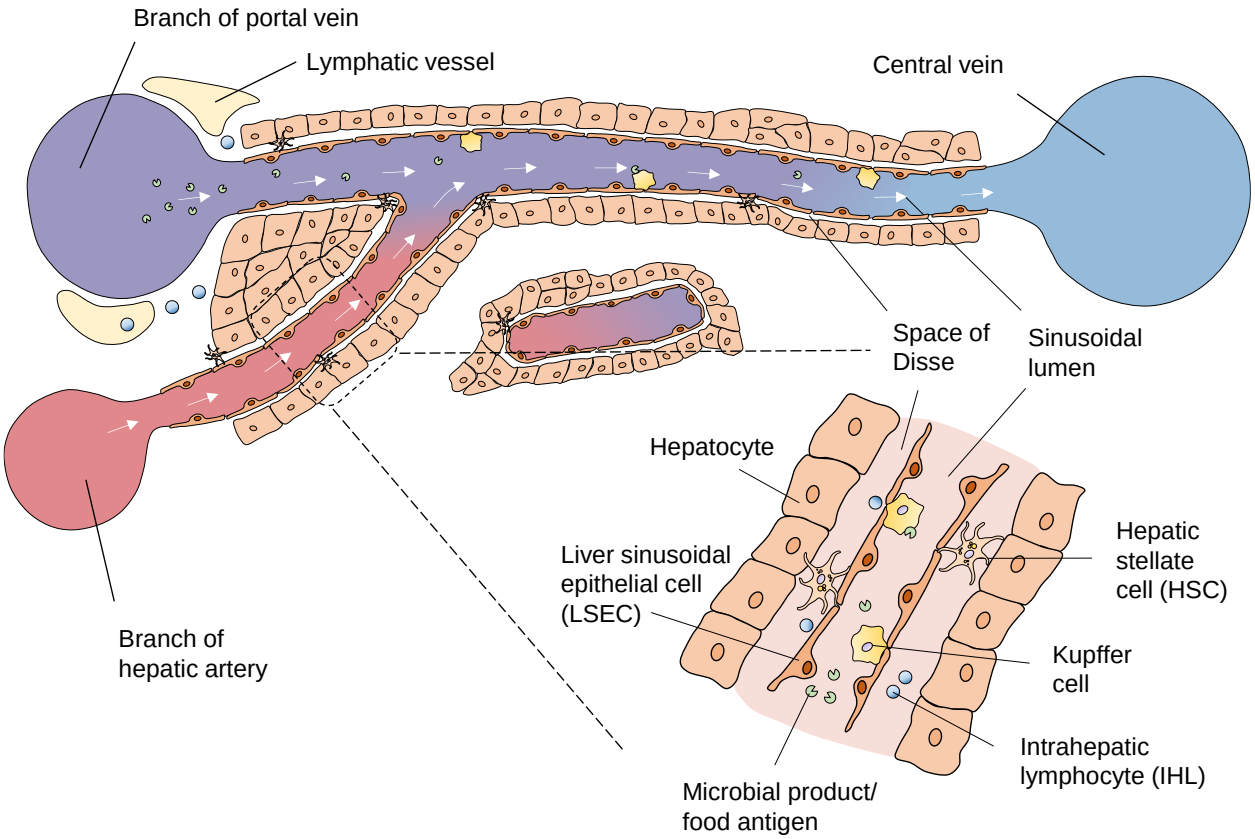

Fig. 1.1: Structural organization of the hepatic immune system (adapted from Ficht and Iannacone (2020)). Blood arriving from the hepatic artery and the portal vein passes through specialized capillary-like vessels, called liver sinusoids. Here, it is scanned by the tissue-resident immune cells of the liver, which have the task of maintaining a fine balance between immunological tolerance and the initiation of robust immune responses.

1.2 Innate lymphoid cells (ILCs)

ILCs are a family of innate immune cells, which emerge from the lymphoid lineage but, unlike B and T cells, do not express rearranged antigen receptors (Artis and Spits, 2015; Vivier et al., 2018). As primarily tissue-resident cells, ILCs mostly reside in peripheral tissues and are particularly abundant at mucosal surfaces. Here, they engage in the initiation and regulation of immune responses but also contribute to non-immunological processes such as tissue metabolism, homeostasis and repair. ILCs exert their effector functions mainly via the secretion of cytokines and in this respect display a functional

diversity which is almost identical to T lymphocytes. This similarity has led to the perception of ILCs as the innate counterpart of the adaptive T cell compartment.

Accordingly, the ILC family includes both cytotoxic natural killer (NK) cells, which like CD8+ cytotoxic T lymphocytes (CTL) are tasked with the killing of infected or malignant cells, as well as helper-like ILCs that specifically mirror the functionality of CD4+ T helper (Th) cells. NK cells and helper ILCs share numerous features, such as their developmental origin, their lymphoid morphology and their rapid engagement in immune responses. Nevertheless, they are considered to represent distinct branches of ILC-mediated immunity, based on their strikingly different effector functions and their distinct developmental trajectories (Vivier et al., 2018).

Beyond these biological differences, both subfamilies are furthermore set apart by the time point of their discovery. Whereas NK cells were first described almost half a century ago (Herberman et al., 1975; Pross and Baines, 1976), the first reports on helper ILCs date back less than 13 years (Cella et al., 2009; Cupedo et al., 2009; Neill et al., 2010; Satoh-Takayama et al., 2008; Spits and Di Santo, 2011). As a consequence, these ILCs remain by far less well characterized up to date, which is only partly due to the neglect of helper ILCs in the years predating their discovery. Moreover, their comparably low overall abundance, their positioning in less accessible tissue as well as a considerably high effort to characterize them significantly impedes scientific progress in this field.

The present thesis specifically focuses on the helper-like, non-NK ILCs, in order to address this existing lack of knowledge. The following review of our current understanding of ILC biology will furthermore place special emphasis on knowledge gained from human studies, citing findings from murine models only when human data is sparse or inconclusive.

1.3 Classification and functions of helper ILCs

Helper ILCs, often merely referred to as ILCs, are generally characterized by the expression of the interleukin 7 receptor α-chain (IL-7Rα or CD127), while lacking any markers related to the lineages of T, B, NK and myeloid cells (Spits et al., 2013). Up to

date, CD127+ ILCs are typically divided into three major subsets, called ILC1, ILC2 and ILC3. These are classified based on their effector cytokine profile and their transcription factor dependency, which largely reflects the Th1/Th2/Th17 paradigm of CD4+ T lymphocytes. Although they represent only a minor subset within the lymphoid spectrum, helper ILCs are potent and versatile cytokine producers that contribute to a variety of immune responses (Castellanos and Longman, 2019; Panda and Colonna, 2019; Vivier et al., 2018).

ILC1, or type 1 ILCs, are IFNγ-producing cells that require the expression of the transcription factor T-bet. In this regard, they closely resemble NK cells, but in contrast to these, ILC1 typically do not express eomesodermin (EOMES) and only low levels of granzyme or perforin. Thus, ILC1 are generally non- or only weakly cytotoxic and primarily convey their functional influence via secretion of IFNγ. Nevertheless, the characterization of ILC1 and their distinction from NK cells is often problematic in humans, due to the significant transcriptional overlap between both subsets and the substantial tissue-specific heterogeneity of ILC1. Up to date, NK cells and ILC1 are therefore often rather distinguished on the basis of conventions and definitions, which have been constantly updated over the past decade. In this work, the distinction of both cell types is based on the NK cell-restricted marker NKp80, which is currently considered not to be expressed by ILC1 (Freud et al., 2016). These NKp80-CD127+ ILC1 are hardly detectable in the circulating bloodstream, yet in return they have been described in numerous non-lymphoid tissues such as the gastrointestinal tract, the female reproductive tract, salivary glands and the liver. They strongly respond to stimulation with IL-12, IL-18 or IL-15 and engage in antiviral immune responses as well as the defense against intracellular bacteria, such as *Toxoplasma gondii* or *Clostridioides difficile* (Abt et al., 2015; Klose et al., 2014).

ILC2, or type 2 ILCs, depend on the transcription factors GATA3 and RORα for their maturation and are potent producers of the type 2 cytokines IL-4, IL-5 and IL-13 (Mjösberg et al., 2011; Vivier et al., 2018). Thereby, they contribute to innate immune responses against large extracellular parasites and allergic inflammation. ILC2 respond to the cytokines IL-33, thymic stromal lymphopoietin (TSLP) and IL-25 which are secreted as alarmins by local tissue-resident cells. Upon clearance of infection, ILC2 further engage in tissue repair by producing the epidermal growth factor amphiregulin (AREG) and also

have been described to contribute to tissue metabolism. Increased frequencies of ILC2 have been observed in lung, skin and adipose tissue. Similar to Th2 cells, they express the receptor for prostaglandin D2 (PTGDR2 or CRTH2) which is commonly used for their identification in humans, alongside characteristically high expression levels of CD161 and KLRG1 (Hazenberg and Spits, 2014).

ILC3, or type 3 ILCs, produce the Th17-associated cytokines IL-17 or IL-22, respond to stimulation with IL-1β and IL-23 and are furthermore characterized by their high expression of the transcription factor RORγt. They are most abundant at the mucosal surfaces of the gastrointestinal tract and are predominantly described in the context of

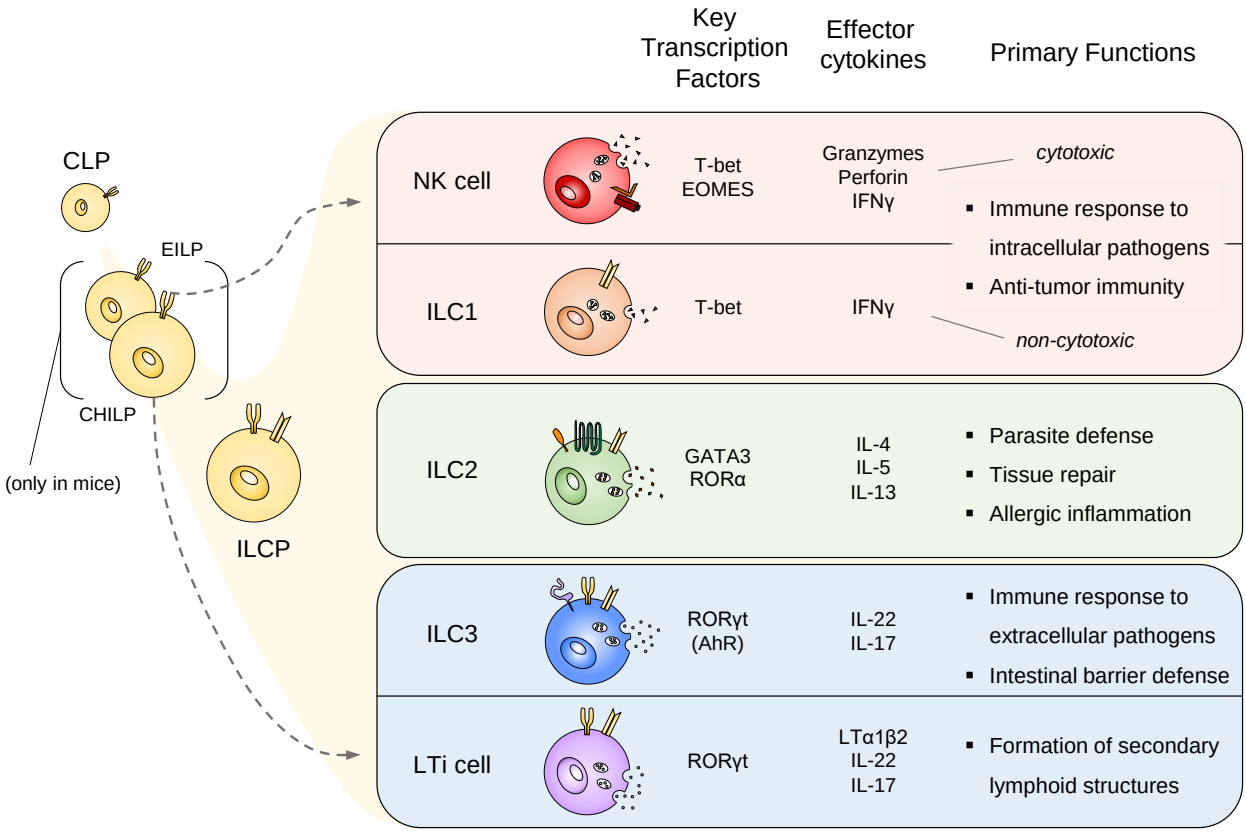

Fig. 1.2: Classification and functions of the major ILC subsets (adapted from Vivier et al. (2018) and Lim and Di Santo (2019)). All members of the ILC family can be classified on the basis of their key transcription factors, their effector cytokine profile, their developmental pathways and their primary biological function. In mice, several distinct stages of ILC development (*EILP = early innate lymphoid progenitor, CHILP = common helper-like ILC progenitor*) have been identified, yet their existence in humans remains controversial.

intestinal barrier maintenance and the containment of commensal bacteria (Cella et al., 2009; Sonnenberg et al., 2012). This role is mainly attributed to the production of the homeostatic cytokine IL-22, which promotes the regeneration of intestinal stem cells and is thus considered to mediate tissue-protective effects. In humans, ILC3 can be identified by surface expression of the receptor tyrosine kinase c-Kit (or CD117) and are generally further subdivided into two functionally distinct cell types, based on the expression of the natural cytotoxicity receptor (NCR) NKp44. While NKp44+ ILC3 are the major source of ILC-derived IL-22, NKp44- ILC3 rather produce IL-17, but also comprise a heterogeneous pool of CD117-expressing ILC precursors (ILCP) (Hoorweg et al., 2012; Lim et al., 2017).

Another cell type, which has been formerly included in the ILC3 subset, are lymphoid tissue-inducer (LTi) cells, which were the only known non-cytotoxic innate lymphocytes for over a decade (Mebius et al., 1997). Like ILC3, they depend on RORγt, express high levels of CD117 and can secrete Th17-associated cytokines. However, LTi cells are also critically involved in the formation of secondary lymphoid structures and Peyer's patches to which they contribute via expression of lymphotoxin α1β2 (LTα1β2). This unique and indispensable biological function as well as an individual developmental trajectory has led to the current perception of LTi cells as a distinct subset of the ILC family.

Accordingly, five major subsets are distinguished within the ILC family up to date, including NK cells, LTi cells and ILC1, ILC2 and ILC3 (Vivier et al., 2018). However, recent advances in the investigation of ILCs have led to the realization that the actual heterogeneity of ILCs across different tissues and states of disease is in fact much greater than initially assumed (Mazzurana et al., 2021; Simoni and Newell, 2018). This diversity, which is especially observed among helper-like ILCs, is essentially facilitated via two mechanisms: the differentiation of multipotent ILCPs and the plasticity of mature ILC subsets (Bal et al., 2020; Diefenbach et al., 2014).

1.4 ILC differentiation and plasticity

Like all lymphoid cell types, ILCs develop from the common lymphoid progenitor (CLP), which gives rise to more committed precursors that eventually differentiate into mature ILC subsets. A large fraction of ILCs is generated in the bone marrow and in the fetal liver,

disseminating to peripheral tissues early in development, where they remain as long-lived, tissue-resident cells (Weiner et al., 2017). During further development however, these local ILC pools are slowly renewed. According to the current understanding, the source of this replenishment are multipotent ILCPs, which circulate in peripheral blood, but also have been identified in lymphoid and non-lymphoid tissues of adult individuals (Lim and Di Santo, 2019).

As the local differentiation of these ILCPs is essentially guided by the environmental conditions of the respective tissue, the wide variety of tissue-specific stimuli shape numerous highly diverse ILC pools. As an example of this diversity, the human intestinal mucosa is virtually void of ILC2, whereas in the skin these represent a highly abundant ILC subset (Bernink et al., 2019; Krämer et al., 2017).
The pool of ILCP has been shown to give rise to all types of mature ILCs, but also to comprise distinct subsets of ILCPs with specific differentiation potential (Chen et al., 2018; Lim et al., 2017). Among circulating progenitors, three multipotent subsets have been identified. These include two NKp46-expressing subsets, which can be further dissected by the expression of CD56, and a KLRG1-expressing ILCP that lacks both NKp46 and CD56 (Nagasawa et al., 2019). Due to their distinct epigenetic configuration of several key transcription factor loci, the differentiation of these individual ILCP subsets is effectively skewed towards specific mature ILC subsets. While NKp46-expressing ILCPs can generate ILC1, ILC3 and even cytotoxic NK cells based on the type of the priming signals, they are unable to differentiate into ILC2. KLRG1-expressing ILCPs on the other hand, predominantly develop into ILC2, although they do not appear to be fully committed to this fate. Accordingly, they also develop into ILC3 when exposed to inflammatory conditions, such as prolonged stimulation with IL-1β and IL-23. Up to date, it remains unclear if the different developmental trajectories of, for instance, ILC3 in fact generate heterogeneous cells with distinct properties and biological functions.

Once matured, the heterogeneity among ILC subsets is further increased by the ability of CD127+ ILCs to change their phenotype and functional profile in response to specific environmental cues they encounter (Bal et al., 2020). This capacity, which resembles the plasticity observed in Th cells, tremendously enhances the versatility of tissue-resident ILC pools by enabling a swift adaptation to changes in the local microenvironment without

the need for external recruitment. In this context, multiple factors and signaling pathways have been described to centrally influence ILC plasticity. These include soluble metabolites such as ligands of the aryl hydrocarbon receptor (AhR), membrane-bound Notch ligands and cytokines such as IL-12, IL-1β and TGFβ (Golebski et al., 2019; Golub, 2021; Hughes et al., 2014; Lim et al., 2016).

Several paths of plasticity have been described in human ILCs, one of the first being the conversion of IL-22-producing ILC3 to IFNγ-producing ILC1 (Bernink et al., 2015; Cella et al., 2010). This process was shown to result from prolonged exposure to IL-12 and IL-1β, which leads to a simultaneous downregulation of RORγt and upregulation of T-bet in the so called “ex-ILC3”. Later on, the same mechanism was found to also occur in mature ILC2, which develop into IFNγ-producing ILC1 by downregulating expression of GATA3 and type 2 cytokines, while upregulating expression of T-bet. As demonstrated in subsequent studies, the ILC1-directed conversion of ILC3 and ILC2 is reversible and ILC plasticity in general appears to be mostly bidirectional. Accordingly, ILC1 differentiate into IL-22-producing ILC3 in the presence of IL-1β and IL-23, while ILC3-directed conversion of ILC2 is partially dependent on additional TGFβ-signaling (Bernink et al., 2019). Interestingly, reversion of ILC2-derived ILC1-like and ILC3-like cells has been shown to occur under the influence of IL-4, but the transdifferentiation of canonical ILC1 and ILC3 into ILC2 has not been proven up to date (Bal et al., 2016; Chen et al., 2018). Whether this reflects an intrinsic limitation in the plasticity of ILC1 and ILC3 or rather suggests that an additional trigger remains to be identified is currently under investigation.

The functional diversity of the ILC spectrum is further enhanced by mixed expression signatures, which can be acquired by individual ILC subsets in response to differential stimuli. As shown among ILC2, cells displaying slightly elevated levels of RORγt expression can give rise to dual cytokine producers of both IL-17 and type 2 cytokines when cultured under ILC3-priming conditions (Bernink et al., 2019; Golebski et al., 2019).

At this point, the plasticity of ILCs exceeds that of Th cells, where direct evidence for the conversion of Th2 to Th17 cells is still lacking (Cooney et al., 2011). Overall, the investigation of ILC plasticity has greatly benefited from the extensive knowledge previously gained from studies of similar mechanisms in Th lymphocytes, yet clear differences exist between both cell types. Distinctive features especially affect the

chromatin landscape of regulatory regions controlling the expression of signature cytokines. Whereas in Th cells, these regions only become accessible upon activational signaling, they are active or directly inducible in ILCs (Shih et al., 2016). As a consequence, ILCs appear to be more prone to adapt to dynamical changes in their microenvironment, as the regulatory components of their transcriptional machinery enables direct access to a diverse set of functional genes.

The investigation of ILC plasticity remains an active area of research and the exact impact on the biological function of ILCs is still incompletely understood. However, it is becoming increasingly evident that the adaptation to environmental changes also enables ILCs to promptly respond to pathological processes, such as tissue inflammation. As a consequence, their flexibility may have an important influence on the role ILCs play in the pathogenesis of inflammatory diseases.

1.5 Role of ILCs in inflammatory diseases and homeostasis

ILCs have been associated with multiple inflammatory diseases in humans and their activation, accumulation and transdifferentiation has been documented in several types of inflamed tissue. Due to their distinct effector functions and distribution in the human body, the individual ILC subsets are typically described to contribute to different pathological settings in different tissues. For instance, IFNγ-producing ILC1 have been reported to be involved in inflammatory bowel diseases (IBD), especially Crohn's disease (CD), whereas IL-13 producing ILC2 have been linked to inflammation affecting the pulmonary system (Fuchs et al., 2013; Smith et al., 2016). The role of ILC3 on the other hand has been discussed in the context of colitis and psoriasis (Teunissen et al., 2014; Zeng et al., 2019). As mentioned above the disease-related changes to tissue-resident ILC pools often involve elements of ILC plasticity (Bal et al., 2020).

In CD, the pathological accumulation of IFNγ-producing, pro-inflammatory ILC1 in the inflamed intestinal mucosa is accompanied by a decrease of NKp44+ ILC3, thus resulting in a loss of IL-22-producing, tissue-protective cells. This shift in the effector cytokine profile of the intestinal ILC pool has been shown to correlate with the presence of CD14+ dendritic cells (DC). Given that CD14+ DCs are potent producers of IL-12 they are

considered to promote the conversion of ILC3 to ILC1, thereby contributing to general features of CD, such as the increased intestinal permeability (Bernink et al., 2013; Forkel et al., 2019; Li et al., 2017).

Similarly, in patients with chronic obstructive pulmonary disease (COPD) or viral lung infections, clusters of ILC2 have been identified in inflammatory foci, where these transdifferentiate into IFNγ-producing cells in an IL-12-dependent manner. In contrast, elevated levels of IL-4 or IL-4-producing eosinophils are associated with an accumulation of ILC2, as reported in patients with chronic rhinosinusitis (Bal et al., 2016; Silver et al., 2016).

Furthermore, alterations of the ILC composition in skin lesions of psoriasis patients indicate a shift from ILC2 to IL-17-producing ILC3. In addition, increased numbers of IL-22-producing NKp44+ ILC3 have been linked to disease-related processes such as epidermal thickening. This ILC3-directed plasticity is associated with elevated levels of IL-1β and IL-23, which are typically observed in psoriatic inflammation. Of note, therapeutic antibodies against IL-17 and IL-23 are highly efficient in the treatment of psoriasis, suggesting that the priming of ILC3 might be of major clinical importance (Bernink et al., 2019; Teunissen et al., 2014; Villanova et al., 2014).

Although numerous reports provide evidence for the involvement of ILCs in a variety of pathological settings, their actual contribution and relevance in these diseases remain unclear and controversial. Given that Th cells mediate similar pathogenic or protective effects under the aforementioned conditions and are mostly also more abundant, ILCs appear to be relatively redundant in inflammatory diseases and not essential for host survival. This perception has been significantly reinforced by a study that investigated the clinical presentation of patients with severe combined immunodeficiency (SCID) after haematopoietic stem cell transplantation (Vély et al., 2016). Following transplantation, SCID patients with common γ-chain mutations showed T cell but not ILC reconstitution, yet they did not display increased susceptibility to infection in comparison to SCID patients with Rag1 or Rag2 mutations, in which ILC development remains intact.

Although these findings suggest that ILCs are dispensable as long as B and T lymphocytes are present, generalizations derived from a small and unique cohort of SCID patients who are under intensive medical surveillance are challenging. At this point, further

research is required to delineate the differential impact of ILC-mediated and T cell-mediated cytokine secretion in inflammatory diseases. Despite a potentially predominant role of Th cells, the additive effects of ILC-derived signaling might certainly remain important with regard to pathologies caused by excess immune activation. Furthermore, ILCs might also modulate T cell responses as recently discussed, either indirectly via interactions with the immunological niche in which both cell types reside or directly via constitutive expression of co-stimulatory molecules (Sonnenberg and Hepworth, 2019).

Given the fact that ILCs have long been overlooked in contrast to T cells, it has been suggested that they might be involved at stages and in processes less well-studied, such as the initiation of chronic inflammatory diseases (Bal et al., 2020; Kotas and Locksley, 2018). Features specific to ILCs support this hypothesis, such as their strategic positioning in peripheral tissues and their ability to polarize their effector functions in the absence of immunological challenges. Moreover, in addition to pathogenic agents, ILCs have also been shown to respond to numerous host-derived stimuli such as metabolites, neuropeptides and hormones, further indicating that ILCs are also engaged in the homeostatic signaling preceding dysregulated immune responses (Jacquelot et al., 2019).

In the human liver, physiological functions encompass elements of inflammation, given the constant exposure to exogenous agents (Robinson et al., 2016). The dysregulation of these processes forms the basis for sustained inflammation of liver tissue, also known as hepatitis, which can lead to liver fibrosis.

1.6 Liver fibrosis

Liver fibrosis arises in response to acute or chronic liver injury and is characterized by the excessive accumulation of extracellular matrix (ECM) proteins such as collagens (Bataller and Brenner, 2005; Xu et al., 2012). If left unchecked, this process results in a critical distortion of the hepatic architecture, where functional parenchymal tissue is increasingly replaced by scar tissue. Due to the high regenerative properties of the liver, hepatic fibrosis typically remains asymptomatic for up to several years in which it can be functionally compensated and even reversed. However, if the underlying cause is not

removed it ultimately progresses to an irreversible end-stage, called cirrhosis, which is associated with functional liver failure, portal hypertension and liver cancer. Cirrhosis and chronic liver disease (CLD) are a major clinical burden of increasing relevance, causing approximately 1.32 million deaths worldwide in 2017 compared to less than 0.9 million deaths in 1990 (Sepanlou et al., 2020). Once in its final stage, liver transplantation becomes the only curative option, underlining the importance of early intervention.

Almost all etiologies of CLD converge to liver fibrosis, including chronic hepatitis B (HBV) and C (HCV) infection, alcoholic liver disease, non-alcoholic steatohepatitis (NASH) or several types of autoimmune hepatitis. Despite the diversity of causative agents, common hallmarks of hepatic fibrogenesis have been described, such as sustained inflammation and the activation of hepatic stellate cells (HSC) (Lee and Friedman, 2011).
HSCs are localized in the subendothelial space of Disse between hepatocytes and the liver sinusoidal endothelium and account for 5-10% of all liver-resident cells (Chen and Tian, 2021). Under homeostatic conditions, HSCs maintain a quiescent phenotype, function as vitamin A-storing cells and regulate the sinusoidal blood flow. Upon activation however, HSCs transdifferentiate into proliferative, fibrogenic myofibroblasts which are the main producers of ECM in liver fibrosis. Accordingly, this process has been identified as a key element of hepatic fibrogenesis and a complex network of activating stimuli has been identified to drive the transition of quiescent HSCs into myofibroblasts. These range from damage- and pathogen-associated molecular patterns (DAMPs/PAMPs), growth factors and adipokines to oxidative stress, autophagy and ECM interactions (Tsuchida and Friedman, 2017; Zhang et al., 2016). Cytokines released by local immune cells further contribute to HSC activation, including TGFβ, one of the most potent fibrogenic triggers of HSCs. Of note, the interactions of HSCs with intrahepatic immune cells such as macrophages and IHLs also have been shown to mediate beneficial effects, for instance, by promoting apoptosis or senescence in HSCs as well as their reversion to a quiescent state.

As such mechanisms are essential to the clearance of liver fibrosis, the role of liver-resident immune cells and their modulatory influence on HSCs have received increasing attention. Whereas numerous reports have addressed the pro- or anti-fibrogenic properties of several IHL subsets, such as NK cells, T cells and NKT cells, data on the

role of human ILCs in liver fibrosis are still sparse (Glässner et al., 2012; Jeong et al., 2008; Wang et al., 2011; Zhang and Zhang, 2020).

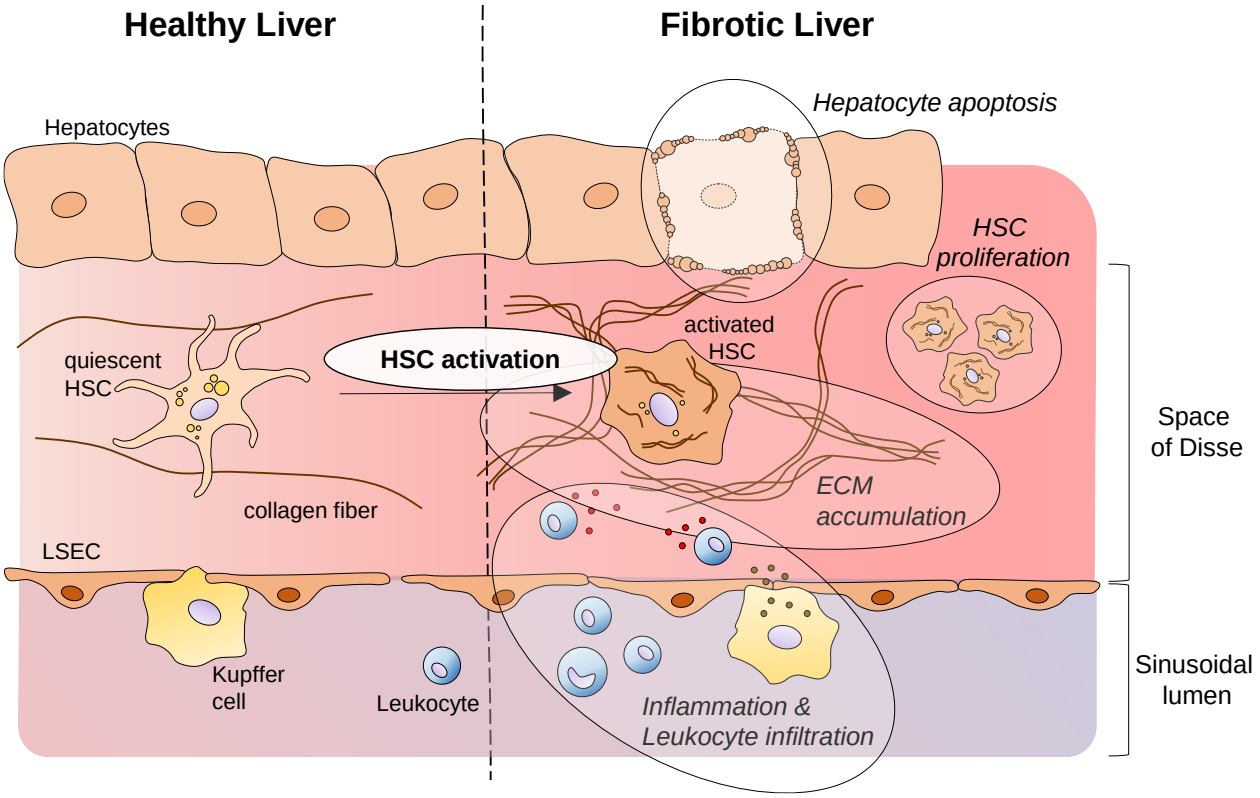

Fig. 1.3: Activation of HSCs as key element of hepatic fibrogenesis. The transdifferentiation of quiescent HSCs into fibrogenic myofibroblasts forms a central element of liver fibrosis. This process is associated with several key features that contribute to the progression of hepatic fibrogenesis, such as the excessive accumulation of ECM, the proliferation of HSCs and sustained hepatic inflammation.

1.7 ILCs in liver fibrosis

While only a minority of studies have addressed the involvement of human ILCs in healthy and fibrotic livers, most of the current knowledge has been derived from murine models. In addition, the functional analogies between ILCs and NK cells or Th cells are often used as a template to assess the impact of ILC-derived cytokine secretion in the human liver (Chen and Tian, 2021; Liu and Zhang, 2017).

Along these lines, the role of ILC1 in CLD is discussed in close relation to their production of IFNγ, which aside its antiviral effects, also has been shown to inhibit the proliferation of

HSCs, and thus is considered to mediate hepatoprotective effects (Jeong et al., 2006; Wynn, 2004). However, multiple liver-resident cell types are potent IFNγ-producers, and some of them, such as NK cells drastically outnumber intrahepatic ILC1 by several orders of magnitude (Chen and Tian, 2021). Moreover, the exact contribution of ILC1 might be more difficult to unravel as indicated by studies of patients with chronic HBV infection. Whereas treatment with IFNγ has been shown to improve fibrosis scores in HBV patients, elevated levels of ILC1 were found to correlate with increased liver damage (Weng et al., 2005; Yang et al., 2015). These findings underline the importance of further research and specifically human studies, given the considerable differences in the abundance of intrahepatic ILC1 between mice and humans.

Types 2 cytokines, such as IL-13 have been shown to contribute to the progression of fibrosis in numerous tissues, including the liver (Chiaramonte et al., 1999; Lee et al., 2001; Oriente et al., 2000). Accordingly, both elevated levels of IL-13, and the Th2/ILC2-specific stimulus IL-33 have been recorded in patients with liver fibrosis (Mchedlidze et al., 2013; Tan et al., 2018; Weng et al., 2009). Mechanistically, IL-13 can activate HSCs via the high affinity alpha chain of the IL-13 receptor (IL-13Rα2) and in rat or murine HSCs, IL-13 has been shown to directly upregulate collagen expression (Liu et al., 2011; Shimamura et al., 2008).

Due to the pro-fibrotic influence of IL-13, the involvement of ILC2 in hepatic fibrogenesis has been a primary subject of investigation in both murine and human studies. As shown in mouse models of induced liver fibrosis, the damage-associated release of IL-33 mediates the accumulation of IL-13-producing, liver-resident ILC2 (Marvie et al., 2009). Moreover, in IL-13-deficient mice (IL-13$^{-/-}$), which show reduced hepatic ECM deposition, the adoptive transfer of ILC2 is sufficient to induce increased collagen expression in the liver, indicating a strong fibrogenic potential for this ILC subset (Mchedlidze et al., 2013). These findings might be also relevant for the pathogenesis of human liver fibrosis, as supportive data has been reported by two studies on human intrahepatic ILC2. As indicated by both reports, the frequency of intrahepatic ILC2 correlates with the severity of fibrotic liver disease and human ILC2 can be activated by hepatocyte- or HSC-derived IL-33 (Forkel et al., 2017; Jeffery et al., 2017). However, with regard to the composition of the intrahepatic ILC pool and the proportion of ILC2, these studies reported drastically

different findings. Therefore, it remains unclear to which extent the findings obtained in mice are transferable to humans.

Given their functional similarities to Th17 cells, the role of ILC3 in liver fibrosis is generally discussed in a similar context and predominantly associated with the production of IL-17 and IL-22. For IL-22, ambiguous effects have been described in the progression of liver fibrosis. On the one hand, IL-22 was found to promote the survival of hepatocytes and induce senescence in activated HSCs, thereby contributing to the amelioration of fibrosis (Kong et al., 2012; Zenewicz et al., 2007). On the other hand, studies in HBV-infected patients demonstrated a pro-inflammatory nature of IL-22, which was associated with detrimental effects such as increased Th17-recruitment and exacerbated liver inflammation (Zhang et al., 2011; Zhao et al., 2014). In addition, elevated systemic levels of IL-22 are a predictive marker for reduced survival in patients with advanced liver cirrhosis (Kronenberger et al., 2012). Thus, an involvement of IL-22-producing cells such as ILC3 in liver fibrosis appears to be evident. However, the above mentioned findings suggest stage- and setting-dependent differences in the effects of IL-22 and direct evidence for the specific contribution of ILC3 remains to be established.
According to previous studies, human intrahepatic ILC3 might predominantly contain NCR- cells that typically produce mostly IL-17 instead of IL-22 (Forkel et al., 2017). In hepatic fibrogenesis, IL-17 has been associated with sustained inflammation and direct pro-fibrotic effects, including the activation of HSCs (Paquissi, 2017; Tan et al., 2013). However, the functional properties of human intrahepatic ILC3 have mostly been neglected so far, as functional studies were either focussed on other ILC subsets or peripheral cells (Forkel et al., 2017; Jeffery et al., 2017; Wang et al., 2018). Consequently, direct evidence for an involvement of ILC3 in liver fibrosis is still missing.

1.8 Aims

Despite the prominent role of the innate lymphocytes in the human liver, the composition of the intrahepatic helper ILC pool and its contribution to local homeostatic and pathological conditions has remained scarcely studied. However, the collective evidence from studies of murine models as well as the documented pro- and anti-fibrotic effects of

ILC-associated cytokines do suggest a significant role for ILCs in hepatic fibrogenesis. Up to date, only few reports have been published, which have investigated tissue-resident ILCs isolated from human hepatic tissue and in addition, these studies have produced inconsistent results.

The work in this thesis aimed to significantly improve our current understanding of ILCs in the human liver by addressing the following key aspects:

- To provide a detailed characterisation of the phenotypic and functional properties of the human intrahepatic helper ILC pool, thereby resolving existing conflicts in the published literature and elucidate the profile of so far neglected subsets.

- To identify tissue-specific features that shape the biological functionality of liver-resident ILCs, screen for evidence of tissue-driven plasticity and study the mechanisms that contribute to the configuration of the intrahepatic ILC pool.

- To investigate the involvement of tissue-resident ILCs in liver fibrosis by assessing disease-related perturbations and the impact of ILC-derived cytokine secretion on other cell types that critically drive hepatic fibrogenesis.

2. Material and methods

2.1 Material

2.1.1 Human tissue samples

Liver tissue of non-fibrotic organs was obtained from resection margins of hepatic carcinomas as well as from liver perfusates of healthy transplant organs. Fibrotic or cirrhotic liver tissue was collected from explanted organs of patients undergoing liver transplantation mainly due to viral hepatitis, alcoholic cirrhosis, nonalcoholic fatty liver disease, primary biliary cholangitis (PBC) or primary sclerosing cholangitis (PSC). Major clinical parameters of the chronic liver disease cohort can be found in **Table 2.1**:

Table 2.1: Patient characteristics of chronic liver disease cohort
[a)] % of total, [b)] mean (range), [c)] median (range); N = number, AST = aspartate transaminase, ALT = alanine transaminase, gammaGT = gamma-glutamyltransferase, MELD = Model for END-Stage Liver Disease; multiple etiologies/patient possible

N (Specimen)	28
Gender	
female : male [a.)]	42.9 : 57.1
Age [b.)]	54.6 (35-69)
Clinical Data	
AST [U/L] [c.)]	45.5 (18-214)
ALT [U/L] [c.)]	28.5 (11-177)
gammaGT [U/L] [c.)]	71.0 (17-867)
Bilirubin [mg/dL] [c.)]	7.29 (0.33-39.75)
MELD score [b.)]	17.2 (7-32)
Thrombocytes [c.)]	83.0 (21-326)
Etiology	
viral (HBV/HCV) [a.)]	32.14
Alcoholic [a.)]	38.46
PBC/PSC [a.)]	19.23
Other [a.)]	30.76

Intestinal tissue was obtained from patients undergoing colonoscopy or prophylactic colectomy (due to inheritance of predispositions for familial adenomatous polyposis (FAP) or hereditary nonpolyposis colorectal cancer (HNPCC). Human tonsils were collected after tonsillectomy from patients suffering from obstructive sleep apnea or recurrent tonsillitis. Peripheral Blood of healthy donors was obtained from the blood donation center of the University Hospital Bonn.

Written informed consent was obtained from all patients and donors. This study had been approved by the local ethics committee of the University of Bonn (#073/19, #275/13, #040/16, #035/14 and #417/17). All examinations were performed on the basis of the revised Declaration of Helsinki of the World Medical Association (2013) and the corresponding legal basis.

2.1.2 Primary human hepatic stellate cells (HSCs)

Primary human HSCs were commercially obtained from ScienCell™ Research Laboratories (Order No. #5300) and expanded according to the manufacturer's protocols. Cells were subcultured 2-4 times when reaching 80 % confluence and subsequently cryopreserved. Different lot numbers (representing different donors) were ordered to account for biological variability.

2.1.3 OP9-DL4 stromal cells

OP9 stromal cells expressing Notch ligand DLL4 (OP9-DL4) were kindly provided by Prof. Dr. Marcus Uhrberg and Prof. Dr. Juan Carlos Zuniga-Pflucker (Mohtashami et al., 2013). The cells were initially expanded and subcultured 2-4 times when reaching 80 % confluence before being cryopreserved.

2.1.4 Reagents and consumables

Table 2.2: Essential reagents and consumables used in this project

Component	Manufacturer	Order No.
2-Mercaptoethanol	Sigma-Aldrich®	M6250-100ML
Antibiotic-Antimycotic	Gibco™	15240062
Ascorbic acid	European Pharmacopoeia	A1300000
Brefeldin A (BFA)	Enzo	BML-G405
Collagenase Type IV	Worthington®	LS004189
Dimethylsulfoxid (DMSO)	Sigma-Aldrich®	D8418
Dithiothreitol (DTT)	Sigma-Aldrich®	10708984001
Ethylenediaminetetraacetic acid	AppliChem	A3145
Fetal Bovine Serum (FBS)	Sigma-Aldrich®	*custom order*
Ham's F-12 Nutrient Mix	Gibco™	21765029
Hanks' Balanced Salt Solution (HBSS)	Gibco™	14180046
Heparin	ratiopharm®	5394.02.00
HS-Nuclease	MoBiTec®	GE-NUC10700
Human AB Serum	Sigma-Aldrich®	H3667-100ML
Human Serum Albumin (HSA)	CSL Behring	001052-31826
Ionomycin	Cell Signaling Technology	9995S
LS MACS colums	Miltenyi Biotec	130-042-401
MojoSort™ Streptavidin Nanobeads	Biolegend®	480016
N-acetylcysteine (NAC)	Sigma-Aldrich®	A7250-10G
Pancoll, human	PanBiotec™	P04-601000
Penicillin-Streptomycin (P/S)	PanBiotec™	P06-07050
Percoll™	GE Healthcare	17-0891-01
Phorbol-12-myristat-13-acetat (PMA)	Cell Signaling Technology	9905
Phosphate-buffered saline (PBS)	Gibco™	18912014
Precision Count Beads™	Biolegend®	424902
RPMI-1640	Gibco™	21875034
Sodium selenite	Sigma-Aldrich®	S5261-10G

2.1.5 Kits

Table 2.3: Pre-manufactured analysis and isolation kits used in this project

Kit	Manufacturer	Order No.
Blue S' Green qPCR Kit	Biozym®	331416
Chromium™ Single Cell 3' Reagent Kits v2	10x Genomics™	*custom order*
Cytofix/Cytoperm™ Fixation/Permeablization	BD Bioscience	554714
eBioscience™ Foxp3 / Transcription Factor	Invitrogen™	00-5523-00
Human CXCL8 DuoSet ELISA	R&D Systems®	DY208
IL-13 Secretion Assay - Cell Enrichment and Detection Kit (PE), human	Miltenyi Biotec	130-093-480
LEGENDplex™ Human Th Cytokine Panel kit	Biolegend®	740001
Pan Monocyte Isolation Kit, human	Miltenyi Biotec	130-096-537
QuantiTect® Reverse Transcription Kit	Qiagen	205313
Qubit™ RNA HS Assay Kit	Invitrogen™	Q32855
SPLIT RNA Extraction Kit	Lexogen	008.48
Zombie Aqua™ Fixable Viability Kit	Biolegend®	423102

2.1.6 Cytokines and ligands

Table 2.4: Cytokines and metabolic ligands used in this project

Cytokine	Manufacturer	Order No.
FICZ	Sigma-Aldrich®	SML1489-1MG
IL-13	ImmunoTools	11340135
IL-1β	ImmunoTools	11340015
IL-2	Miltenyi Biotec	130-097-743
IL-22	ImmunoTools	11340225
IL-23	ImmunoTools	11340233
IL-33	Miltenyi Biotec	130-109-378
IL-7	Miltenyi Biotec	130-095-367
TGFβ	Miltenyi Biotec	130-095-066
TSLP	ImmunoTools	11343494

2.1.7 Antibodies

Table 2.5: Comprehensive list of antibodies used for flow cytometric analyses in this project

Antigen	Conjugate	Clone	Company	Cat. No.
AhR	PE	T49-550	BD Bioscience	565711
CD103	AF700	Ber-ACT8	Novus	NBP1-
CD103	BV421	Ber-ACT8	BD Bioscience	563882
CD117 (ckit)	BV785	104D2	BioLegend®	313238
CD117 (ckit)	PE-Cy7	104D2	BioLegend®	313212
CD117 (ckit)	PE-Vio615	REA787	Miltenyi Biotec	130-111-598
CD123	FITC	6H6	BioLegend®	306014
CD127	BV605	A019D5	BioLegend®	351334
CD127	PE	hIL-7R-M21	BD Bioscience	557938
CD14	FITC	M5E2	BioLegend®	301804
CD14	Biotin	TÜK4	Miltenyi Biotec	130-098-380
CD16	FITC	3G8	BioLegend®	302006
CD161	APC-Cy7	HP-3G10	BioLegend®	339928
CD19	FITC	HIB19	BioLegend®	302206
CD19	Biotin	REA675	Miltenyi Biotec	130-110-247
CD1a	FITC	HI149	BioLegend®	300104
CD20	FITC	2H7	Biolegend®	302304
CD294 (CRTH2)	AF647	BM16	BD Bioscience	558042
CD294 (CRTH2)	PerCP-Cy5.5	BM16	BioLegend®	350116
CD3	FITC	UCHT1	BioLegend®	300406
CD3	Biotin	BW264/56	Miltenyi Biotec	130-113-127
CD303 (BDCA-2)	FITC	AC144	Miltenyi Biotec	130-090-510
CD336 (NKp44)	BV786	P44-8	BD Bioscience	744304
CD336 (NKp44)	PE	P44-8	BioLegend®	325108
CD336 (NKp44)	PerCP-Cy5.5	P44-8	BioLegend®	325114
CD34	FITC	581	BioLegend®	343504
CD45	BUV805	HI30	BD Bioscience	564914
CD45	BV421	HI30	BioLegend®	304032

CD49a	PerCP-	TS2/7	Invitrogen	46-9490-42
CD56	BUV395	NCAM16.2	BD Bioscience	563554
CD56	BUV563	NCAM16.2	BD Bioscience	565704
CD62L	BV421	DREG-56	BD Bioscience	563862
CD69	BV421	FN50	BioLegend®	310930
CD69	BV786	FN50	BD Bioscience	563834
CD94	AF700	MM0181-5F26	Novus	NBP2-
CD94	FITC	HP-3D9	BD Bioscience	555888
FcεR1α	FITC	AER-37	BioLegend®	334608
GATA3	BUV395	L50-823	BD Bioscience	565448
GATA3	BV421	L50-823	BD Bioscience	563349
IFNγ	BV421	4S.B3	BioLegend®	502532
IL-13	BV421	JES10-5A2	BioLegend®	501916
IL-13	PE	JES10-5A2	BioLegend®	501903
IL1R1	APC	*Polyclonal*	R&D Systems®	FAB269A-100
IL1R1	PE	*Polyclonal*	R&D Systems®	FAB269P-100
IL-22	APC	IL22JOP	Invitrogen	17-7222-82
IL-8 (CXCL8)	FITC	BH0814	BioLegend®	514604
IL-8 (CXCL8)	PE	E8N1	BioLegend®	511408
KLRG1	BV421	SA231A2	BioLegend®	367706
KLRG1	PE-Vio 615	REA261	Miltenyi Biotec	130-108-366
NKp80	FITC	4A4.D10	Miltenyi Biotec	130-094-843
RORC	APC	AFKJS-9	eBioscience™	17-6988-82
RORC	PE	AFKJS-9	eBioscience™	12-6988-82
T-bet	BV421	4B10	BioLegend®	644816
TCRαβ	FITC	IP26	BioLegend®	306706
TCRγδ	FITC	B1	BioLegend®	331208
Isotype controls				
	APC	eBR2a	eBioscience™	17-4321-81
	PE	eBR2a	eBioscience™	12-4321-80
	BV421	MOPC-21	BioLegend®	400158
	BUV395	X40	BD Bioscience	563547
	BV421	X40	BD Bioscience	562438

2.1.8 Oligonucleotides

Table 2.6: List of oligonucleotide primers used for quantitative PCR analysis in this project (bp = base pairs, fwd = forward, rev = reverse)

Gene Name	**5'-3' Sequence**	**Amplicon Size [bp]**
ACTA2-fwd	CCA GAG CCA TTG TCA CAC AC	91
ACTA2-rev	CAG CCA AGC ACT GTC AGG	
ACTG2-fwd	TTG ATG TCT CGC ACA ATT TCT CT	246
ACTG2-rev	CAT GTA CGT CGC CAT TCA AGC	
AHR-fwd	TAC AAA GCC ATT CAG AGC CTG T	274
AHR-rev	TTC CAA GCG GCA TAG AGA CC	
CCL20-fwd	TTA GGA TGA AGA ATA CGG TCT GTG	130/133
CCL20-rev	CCA TGT GCT GTA CCA AGA GT	
CD2-fwd	CTA CTC TGT GGG CTC TTG TC	105
CD2-rev	TCT TGA TGG TCT TTG TGG CA	
COL1A1-fwd	CAC ACG TCT CGG TCA TGG TA	91
COL1A1-rev	AAG AGG AAG GCC AAG TCG AG	
CXCL1-fwd	GCC CCT TTG TTC TAA GCC AG	262
CXCL1-rev	CTG GCG GAT CCA AGC AAA TG	
CXCL8-fwd	AAA TTT GGG GTG GAA AGG TT	107
CXCL8-rev	TCC TGA TTT CTG CAG CTC TGT	
EEF1A1-fwd	CCG TTC TTC CAC CAC TGA TT	183
EEF1A1-rev	CTT TGG GTC GCT TTG CTG TT	
EREG-fwd	CAG AGC TAC ACT TTG TTA TTG ACA C	100
EREG-rev	TCA TGT ATC CCA GGA GAG TCC	
FASLG-fwd	GTG GCC TAT TTG CTT CTC CA	95
FASLG-rev	TTC AGC TCT TCC ACC TAC AGA	
FCER1G-fwd	CTC ATG CTT CAG AGT CTC GTA	113
FCER1G-rev	GAC TGA AGA TCC AAG TGC GAA	
GAPDH-fwd	GAA GGT GGT GAA GCA GGC	229
GAPDH-rev	CTC CTT GGA GGC CAT GTG	
GATA3-fwd	CCT CCA GTG AGT CAT GCA C	

GATA3-rev	CCT GTC TGC AAT GCC TGT	145
HPGD-fwd	GCA AGA TAT GAC AAC ATT CCA GT	109
HPGD-rev	AGT GAC TCA TCC TGT CTG CT	
HPGDS-fwd	TCC CCC TCA TAT TAA AAT AAG TGA GT	112
HPGDS-rev	CCA AGG CAC AGT CAC ATA CC	
ID2-fwd	CTT AAA AGA TTC CGT GAA TTT GTT GT	150
ID2-rev	ATC AGC ATC CTG TCC TTG C	
IL10RA-fwd	AGC GAC AGA TGG TTT CAC C	141
IL10RA-rev	TTC CGA GAG TAT GAG ATT GCC	
IL13-fwd	CAA GGG GAA GGC TGA GGT	212
IL13-rev	TTT CGC GAG GGA CAG TTC	
IL17RB-fwd	CAA GTA GGA AAA TAT GGA GTC AGC	139
IL17RB-rev	TCC AAC ACA GCA CTA TCA TCG	
IL1B-fwd	GAA GCT GAT GGC CCT AAA CA	110
IL1B-rev	AAG CCC TTG CTG TAG TGG TG	
IL1R1-fwd	ACC ACG CAA TAG TAA TGT CCT G	184
IL1R1-rev	ATG AAA TTG ATG TTC GTC CCT GT	
IL1RL1-fwd	ACA TGA GGC AGT TGG TGA TAC	117
IL1RL1-rev	AAC TAT TCT TAG CTC CGT CAC TG	
IL22-fwd	CTC TGG ATA TGC AGG TCA TCA C	123
IL22-rev	AGT GCT GTT CCC TCA ATC TG	
IL23R-fwd	TGT TAG CCC AGA ATT CCA TGT	125
IL23R-rev	GTC AAG AAA CAG GCA AAA GGT	
IL32-fwd	TTG TGC CAG GAA GAC TGC	129/225
IL32-rev	CAG CTT CTT CAT GTC ATC AGA GA	
IL33-fwd	AAG GCA AAG CAC TCC ACA GT	180
IL33-rev	CAA AGA AGT TTG CCC CAT GT	
KIT-fwd	CAG AAT TGG ACA CTA GGA ATG TG	137
KIT-rev	CAG AAC CTT CAC TGA TAA ATG GG	
KLRG1-fwd	CCA GAC CGC TGG ATG AAA TAT G	126
KLRG1-rev	CTG ATT GTC CGT TAT CAC AAG GA	
MMP2-fwd	TTC TTG TCG CGG TCG TAG TC	180
MMP2-rev	TGG CAA GTA CGG CTT CTG TC	

NCAM1-fwd	CAT CAT TCC ACA CCA CTG AGA	139
NCAM1-rev	GAG ATC AGC GTT GGA GAG TC	
NCR2-fwd	CCA GAT TGT GAA TCG AGA GGT C	102
NCR2-rev	AAG AAA GGC TGG TGT AAG GAG	
PLCG2-fwd	GTA GTA ACT GAC GAG CTC CAC	129
PLCG2-rev	GAC TCC TAT GCC ATC ACC TT	
RORC-fwd	TGC AGC TGT TCT ACT TTC CTT	127
RORC-rev	TTG ACT TCT CCC ACT CCC TAA	
TOX-fwd	TAT GAG CAT GAC AGA GCC GAG	109
TOX-rev	GGA AGG AGG AGT AAT TGG TGG A	
TOX2-fwd	TGG CCT GAT AGG AGT AGG CAG	159
TOX2-rev	AGA GCG AGA ACA ACG AAG ACT	
TYROBP-fwd	GTT GCT GAC TGT CAT GAT TCG	106
TYROBP-rev	CGA GTC GCC TTA TCA GGA G	
XCL1-fwd	AAG GCT CCT TGA GAG CAG TAA	167
XCL1-rev	ATT GGT CGA TTG CTG GGT TCC	

2.1.9 Devices

Table 2.7: Main devices used for data analysis and sample processing

Device	**Manufacturer**
FACSCanto™ II	BD Bioscience
FACSAria™ Fusion	BD Bioscience
LSRFortessa™	BD Bioscience
LightCycler® 96 Real-Time PCR System	Roche
NanoDrop™ 1000	Thermo Scientic™
Qubit 4 Fluorometer	Invitrogen™
Stomacher® 400 Circulator	Seward Ltd.
Sunrise™ Absorbance Microplate Reader	Tecan

2.1.10 Cell culture media

Table 2.8: Definition of cell culture media used in this project

Medium	Component	Concentration/Dilution
Pre-Digestion Medium	HBSS	
	DTT	154 µg/ml
	EDTA	5 mM
	NAC	0.25 %
	P/S	1 %
Digestion Medium	RPMI-1640	
	FBS	10 %
	P/S	1 %
	Collagenase Type IV	125 U/ml
	HS-Nuclease	25 U/ml
Freezing Medium	RPMI-1640	
	FBS	10 %
	DMSO	10 %
	P/S	1 %
Thawing Medium	HBSS	
	HSA	1 %
	P/S	1 %
	HS-Nuclease	25 U/ml
Differentiation Medium	Ham’s F12 Nutrient Mix	
	Human AB Serum	10 %
	Antibiotic-Antimycotic	1 %
	Ascorbic acid	20 mg/ml
	Sodium selenite	0.05 mg/ml
	2-Mercaptoethanol	24 mM

2.2 Methods

2.2.1 Isolation of tissue-resident lymphocytes

Liver-infiltrating lymphocytes were isolated from explanted or resected liver tissue as well as from perfusation liquid of transplant organs. Solid tissue was cut into small pieces, washed with PBS containing 100 U/ml Heparin and then incubated in digestion medium (**Table 2.8)** at 37 °C for 45 min. The suspension was then homogenized using a Stomacher® 400 Circulator (230 rpm, 10 min, 3 repetitions) and filtered through a sterile 100 µm gauze tissue. Isolation of the lymphocyte fraction was achieved by density centrifugation (1000 x g, 15 min) using a Percoll™ gradient of 40.5 % : 58.5 %.

Isolation of lymphocytes from liver perfusation liquid was achieved by density gradient centrifugation (1000 x g, 15 min) using Pancoll (human).

For the preparation of lymphocytes from intestinal biopsies or resections, tissue specimen were cut into small pieces and incubated in pre-digestion medium (**Table 2.8)** at 37 °C for 45 min to dissolve epithelial tight junctions and excess mucus. The mucosal tissue was then washed with PBS and further incubated in digestion medium at 37 °C for 45 min before being filtered through sterile 70 µm gauze tissue. The obtained cell suspension was merged with pre-digestion supernatant containing the intraepithelial lymphocyte fraction.

Tonsillar lymphocytes were isolated from whole ectomized tonsils which were cut into small pieces and passed through a sterile stainless stell strainer. Lymphocyte isolation was achieved by density gradient centrifugation (1000 x g, 15 min) of the obtained cell suspension using Pancoll (human).

Following the isolation procedure, cells were either used directly for experimentation or cryopreserved.

2.2.2 PBMC isolation

Human peripheral blood mononuclear cells (PBMCs) were isolated from whole blood samples by density gradient centrifugation (1000 x g, 15 min) using Pancoll (human). Cells were either used directly for experimentation or cryopreserved.

Further isolation of circulating monocytes was performed using the Pan Monocyte Isolation Kit (human) from Miltenyi Biotec according to the manufacturer's protocols. Monocytes were used directly after isolation and were not subjected to cryopreservation.

2.2.3 Cryopreservation and thawing of cell suspensions

For long-term storage of specimens, isolated cells were resuspended in 0.5-1 ml freezing medium (**Table 2.8)**, transferred to a cryopreservation vial and frozen to -80 °C at a cooling rate of 1 °C/min. This was achieved by placing the cryopreservation vial in a 15 mm thick polystyrene tray. After 24 h, cell specimens were transferred to -150 °C.

Retrieving cells from cryopreservation was performed by rapidly thawing the cell suspension in a 37 °C water bath until all ice crystals had melted. In a drop-wise fashion, thawing media (**Table 2.8)** was added to the cryopreservation vial until the suspension volume was doubled. The cells were then transferred to a 15 ml Falcon tube, and additional thawing medium was slowly added until DMSO concentration had been diluted to at least <0.1 %. Following a resting phase of 10 min to achieve complete osmotic equilibration, freezing and thawing media were removed by centrifugation (250 x g, 10 min) and cells were recovered in the appropriate medium.

2.2.4 Maintenance of lymphocyte/ILC suspensions

For short-term cultures (≤3 d), lymphocyte suspensions or purified ILCs were maintained in RPMI-1640, supplemented with 10 % FBS and 1 % P/S at 37 °C and 5 % CO_2. Prior to functional assays, cells were rested for at least 2 h if they had been previously recovered from cryopreservation, in order to restore their metabolic activity.

2.2.5 Stimulation of lymphocyte/ILC suspensions

Stimulation with PMA (50 ng/ml) and Ionomycin (1 µg/ml) was used to assess the overall functional capacity of mixed lymphocyte suspensions and sort-purified or expanded ILCs. Cells were stimulated for 2 h with PMA/Ionomycin and subsequently treated with BFA (5 µg/ml) for another 2 h, if a flow cytometric analysis was intended.

Cytokine-specific stimulation of cells was performed overnight (18-20 h) with IL-1β, IL-23, IL-33 or TSLP in the indicated combination and concentration. In this setting, BFA was added during the last 4-6 h of the experiment, to account for the more moderate induction of cytokine secretion.

Supernatant was collected at the end of the stimulation, if quantification of cytokine secretion was intended.

2.2.6 Maintenance of HSCs

Following the recovery from cryopreservation, HSCs were cultured according to the manufacturer's protocols, with the exception of FBS being replaced by 1 % HSA. Cells were seeded into 96 well flat-bottom plates (10'000 cells per well) and maintained overnight before being stimulated with recombinant human cytokines or co-cultured with sort-purified ILCs.

2.2.7 Stimulation of HSCs

HSCs were treated with the indicated concentrations of recombinant human IL-13, IL-22 and TGFβ to assess the cytokine-specific effects on gene expression and cytokine secretion. After 48 h of treatment, the complete supernatant was removed and collected. The adherent cell layer was then directly lysed by the addition of RNA isolation buffer (Lexogen). Flow cytometric analyses were performed after 24 h of treatment, including addition of BFA for the last 4-6 h of culture.

To investigate the impact of ILC-derived cytokine secretion on HSCs, both cell types were co-cultured in RPMI-1640, supplemented with 10 % FBS and 1 % P/S at 37 °C and 5 % CO_2. Sort-purified ILCs were previously stimulated with PMA/Ionomycin for 4 h. Prior to the initiation of co-culture, the activating agents were removed by extensive washing (dilution > 1:1 x 10^6) in order to avoid unspecific activation of HSCs. Appropriate stimulation controls were included. Flow cytometric analyses were performed after 24 h of co-culture, which included addition of BFA for the last 4-6 h of culture.

2.2.8 Monocyte migration assay

The chemotactic potential of HSCs-derived cytokine secretion on circulating monocytes was evaluated in 24-transwell assay plates with a pore diameter of 5 µm. Previously collected supernatant of HSCs treated with IL-13 for 48 h was added to the lower chamber and 2 x 10^5 freshly isolated monocytes were added to the upper chamber. After 4 h, all migrated cells were harvested from the lower chamber using PBS supplemented with 0.2 % EDTA to detach adherent monocytes. Cells were stained for flow cytometric counting analysis and a defined volume of Precision Count Beads™ (Biolegend®) for normalization was added before starting acquisition.

2.2.9 Maintenance of OP9-DL4

OP9-DL4 stromal cells were continuously maintained in DMEM, supplemented with 10 % FBS and 1 % P/S at 37 °C and 5 % CO_2. One batch of cells was subcultured for up to 6 weeks, before being discarded and a new batch was thawed. Cells were maintained at least for one week before serving as a feeder cell layer in bulk or clonal expansion cultures.

2.2.10 Bulk and clonal expansion culture of ILCs

Two days before the addition of purified ILCs, OP9-DL4 stromal cells were growth-inhibited by irradiation (25 Gy), recovered in differentiation medium (**Table 2.8**) (Cichocki and Miller, 2010) and seeded either in 24 well plates (10'000 cells/well) for bulk culture or 96 well plates (3'500 cells/well) for clonal expansion assays. ILCs were added to the feeder cells either as sort-purified bulk population (100-1000 cells) or sorted directly as single cells into a prepared 96 well plate. Medium was supplemented as indicated with the following cytokines (10 ng/ml each): IL-2, IL-7, TGFβ, IL-1β, IL-23, IL-33, TSLP and FICZ. Both medium and cytokines were refreshed every 3 days for bulk cultures and every 7 days for clonal expansion assays by exchanging half of the culture volume.

Clone splitting experiments were performed by dividing all wells of a plate on two freshly prepared plates after an initial expansion period of 7 days. Medium was renewed after the splitting procedure. All long-term cultures were maintained for 12-14 days, depending on the density of the expanded cells.

2.2.11 Flow cytometric analysis and cell sorting

Following cell isolation or cell culture, samples were prepared as single-cell suspension, stained with the Zombie Aqua™ Fixable Viability Kit (Biolegend®) for live-dead discrimination and labelled with conjugated antibodies. For the detection of nucleic antigens such as transcription factors the eBioscience™ Foxp3/Transcription Factor Staining Buffer Set (Invitrogen™) was used in accordance with the manufacturer's instructions.

For the detection of intracellular cytokines, cells were stimulated as indicated and treated with BFA (5µg/ml) for the last 2-4 h of culture. Fixation and permeabilization was performed using Cytofix/Cytoperm™ (BD Bioscience).

All flow cytometric data was acquired on a BD LSRFortessa™ cell analyzer (BD

Bioscience). Data analysis was performed using FlowJo® Software V10 (continuously updated version), including the following packages: *DownSample v3, FlowAI, FlowSOM, IndexSort v3 and UMAP v3*.

Sort-purification of total ILCs and ILC subsets was performed with a FACSAria™ III or FACSAria™ Fusion cell sorter (BD Bioscience). Larger batches of cell samples (> 2 x 10^7 cells) were previously depleted of CD3+, CD19+ and CD14+ cells, using the respective biotinylated antibodies, MojoSort™ Streptavidin Nanobeads (Biolegend®) and MACS columns (Miltenyi Biotec) as specified by the manufacturers.

A comprehensive list of all antibodies used in this study can be found in **Table 2.5**.

2.2.12 Post-culture analysis of IL-13-secreting cells

Expanded bulks were stained for flow cytometric analysis and Lin-CRTH2-CD117+NKp44+ cells were sort-purified by FACS. These cells were recovered in differentiation medium and stimulated with PMA/Ionomycin for 2 h. Next, IL-13 secreting cells were labelled and isolated using the IL-13 Secretion Assay - Cell Enrichment and Detection Kit from Miltenyi Biotec according to the manufacturer's instructions. Positively selected cells were then lysed in mRNA isolation buffer (Lexogen) and stored at -80 °C.

2.2.13 Quantitative PCR analysis

Isolation of RNA samples was performed utilizing the SPLIT RNA Extraction Kit (Lexogen). Cultured cells were lysed immediately after aspiration of the supernatant and further processed following the manufacturer's instructions. RNA concentration was measured with a Qubit Fluorometer using the Qubit™ RNA HS Assay Kit (Invitrogen™) and RNA purity was assessed with a NanoDrop™ 1000 Spectrophotometer (Thermo Scientic™). Transcription of cDNA was done using the QuantiTect® Reverse Transcription Kit (Qiagen) in accordance with the manufacturer's protocol.

Quantitative PCR was performed in a LightCycler® 96 Real-Time PCR System (Roche). Reactions were set up with the Blue S' Green qPCR Kit (Biozym®) and the customized primers listed in **Table 2.6**. The individual primers were designed using the Primer-BLAST online platform of the U.S. National Library of Medicine and selected to specifically amplify the respective gene and potential splice variants. Gene-specific amplification was tested by agarose gel electrophoresis of the PCR product and amplicon size evaluation. Alternatively, pre-designed assays were commercially obtained from IDT™. Relative

target gene expression was calculated with the 2^-ΔCt-method using mean expression of the house keeping genes *EEF1A1* and *GAPDH* as reference for normalization.

2.2.14 Analysis of cytokine secretion

Cell culture supernatants were measured for secreted CXCL8 using the Human CXCL8 DuoSet ELISA (R&D Systems®) according to the manufacturer's instructions. Photometric analysis was performed with a Sunrise™ Absorbance Microplate Reader (Tecan).
In addition, culture supernatants were screened for further secreted cytokines such as IFNγ, TNFα, IL-13, IL-17A, IL-17F and IL-22 using the LEGENDplex™ Human Th Cytokine Panel Kit (Biolegend®). Data acquisition was performed on a BD FACSCanto II flow cytometer and samples were analysed using the LEGENDplex™ Data Analysis Software.

2.2.15 Single-cell RNA-sequencing (scRNA-seq) of intrahepatic ILCs

Total viable intrahepatic CD45+Lin-CD127+ ILCs from three individual donors were sort-purified, recovered in supplemented RPMI-1640 (10 % FCS, 1 % P/S) and cultured at 37 °C for post-sort stimulation (1 h PMA/Ionomycin). Cells with faint CD127 expression were also included to cover the full spectrum of CD127+ ILCs. Although this strategy was associated with an increased risk of potential contamination, subsequent scRNA-seq analysis would allow the exclusion of non-ILCs based on their differential expression patterns. In the following, samples were processed with the Chromium™ Single Cell 3' Reagent Kits v2 (10x Genomics®) according to the manufacturer's instructions in order to generate barcoded sequencing libraries for scRNA-seq.

Subsequent data processing and analysis were performed at the Interdisciplinary Center for Clinical Research (IZKF) at the RWTH Aachen University in cooperation with Ali T. Abdallah (NGS-Research Group). In brief, all samples were sequenced on a NextSeq 500 sequencing system with the following run parameters: 26 cycles for read 1, 98 cycles for read 2, 8 cycles for sample Index. The mkfastq command of CellRanger (v2.0.0; 10x Genomics®) was then used to demultiplex sequencing data, converting them to the fastq format. The count command of mkfastq was used to align the sequences to the human genome reference sequence GRCh38 (pre-processed release 84; 10x Genomics®) and generate gene expression matrices across all cells for all samples. Using the Seurat package (v v2.3.0) (Satija et al., 2015), the filtered digital gene expression matrices (UMI

counts per gene per cell) were merged and further processed by filtering, normalizing and clustering the cells and performing differential expression analyses. Imputation procedures were performed using Rmagic r package (v1.4.0) (van Dijk et al., 2018).
All scRNA-seq data including relevant supplemental information have been deposited at GEO and are currently available upon request.

2.2.16 Statistical analysis

Further statistical analysis and data visualization was performed using GraphPad Prism 9 and R (including R packages *"ggplot2", "Rtsne", "uwot", "pheatmap"*). Gaussian distribution of datasets was tested by D'Agostino & Pearson omnibus normality test (N ≥ 8) or Shapiro-Wilk normality test (N ≥ 4). Statistical significance was determined as indicated by means of the appropriate test and corrected for multiple comparisons, if applicable, by controlling the False Discovery Rate (FDR; Two-stage step-up method (Benjamini et al., 2006)). P values (corrected for multiple comparisons, if applicable) are indicated in figures as follows: ns = $p > 0.05$, * = $p < 0.05$, ** = $p < 0.01$, *** = $p < 0.001$, **** = $p < 0.0001$. For data visualization in heatmaps, individual values were z-score-normalized ($z\text{-score} = (x - mean_{row})/SD_{row}$) to enable transcript-specific resolution of expressional differences by global colour coding. Exemplary depiction of flow cytometric data in form of histograms, dot plots or contour plots is representative for multiple (N > 3) independent experiments. For expression level analyses in flow cytometric data, the mean fluorescent intensity (MFI) was calculated using the geometric mean. Depicted boxplots indicate 25^{th} – 75^{th} percentiles with a horizontal line indicating the median. Unless otherwise specified, whiskers indicate min-max range, in contrast to error bars which indicate standard deviation (SD).

3. Results

This study was designed to initially provide a general overview of the phenotypical and functional properties of human liver ILCs, as previously published reports have provided inconsistent results with regard to these basic aspects (Forkel et al., 2017; Jeffery et al., 2017). For this purpose, tissue-resident ILCs were investigated in isolates of liver-infiltrating mononuclear cells obtained from non-fibrotic liver tissue using a flow cytometric approach. To identify liver-specific features, a comparative evaluation of liver ILCs and tonsillar, colonic or circulating ILCs was performed.

3.1 Phenotypical characterisation of the intrahepatic ILC pool

Following established gating protocols (Hazenberg and Spits, 2014; Spits et al., 2013), all conventionally described ILC subsets could be identified within the human liver (**Fig. 3.1A**). ILCs were defined as lineage-negative, CD127-expressing cells and further subdivided based on their expression of the surface markers CRTH2 and CD117. Since all further analyses were focussed on helper-like ILCs, NK cells were excluded based on their expression of CD94 and NKp80. Among these ILC subsets, CRTH2-CD117+ ILCs, typically referred to as ILC3, formed the most abundant subset in the liver, followed by CRTH2-CD117- ILC1 and CRTH2+ ILC2 (**Fig. 3.1B**).

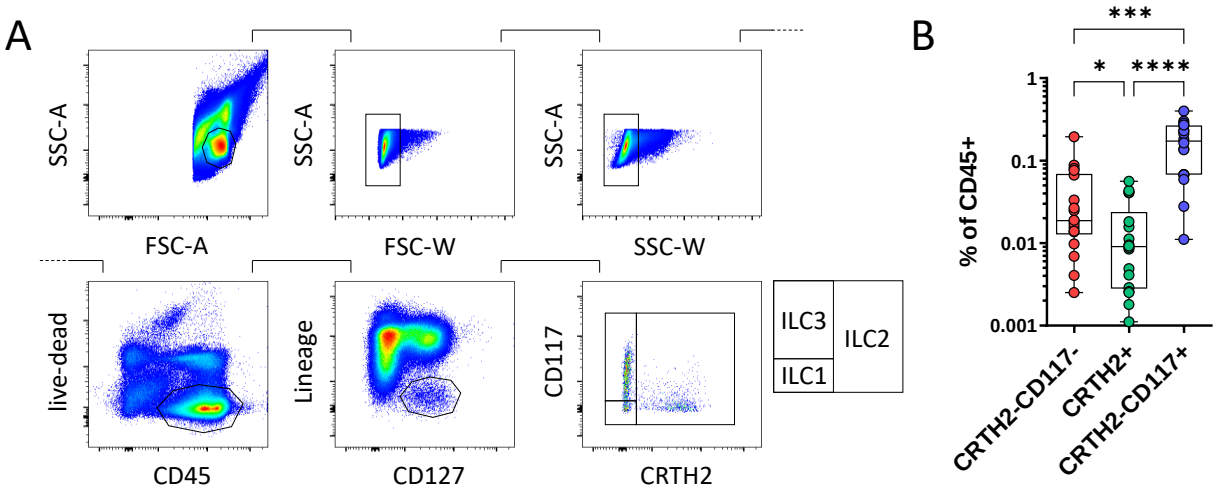

Fig. 3.1 Identification of human intrahepatic ILCs in healthy livers by flow cytometry **(A)** Applied gating strategy defining non-NK ILCs as single viable CD45+, lineage-negative (CD3-, TCRαβ-, TCRγδ-, CD14-, CD19-, CD20-, CD14-, CD16-, NKp80-, CD94-,

CD1a-, CD123-, CD34-, FcεR1α-, BDCA-2-) CD127+ cells. Subdivision into conventionally described subsets based on expression of CD117 and CRTH2. **(B)** ILC subset frequency as percentage of CD45+ cells for CRTH2-CD117- ILC1, CRTH2+ ILC2 and CRTH2-CD117+ ILC3 (N = 18). Statistical significance determined by Kruskal-Wallis test (B), corrected for multiple comparisons by controlling FDR.

To evaluate if the identified intrahepatic ILCs matched the commonly reported subset-specific expression patterns (Artis and Spits, 2015; Simoni and Newell, 2018), an extended phenotypical characterisation was performed next. As expected and described, CRTH2+ ILC2 expressed high levels of their canonical transcription factor GATA3 and the surface markers CD161 and KLRG1, while lacking expression of CD56 and NKp44 (**Fig. 3.2A, B**). CRTH2-CD117+ ILC3 displayed prominent expression of the transcription factor RORγt and the surface markers IL1R1 and NKp44. Low levels of the ILC1-specific transcription factor T-bet could be observed in CRTH2-CD117- ILCs, nevertheless these cells expressed a typical pattern of surface markers such as CD161, CD49a and CD56. Overall, all ILC subsets identified in the human liver displayed a conventional phenotype, as far as assessed by this initial flow cytometric characterisation.

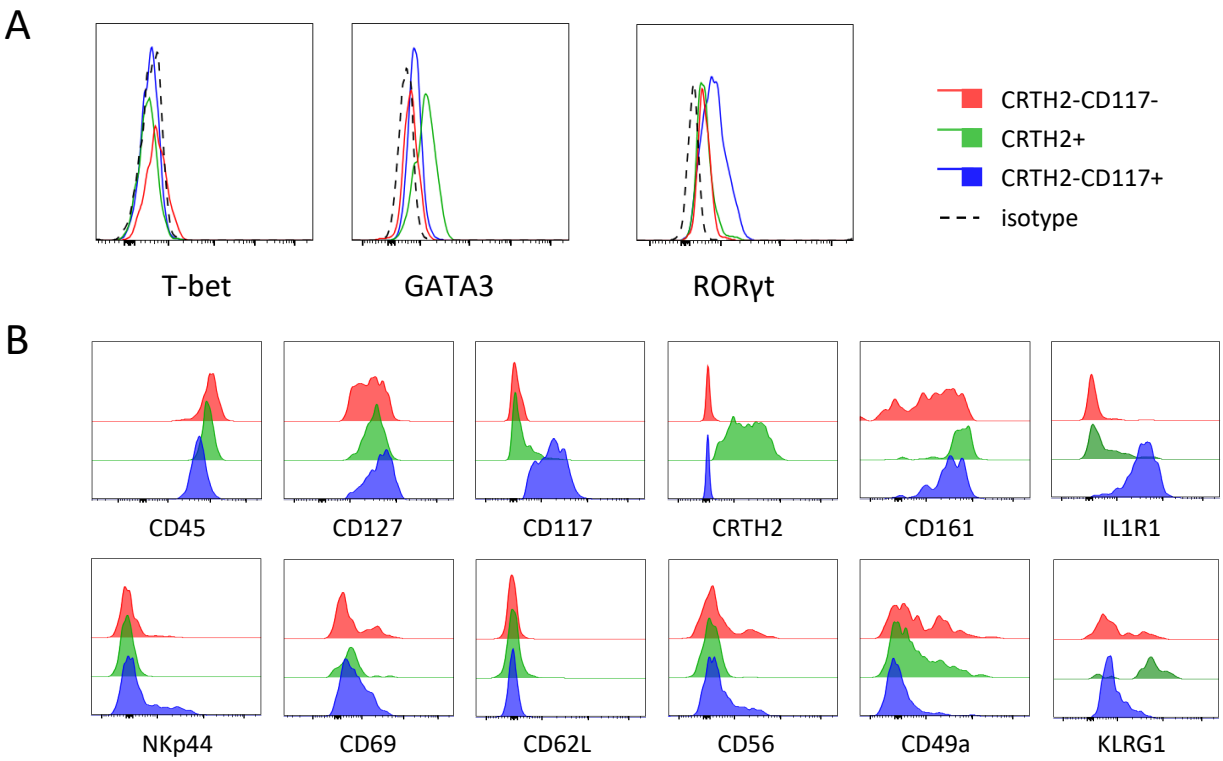

Fig. 3.2 Phenotypical profile of ILC subsets (A) Histograms showing expression of

transcription factors and **(B)** surface markers in CRTH2-CD117-, CRTH2+ and CRTH2-CD117+ ILCs in relation to isotype controls or among each other.

In order to evaluate tissue-specific features of the intrahepatic ILCs pool, further analyses were performed comparing liver ILCs to ILCs isolated from tonsils, colon and peripheral blood. In contrast to the low frequency of circulating ILCs, the liver contained an enriched proportion of CD45+Lin-CD127+ cells, although even higher numbers were found in tonsillar or colonic tissue (**Fig. 3.3A**). The composition of the hepatic ILC pool on the other hand, appeared to be more balanced than in tonsils and colon, containing also CRTH2+ ILC2, which were hardly detectable in the other tissues (**Fig. 3.3B**).

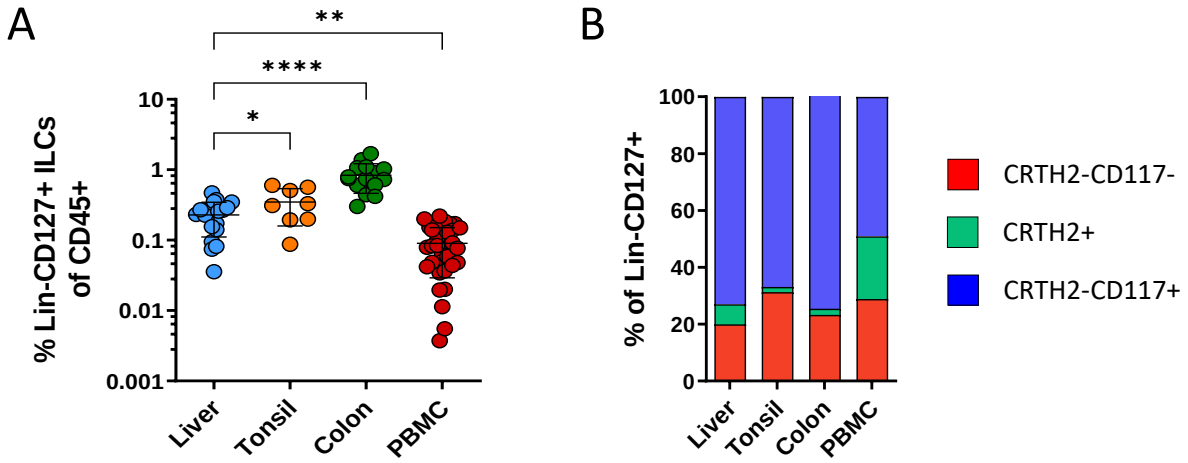

Fig. 3.3 Frequency and composition of the ILC pool in different compartments of the human body (A) Frequency of intrahepatic Lin-CD127+ ILCs (N = 18) as percentage of CD45+ cells in comparison to ILCs from tonsils (N = 8), colon (N = 15) and peripheral blood (N = 34). **(B)** Compartment-specific composition of ILC pool as mean percentages of individual subsets among Lin-CD127+ ILCs in assessed samples. Statistical significance determined by ANOVA (A), corrected for multiple comparisons by controlling FDR. Error bar showing SD.

To investigate this compartment-specific heterogeneity in an unbiased manner and in more detail, equal proportions of Lin-CD127+ ILCs from liver, tonsil, colon and peripheral blood of multiple representative donors were merged to form a composite dataset. Using the FlowSOM algorithm for unsupervised clustering (Van Gassen et al., 2015), eight distinct clusters could be identified in the dataset (**Fig. 3.4A**), based on the expression of 11 different flow cytometric parameters (**Fig. 3.4B**). All clusters as well as all analysed

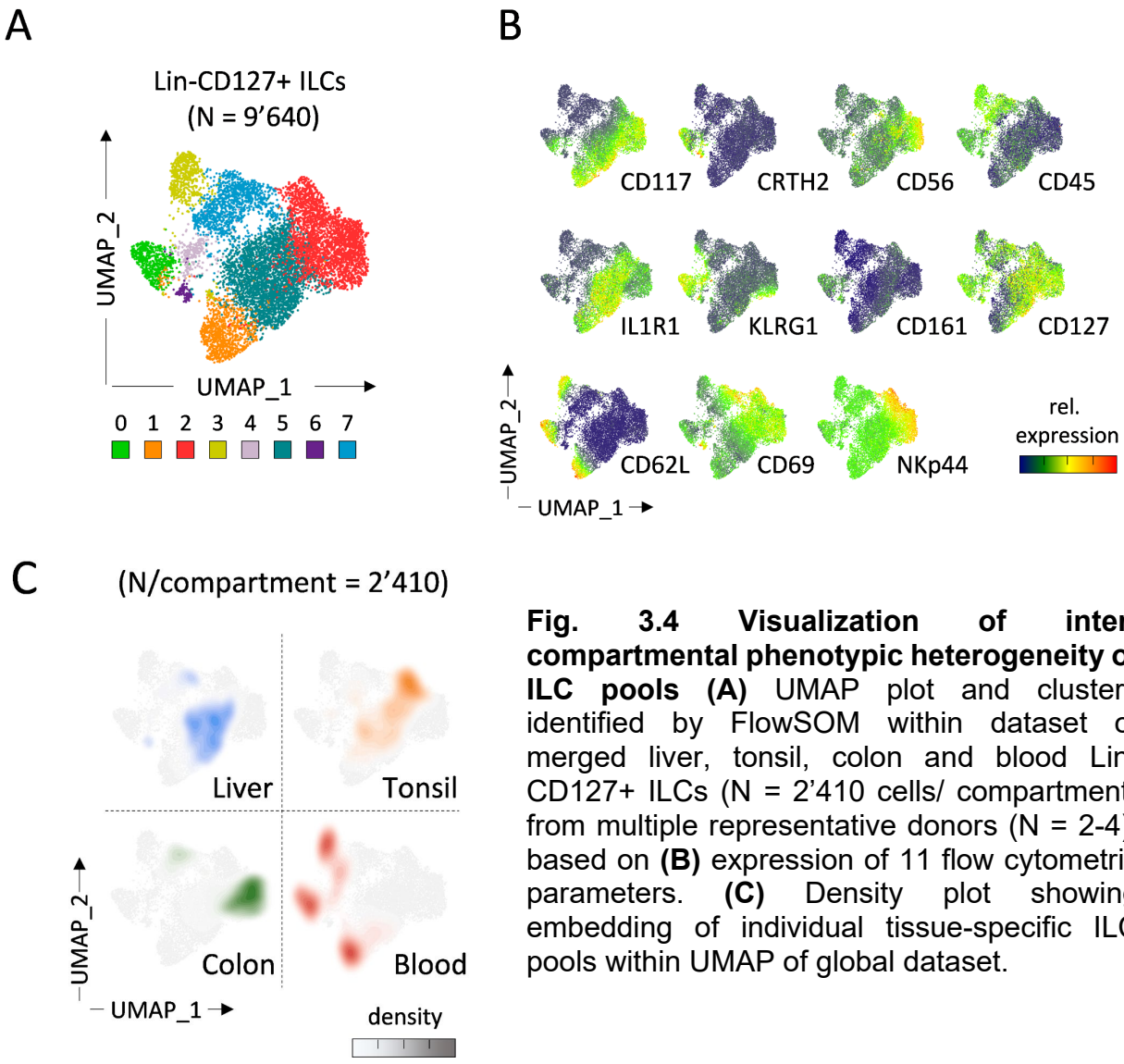

Fig. 3.4 Visualization of inter-compartmental phenotypic heterogeneity of ILC pools (A) UMAP plot and clusters identified by FlowSOM within dataset of merged liver, tonsil, colon and blood Lin-CD127+ ILCs (N = 2'410 cells/ compartment) from multiple representative donors (N = 2-4), based on **(B)** expression of 11 flow cytometric parameters. **(C)** Density plot showing embedding of individual tissue-specific ILC pools within UMAP of global dataset.

compartments were specifically embedded in a UMAP plot, used for reduction of dimensionality and data visualization, highlighting their distinctive phenotypical profiles (**Fig. 3.4C**).

Based on their expressional properties, all clusters could be unambiguously assigned to a distinct ILC subset: Clusters 3 and 7 as CRTH2-CD117- ILC1-like, clusters 0, 4 and 6 as CRTH2+ ILC2-like and cluster 1, 2 and 5 as CRTH2-CD117+ ILC3-like cells (**Fig. 3.5A**). Further separation was driven by the specific expression of CD62L (associated with circulating cells) and CD69 (associated with tissue-resident cells), as well as the expression of NKp44 among the subsets with an ILC3-like phenotype. The distribution of

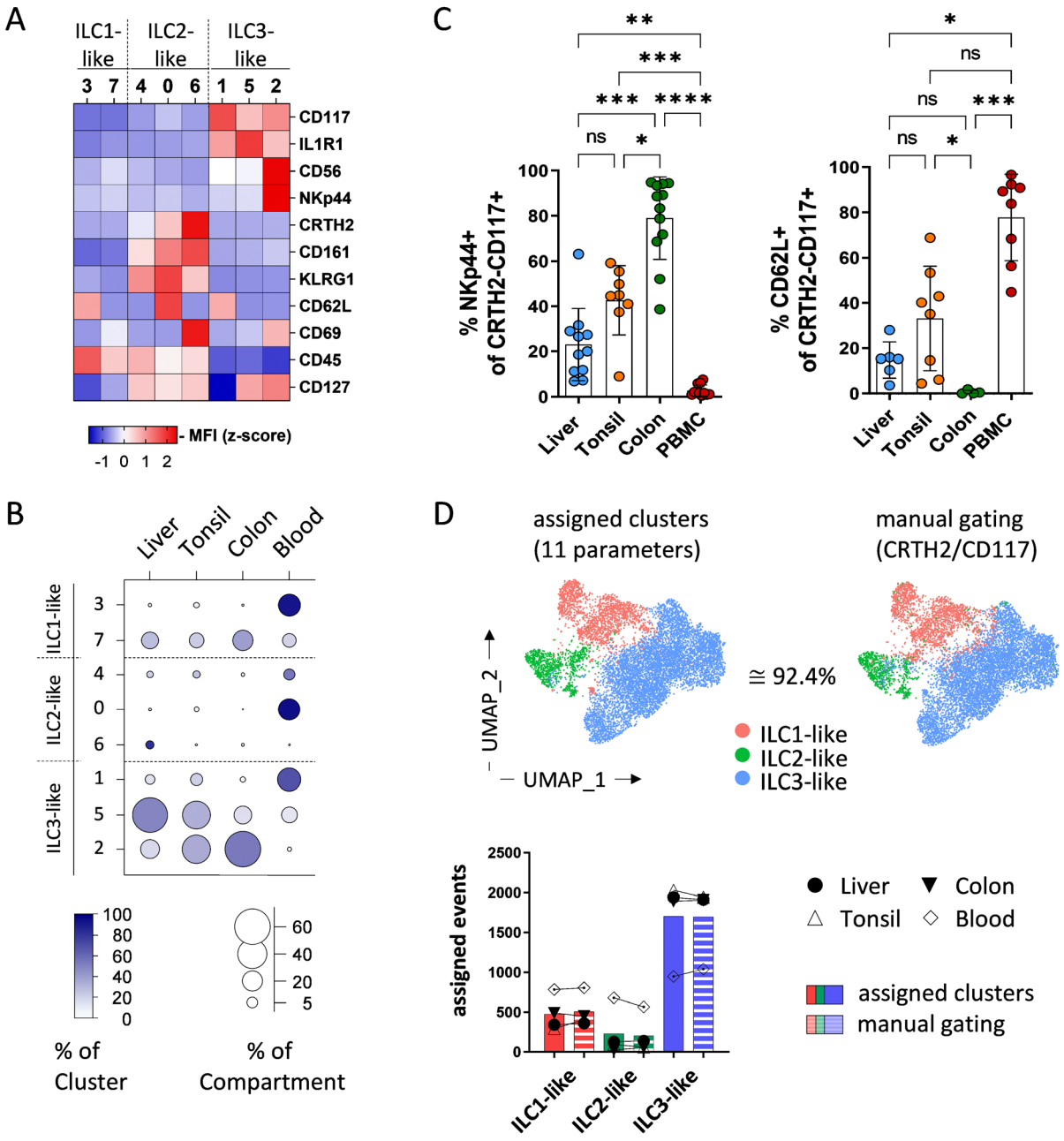

Fig. 3.5 Identification of subclusters within intrahepatic ILC pool in comparison to other compartments (A) Expression signature of FlowSOM clusters depicted as heatmap, displaying MFI z-score of individual markers. Assignment of clusters to ILC subsets (ILC1-, ILC2-, ILC3-like) based on expression pattern of CRTH2 and CD117. **(B)** Bubble chart displaying proportion of clusters within (area) and across (colour) different compartments. **(C)** Percentage of NKp44+ and CD62L+ CRTH2-CD117+ ILCs in additionally sampled donors (N_{liver}=11, N_{tonsil}=8, N_{colon}=12, N_{blood}=11). **(D)** ILC1-like, ILC2-like and ILC3-like cells identified by clustering (top left) versus manual gating (top right) embedded in global UMAP plot. Bar chart (bottom panel) displaying mean number of assigned events, with symbol and lines depicting paired observations within individual compartments. Statistical significance determined by Kruskal-Wallis test (C), corrected for multiple comparisons by controlling FDR. Error bars showing SD.

clusters yielded a specific pattern for each compartment (**Fig. 3.5B**). While tissue-resident NKp44- ILC3 (cluster 5) predominated particularly in the intrahepatic ILC pool, tonsil and colon ILCs displayed higher proportions of NKp44+ ILCs (cluster 2), whereas among circulating ILCs CD62L-expressing cells (cluster 0, 1 and 3) were most abundant. These findings, which were in line with previous observations (Bar-Ephraim et al., 2019; Glatzer et al., 2013; Krämer et al., 2017), could also be confirmed by analysing a larger number of samples (**Fig. 3.5C**). In addition, the liver contained the highest proportion of tissue-resident ILC2 (cluster 6) which were virtually absent in all other assessed compartments.

Furthermore, the assignment of clusters identified in an unbiased manner validated the manual gating approach, yielding a level of congruence of 92.4 % matched items (**Fig. 3.5D**) between both methods.

Taken together, all major ILC subsets could be detected in the human liver. While intrahepatic ILCs displayed conventional surface marker patterns, a tissue-specific composition of the liver ILC pool could be outlined by this initial analysis, identifying tissue-resident ILC3 to represent the predominant subset among Lin-CD127+ liver ILCs.

3.2 Functional characterisation of the intrahepatic ILC pool

Tissue-specific cues of the local microenvironments have been reported not only to shape development and phenotype of distinct ILC pools, but also to affect the functional properties of the individual subsets (Bal et al., 2020). Given the unique composition of the intrahepatic ILC pool, further analyses were performed to assess if the cytokine profile of liver-resident ILCs exhibited tissue-specific features as well. In contrast to former studies (Forkel et al., 2017; Jeffery et al., 2017), these analyses were designed to initially address cytokine production by pan-ILCs, in order to allow for the unbiased detection of cytokine expression beyond the expectable repertoire of individual ILC subsets.

For this purpose, isolated liver-infiltrating lymphocytes were stimulated with PMA/Ionomycin for 4h and the induction of IFNγ, IL-17A, IL-22 and IL-13 was assessed among total Lin-CD127+ ILCs using flow cytometry (**Fig. 3.6A**). As expected and commonly described (Nagasawa et al., 2018; Vivier et al., 2018), most of the IFNγ-producing ILCs were found among CRTH2-CD117- ILC1, whereas the ILC3-specific

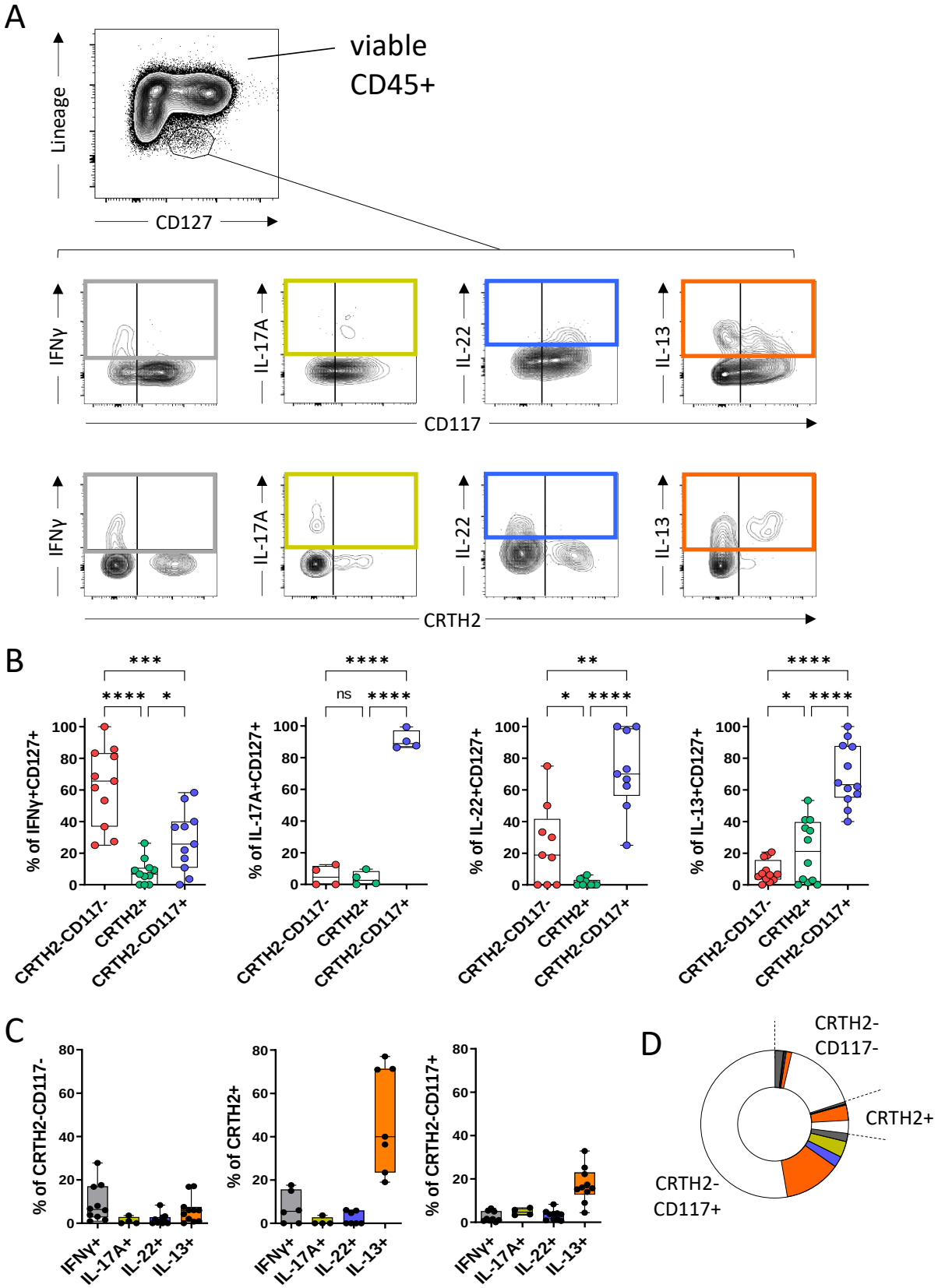

Fig. 3.6 Assessment of functional capacity in intrahepatic non-NK ILCs (A) Flow cytometric analysis of cytokine production in gated CD45+Lin-CD127+ pan-ILCs after

stimulation with PMA/Ionomycin. **(B)** Percentage of cytokine-positive cells within each ILC subset in relation to IFNγ+, IL-17A+, IL-22+ or IL-13+ pan-ILCs. **(C)** Percentage of IFNγ+, IL-17A+, IL-22+ and IL-13+ cells within individual subsets. **(D)** Mean percentages of cytokine-positive subsets as fraction of total ILC pool. Statistical significance determined by ANOVA (B: IFNγ, IL-17A, IL-13) and Kruskal-Wallis test (B: IL-22), corrected for multiple comparisons by controlling FDR.

cytokines IL-17A and IL-22 were predominantly expressed by CRTH2-CD117+ ILC3 (**Fig. 3.6B**), although only a minor induction of cytokine production was observed in these cells (**Fig. 3.6C**).

With regard to the ILC2-specific cytokine IL-13 however, a substantial proportion of PMA/Ionomycin-responsive cells was not only detected among CRTH2+ ILC2 but also among CRTH2-CD117+ ILCs. Within this ILC3-like subset, the amount of IL-13+ cells constituted even the dominant fraction of cytokine-producing cells. Although the subset-intrinsic frequency of IL-13-producing cells was higher in CRTH2+ compared to CRTH2-CD117+ ILCs, the latter represented the major IL-13+ as well as cytokine-positive population within the intrahepatic ILC pool given their higher overall abundance (**Fig. 3.6D**).

This enrichment of IL-13-producing CRTH2-CD117+ ILC3 appeared to be specific for the hepatic compartment, as only marginal numbers could be observed among tonsil, colon and blood ILC3 (**Fig. 3.7A**). To evaluate if this particular functional profile of intrahepatic CRTH2-CD117+ ILCs also manifested upon physiologic stimulation, cells were treated with the ILC3-priming cytokines IL-1β and IL-23 instead of PMA/Ionomycin and analysed after overnight incubation (**Fig. 3.7B**). Here however, no IL-13 expression could be observed in liver ILC3, indicating that the activation of intrahepatic IL-13-producing CRTH2-CD117+ ILCs required different or additional stimuli.

Of note, both pharmacological and physiological stimulation of liver ILC3 induced only low levels of ILC3-specific cytokines such as IL-22, similar to colon or peripheral blood ILC3 (**Fig. 3.7C, D**). This was in contrast to tonsillar ILC3 that displayed a robust induction of IL-22 after PMA/Ionomycin- or IL-1β/IL-23-stimulation, thereby validating the overall efficacy of the treatment and emphasizing the tissue-specific differences in ILC functionality.

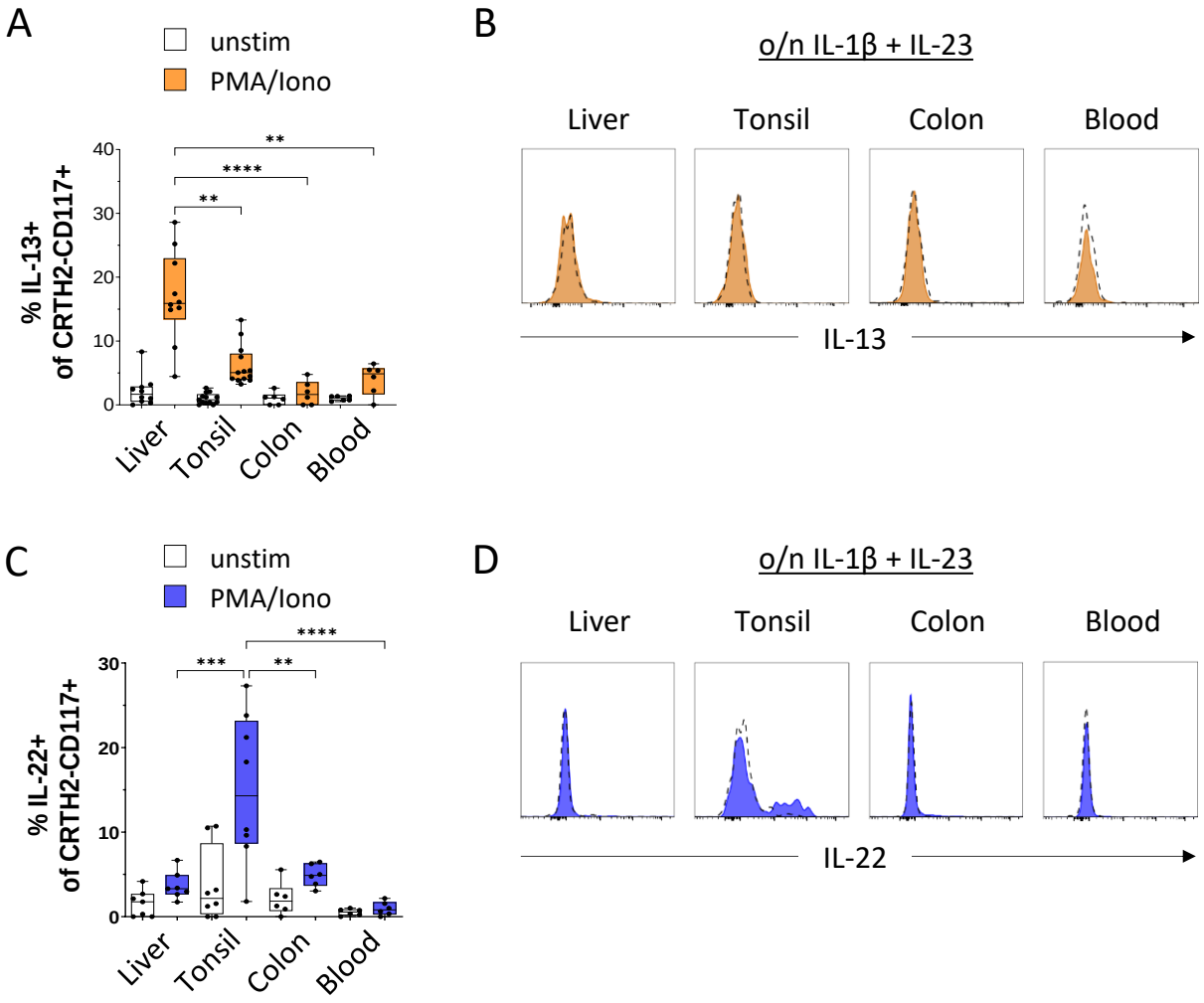

Fig. 3.7 Comparison of functional capacity in liver ILCs to other compartments **(A)** Percentage of IL-13+ and **(C)** IL-22+ cells among CRTH2-CD117+ ILCs in PMA/Ionomycin-stimulated liver (N = 10), tonsil (N = 9), colon (N = 6) and peripheral blood (N = 6) ILCs. **(B)** Histograms showing intracellular expression of IL-13 and **(D)** IL-22 in CRTH2-CD117+ ILCs from indicated compartments after overnight stimulation with IL-1β and IL-23. Statistical significance determined by Kruskal-Wallis test (A) and ANOVA (C), corrected for multiple comparisons by controlling FDR.

In summary, this functional analysis of human intrahepatic ILCs identified a formerly unrecognised subset with an ILC3-like phenotype and the capacity to produce the ILC2-specific cytokine IL-13. This subset appeared to be specifically enriched in the human liver, where it constituted a substantial proportion of the cytokine-producing liver ILCs. Aside from IL-13+ CRTH2-CD117+ ILCs, these included only minor proportions of conventionally described IFNγ+ ILC1-like cells, IL-17A+ or IL-22+ ILC3-like cells or IL-13+ ILC2-like cells.

3.3 Assesment of the heterogeneity of intrahepatic IL-13-expressing ILCs

In the next step, a detailed phenotypic profiling of the IL-13-producing CRTH2-CD117+ liver ILCs was performed, in order to define this subset more precisely, since the initial analysis had only accounted for CD127, CRTH2 and CD117 expression. Given that an activation-induced downregulation of CRTH2 expression has been described in Th2 cells (MacLean Scott et al., 2018), the observation of IL-13+CRTH2-CD117+ might have merely resulted from an erroneous identification of conventional ILC2 with downregulated CRTH2 expression.

To address this hypothesis, the expression of further ILC2-specific markers was assessed in PMA/Ionomycin-induced IL-13+ CRTH2-CD117+ ILCs and compared to their CRTH2+ counterparts (**Fig. 3.8A**). In contrast to the ILC2-like cells however, no prominent expression of GATA3, KLRG1 or CD161 could be observed in IL-13-producing CRTH2-CD117+ cells, which instead resembled the phenotype of IL-13-CRTH2-CD117+ ILC3 (**Fig. 3.8B**). Moreover, the CRTH2-CD117+ subset also appeared to be unresponsive to the ILC2-specific stimuli IL-33 and TSLP, unlike CRTH2+ ILCs (**Fig. 3.8C**). Following overnight stimulation, no expression of IL-13 could be observed among ILC3-like cells, indicating that these cells were also functionally distinct from conventional ILC2.
In return, IL-13+ CRTH2-CD117+ ILCs displayed a substantial expression of the ILC3-specific transcription factor RORγt, similar to that observed in conventional IL-13-CRTH2-CD117+ ILC3 (**Fig. 3.9A**). In addition, expression of two ILC2-exclusion markers, CD56 and NKp44, could be detected, which marked another sharp distinction to IL-13+ CRTH2+ ILC2 (**Fig. 3.9B**).
Interestingly, IL-13 was the only cytokine produced by CRTH2-CD117+ liver ILC3, which was found among both the NKp44- as well as the NKp44+ subset. This was in contrast to the expression of IFNγ, IL-17A or IL-22, which were predominantly found in only one of these subsets (**Fig. 3.9C**), and thus appeared to be more dependent on the maturation-associated upregulation of NKp44 in ILC3.

Altogether, these observations suggested a profound distinction between conventional IL-13+ CRTH2+ ILC2 and IL-13+ CRTH2-CD117+ ILC3-like cells in the human liver, based on the differential phenotypical and functional properties of both cell types.

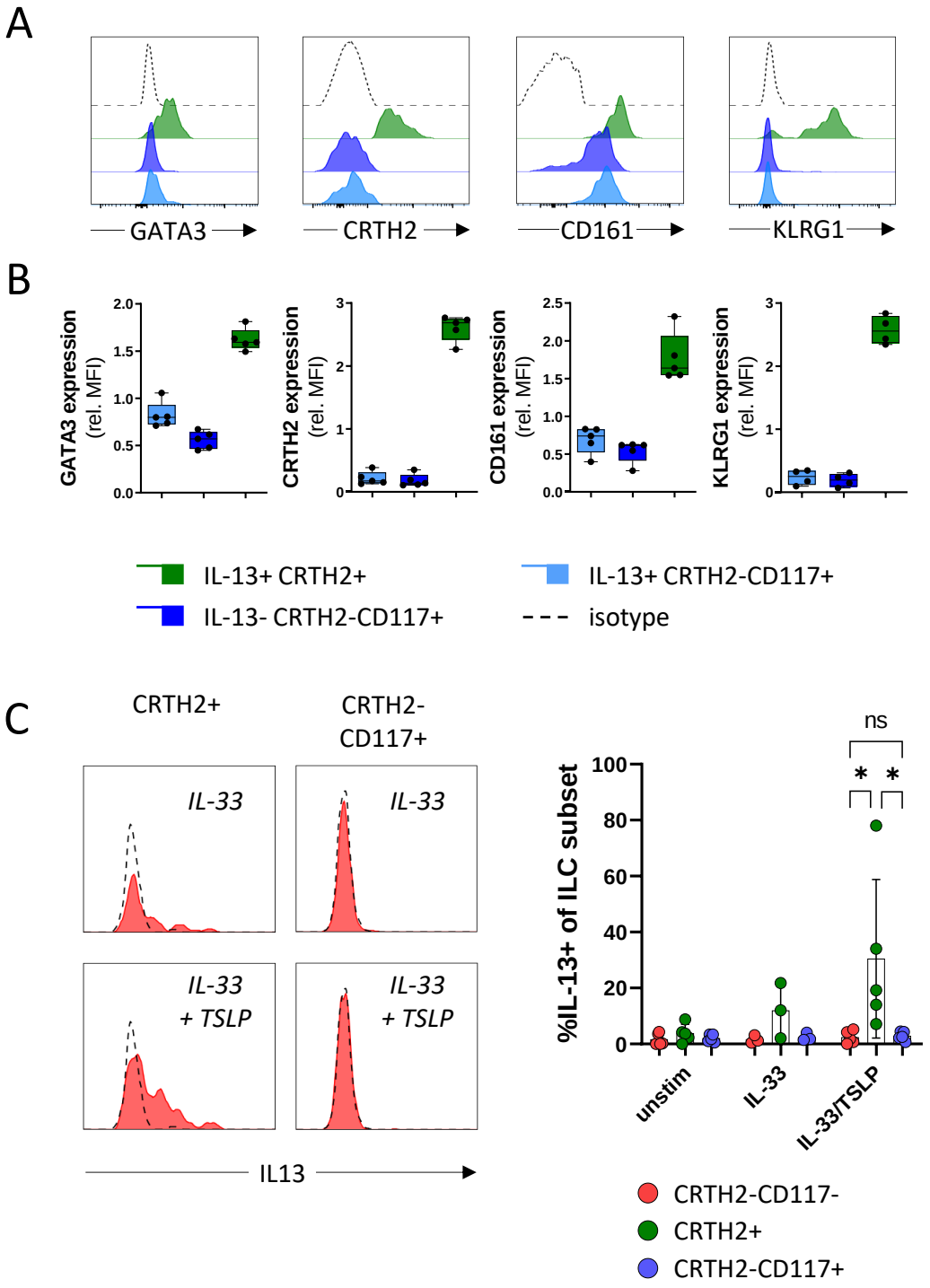

Fig. 3.8 Evaluation of ILC2-specific features in IL-13+ CRTH2-CD117+ ILCs (A) Histograms showing expression levels of indicated markers in IL-13+ CRTH2+ and IL-13+/- CRTH2-CD117+ ILCs in comparison to isotype control after stimulation with PMA/Ionomycin. **(B)** MFI of indicated markers between the different subsets in relation to sample-intrinsic mean. **(C)** Proportion of IL-13+ cells among CRTH2+ and CRTH2-CD117+ ILCs after overnight stimulation with IL-33 +/- TSLP depicted as histogram and bar chart. Statistical significance determined by ANOVA (C), corrected for multiple comparisons by controlling FDR. Error bars showing SD.

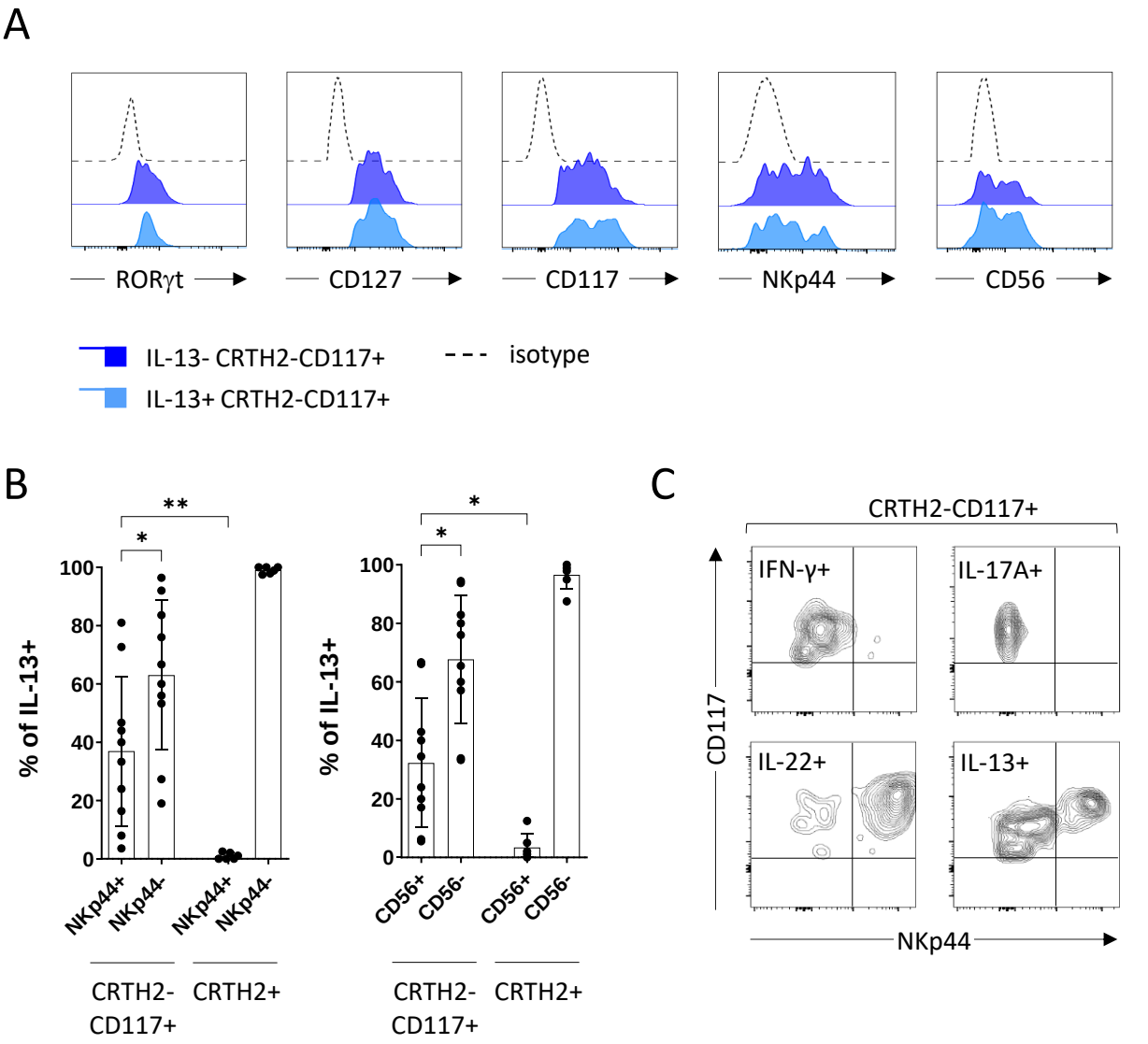

Fig. 3.9 Evaluation of ILC3-specific features in IL-13+ CRTH2-CD117+ ILCs (A) Histograms showing expression levels of indicated markers in IL-13+ and IL-13- CRTH2-CD117+ ILCs in comparison to isotype control after stimulation with PMA/Ionomycin. **(B)** Percentage of NKp44+/- (*left*) and CD56+/- (*right*) cells among IL-13+CRTH2+ and IL-13+CRTH2-CD117+ ILCs. **(C)** Contour plots showing distribution of cytokine-positive cells across NKp44+ and NKp44- subset among CRTH2-CD117+ ILCs. Statistical significance determined by Kruskal-Wallis test (B), corrected for multiple comparisons by controlling FDR. Error bars showing SD.

In order to substantiate these findings and to allow for a more detailed characterization of the intrahepatic IL-13+ ILC3-like cells, an in-depth transcriptional analysis was performed next. Since this approach partially aimed to exclude the possibility of biases stemming

from contaminated bulk populations, the resolution of gene expression on single cell level was of vital importance in this context. For this purpose, intrahepatic CD45+Lin-CD127+ pan-ILCs of three different donors were sort-purified, stimulated with PMA/Ionomycin and then processed using a droplet-based platform for scRNA-seq (10x Genomics®).

Liver specimens with an above-average frequency of CRTH2+ ILCs were chosen, to allow for a balanced representation of the full spectrum of ILC subsets in the scRNA-seq dataset. Furthermore, stimulation with PMA/Ionomycin was reduced to 60 min in order to limit global, activation-induced changes in gene expression and potential non-physiological apoptotic responses.

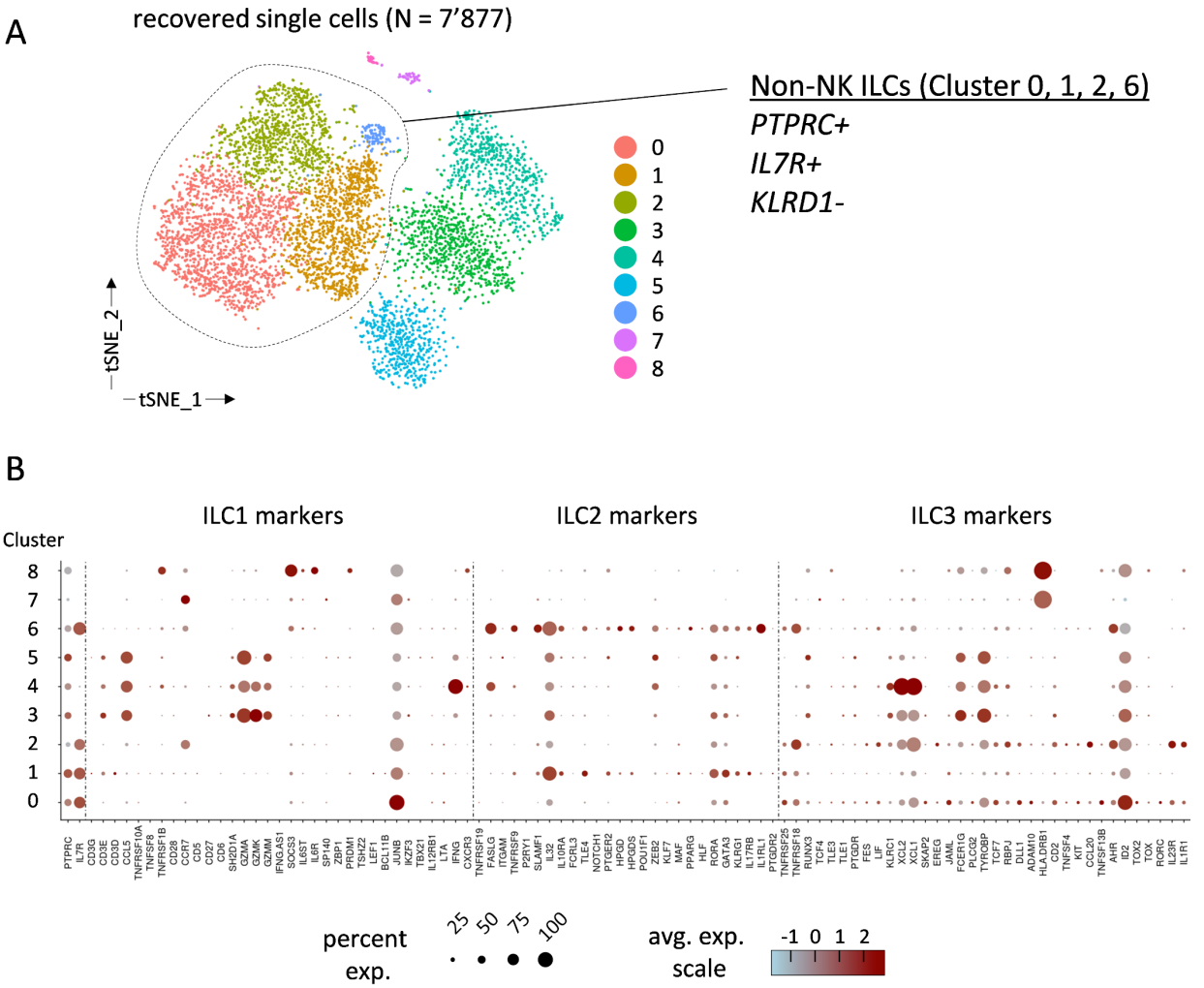

Fig. 3.10 Identification of ILCs in global scRNA-seq dataset (A) tSNE projection of global dataset including all recovered viable single cells (N = 7'877) from total input of sort-purified, PMA/Ionomycin-stimulated CD45+Lin-CD127+ cells. Distinct identified clusters (graph-based, *Seurat*) indicated by colour. **(B)** Reflection of ILC (subset)-specific

expression signature in identified clusters, depicting the percentage of expressing cells (area) and mean expression level (colour) in each cluster. *Figures (A, B) created in cooperation with A. T. Abdallah (IZKF, RWTH Aachen).*

Starting with a total input of 23'762 recorded cells, 7'877 items (33.14 %) could be recovered as viable single cells for further analysis after the pre-processing workflow, which accounted for the removal of technical artefacts and items with insufficient quality. These removed items included cells with a very small (fragmented cells) or very high library size (multiplets) and cells with a high genome-transcript ratio of ribosomal, mitochondrial or cell cycle genes.

An initial clustering analysis of the cleansed dataset identified nine distinct clusters which were specifically embedded in a tSNE projection, used for data visualization (**Fig. 3.10A**). Of these, clusters 0, 1, 2 and 6 displayed a clear ILC signature with a marked expression of the ILC-defining transcripts *PTPRC* and *IL7R* (**Fig. 3.10B**). Within the other grouped subpopulations, only low levels of these features could be observed, indicating a contamination with other cell types. Indeed, high expression of NK-cell-associated transcripts such as *GZMB*, *IFNG* and *KLRD1* could be observed in clusters 3, 4 and 5, while the smaller clusters 7 and 8 showed an enrichment of antigen presenting cell-associated genes (*data not shown*). Consequently, these items were removed from the global dataset, leaving a total of 4'693 non-NK ILCs for downstream analysis.

To assess the ILC-intrinsic heterogeneity in the following, the processed dataset was then subjected to a renewed clustering and tSNE analysis. This resulted in the identification of seven transcriptionally and spatially distinct ILC subclusters (**Fig. 3.11A**). Using previously published ILC subset-specific expression signatures (Björklund et al., 2016), these clusters could be unambiguously classified as either ILC1 (cluster 5), ILC2 (clusters 2, 4, 6) and ILC3 (clusters 0, 1, 3). This was achieved by evaluating the mean enrichment of subset-specific transcripts in each cluster in an overall comparison (**Fig. 3.11B, C**). Thereby a total number of 251 ILC1, 1'318 ILC2 and 3'124 ILC3 could be identified within the dataset (**Fig. 3.11D**). Of note, a paired comparison of transcriptional data and flow cytometric data from matched donors indicated an overrepresentation of ILC1 in the latter (**Fig. 3.11E**). This finding might either indicate a lower abundance of intrahepatic ILC1-

like cells than initially assumed or instead might have resulted from a loss of ILC1 alongside the removal of the transcriptionally similar NK cells from the global dataset.

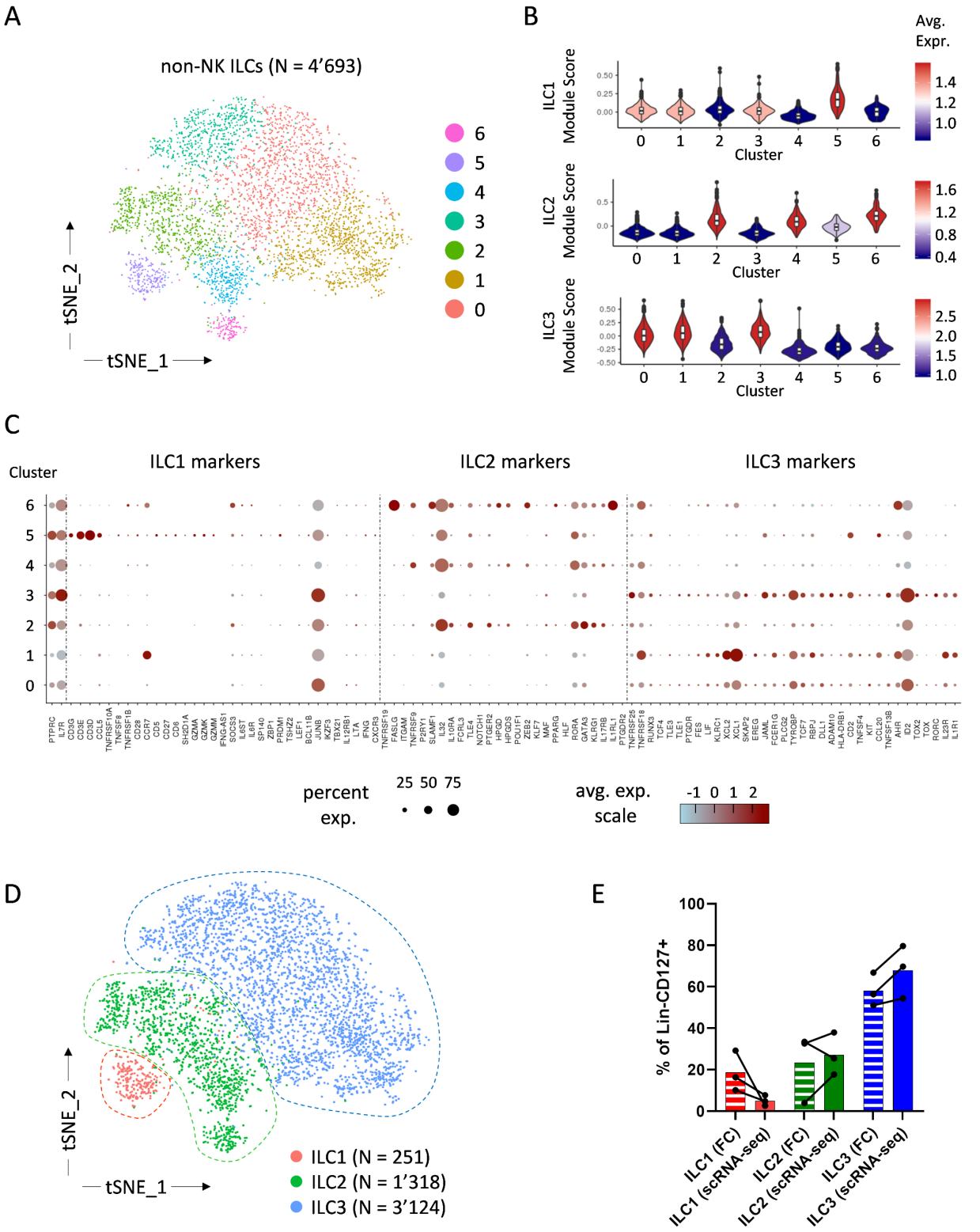

Fig. 3.11 Identification of ILC subsets in cleansed scRNA-seq dataset

(A) tSNE projection of cleansed dataset (N = 4’693 cells) after removal of contaminating non-ILCs, including renewed clustering analysis indicated by colour. **(B)** Violin plots showing mean cluster expression of ILC1-, ILC2- or ILC3-related genes, calculated as modular score (*Seurat*) of all subset-specific transcripts. **(C)** Reflection of ILC (subset) - specific expression signature in re-defined clusters, depicting the percentage of expressing cells (area) and mean expression level (colour) in each cluster. **(D)** Embedding of identified ILC subsets in tSNE projection. **(E)** Percentages of ILC1, ILC2 and ILC3 among Lin-CD127+, identified in matched donors by flow cytometry (FC) versus scRNA-seq. *Figures (A-D) created in cooperation with A. T. Abdallah (IZKF, RWTH Aachen).*

In line with the previous observations, expression of *IL13* could be detected in both the ILC2 and ILC3 supercluster, while *IL13*+ ILC1-like cells were absent (**Fig. 3.12A**). In addition, a direct comparison of both *IL13*+ cell types indicated that their distinction was indeed driven by relevant ILC-defining genes, as ILC2- and ILC3-specific transcripts were found among the respective top 30 differentially expressed (DE) genes. These included genes such as *IL1RL1*, *IL17RB* and *HPGDS* which are phenotypically and functionally associated with conventional ILC2 (Maric et al., 2019; Mjösberg et al., 2011), as well as, respectively, *IL1R1*, *IL23R* and *TYROBP*, which mark ILC3-defining features (Sonnenberg, 2016) (**Fig. 3.12B**), altogether underlining the significance of the observed heterogeneity.

Accordingly, this distinction was also preserved upon a renewed clustering and tSNE analysis of an isolated dataset of all *IL13*-expressing cells **(Fig. 3.12C)**. Here, the two newly identified clusters almost completely overlapped with the superordinate cluster annotation, which confirmed the inherently different gene expression profiles of cells derived from the ILC2-supercluster (*IL13*+ cluster 0) and those derived from the ILC3-supercluster (*IL13*+ cluster 1).

In order to validate their ILC2-like and ILC3-like phenotypes, the enrichment of the complete subset-specific gene expression signatures was evaluated in the *IL13*+ sub-clusters next. Here, cluster 0 displayed a distinct upregulation of ILC2-related transcripts whereas in cluster 1 an upregulation of the ILC3-specific profile could be observed (**Fig. 3.12D**). This did not only manifest in the mean enrichment of the entire signatures, but also with regard to the expression of multiple hallmark genes, which were initially used for the discrimination of the ILC subsets, such as *GATA3*, *RORC*, *PTGDR2* and *KIT* **(Fig.**

3.12E). Moreover, as observed in the flow cytometric analysis, *IL13*+ ILC3 were not only distinct from *IL13*+ ILC2 but also reflected the expressional profile of *IL13*- ILC3.

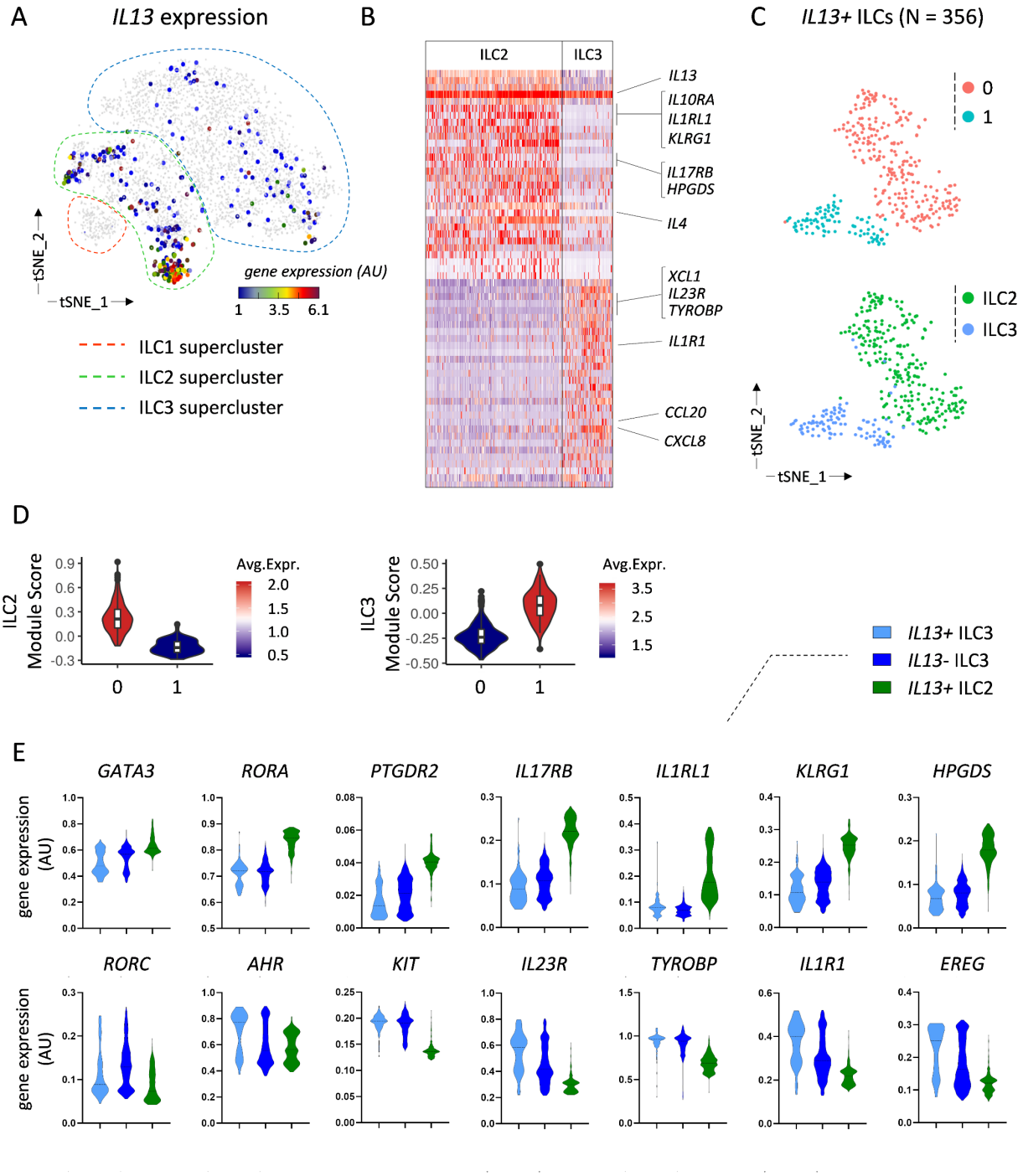

Fig. 3.12 Transcriptional analysis of ILC2-specific and ILC3-specific features in *IL13*+ ILCs (A) Representation of *IL13*-expressing in tSNE-projection of cleansed ILC dataset. Level of expression, as relative arbitrary units (*AU*), coloured as indicated. Dashed Lines indicating outlines of ILC1, ILC2 and ILC3 supercluster. **(B)** Differential Gene Expression (DGE) analysis of *IL13*+ cells from ILC2 versus ILC3 supercluster. Top

30 DE genes are depicted, annotated individual gene names as indication of ILC2- or ILC3-specific features. **(C)** tSNE projection of isolated *IL13*+ dataset, indicating representation of newly defined clusters (*top*) in comparison to affiliation of original supercluster (*bottom*). **(D)** Violin plots showing the enrichment of ILC2-specific and ILC3-specific transcriptional signatures (Björklund et al., 2016) within clusters identified in (C). **(E)** Violin plots depicting expression (as *AU*) of individual ILC2-specific (*top row*) and ILC3-specific (*bottom row*) hallmark genes in a comparison of *IL13*+/- ILC3 and *IL13*+ ILC2. Dashed lines indicating median. *Figures (A-D) created in cooperation with A. T. Abdallah (IZKF, RWTH Aachen).*

In summary, this extensive proteomic and transcriptional analysis comprehensively validated the initially observed heterogeneity among IL13-producing liver ILCs. Thus, the intrahepatic ILC pool can be characterized by the presence of a previously unrecognized subset of ILC3-like cells with the capacity to produce the ILC2-specific cytokine IL-13. Due to its relative abundance among tissue-resident Lin-CD127+ ILCs, these IL-13+ ILC3-like cells might considerably influence the overall effects mediated by ILCs in the liver microenvironment.

3.4 Involvement of pan-ILCs and IL13-producing ILC3 in chronic liver disease

Based on the previous findings, which were observed in histologically normal livers, subsequent analyses aimed to address the potential involvement of ILCs and IL-13-producing ILC3-like cells in the context of chronic liver disease (CLD).

So far, the contribution of ILCs in this setting has been typically discussed in light of their conventional subset-specific cytokine-profiles. As such, both protective as well as detrimental effects have been described for ILC3 in hepatic fibrogenesis (Kong et al., 2012; Zhao et al., 2014), primarily due to their assumed expression of IL-22. Given the atypical functional profile of human liver ILC3 however, they might in fact exert similar effects as IL-13-producing ILC2 for which murine studies have suggested a pro-fibrotic role in liver fibrosis (Marvie et al., 2009; Mchedlidze et al., 2013).

In order to screen for an overall disease-related perturbation of the intrahepatic ILC pool, first, the frequency of Lin-CD127+ ILCs was assessed in isolates of fibrotic or cirrhotic livers and compared to non-fibrotic controls. In fact, all ILC subsets were found to be significantly increased in CLD patients (**Fig. 3.13A**). In CRTH2-CD117+ ILC3, this was

mainly due to a substantial expansion of the NKp44-expressing subset, which represented the dominant ILC subset in fibrotic livers (**Fig. 3.13B**). To evaluate, whether this was due to a systemic increase of ILCs in the diseased patient cohort, pan-ILC frequency was further analysed in colon and peripheral blood samples of CLD patients (**Fig. 3.13C, D**). However, no significant alterations could be detected in comparison to samples from non-fibrotic control donors, indicating a liver-specific expansion of ILCs.

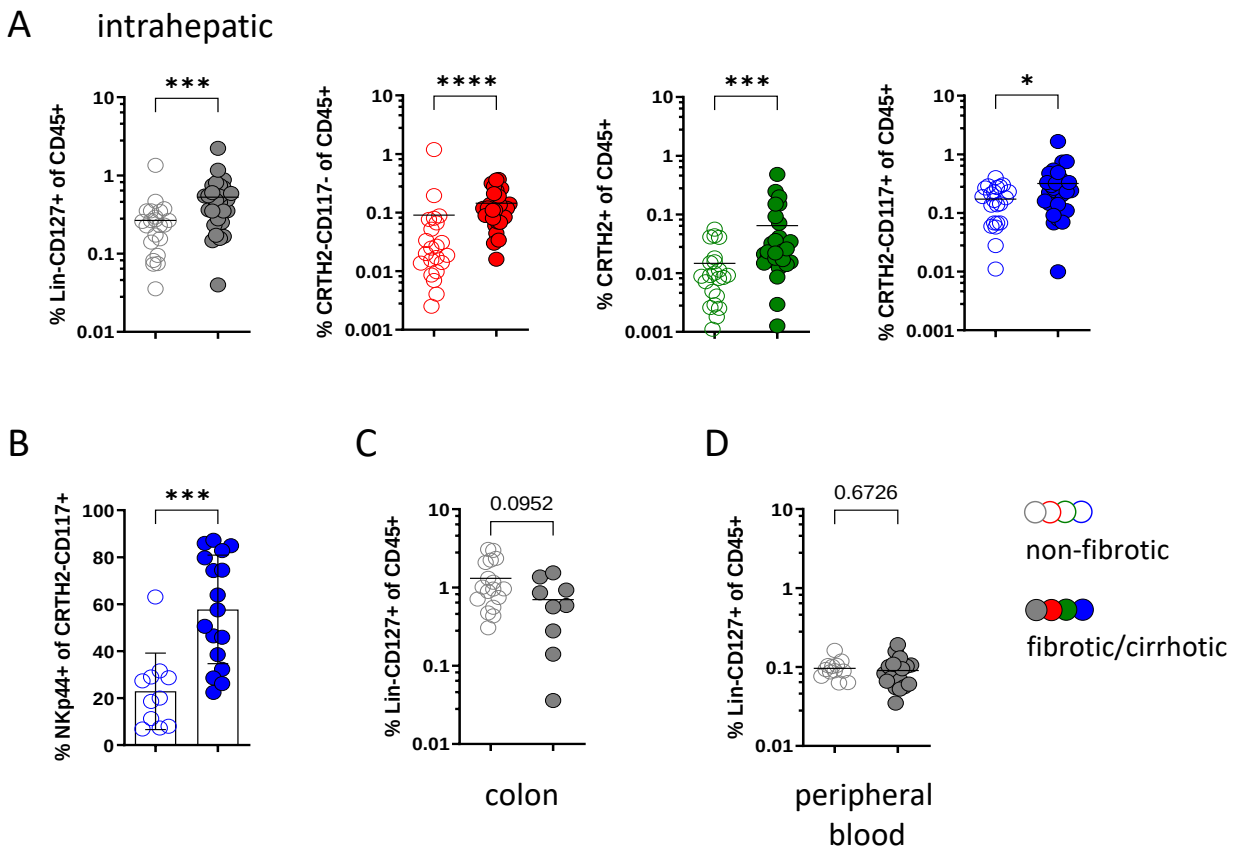

Fig. 3.13 Frequency of pan-ILCs and ILC subsets in controls vs CLD patients (A) Percentage of intrahepatic pan-ILCs and individual subsets among CD45+ cells as well as **(B)** percentage of NKp44+ cells among CRTH2-CD117+ ILCs in isolates of fibrotic or cirrhotic livers compared to non-fibrotic controls. **(C)** Percentage of pan-ILC frequency in colon tissue and **(D)** peripheral blood among CD45+ cells in samples of CLD patients compared to non-fibrotic controls. Statistical significance determined by Mann-Whitney test (A, B, C) or unpaired t-test (D). Error bars indicating SD.

Furthermore, fibrotic or cirrhotic livers also contained an enriched proportion of IL-13-producing ILC3-like cells, indicating an involvement of this previously identified liver-specific cell type in a pathological setting (**Fig. 3.14A**). Of note, IL-13+CRTH2+ ILC2 were

not increased in livers of diseased patients, thus implying that the disease-related expansion of IL-13-producing cells only affected the ILC3-like subset (**Fig. 3.14B**).

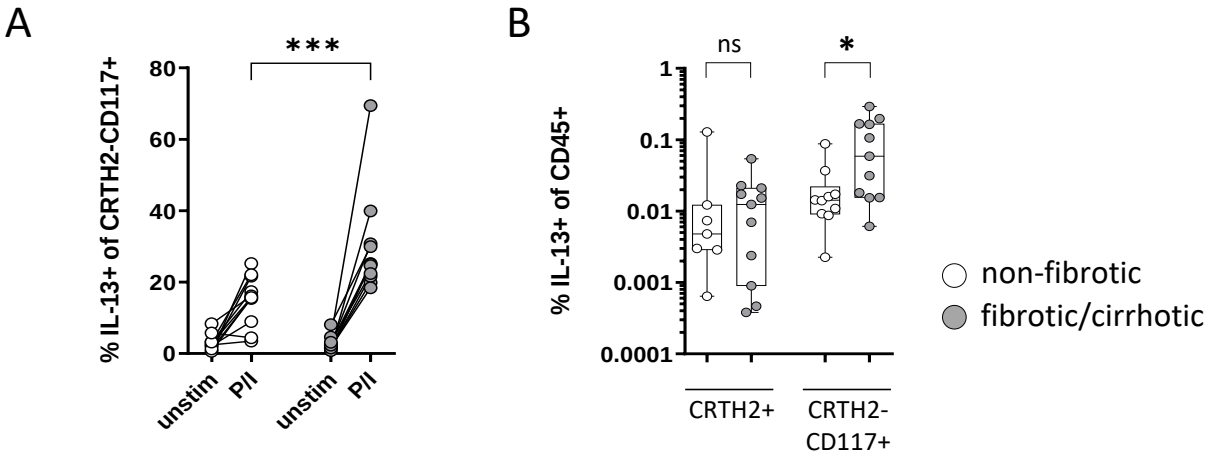

Fig. 3.14 Frequency of IL-13-producing ILCs in controls vs CLD patients (A) Frequency of intrahepatic IL-13+ cells among CRTH2-CD117+ ILCs in samples of CLD patients compared to non-fibrotic controls after stimulation with PMA/Ionomycin. **(B)** Percentage of IL-13+CRTH2+ or IL-13+CRTH2-CD117+ ILCs among CD45+ cells in samples of CLD patients compared to non-fibrotic controls. Statistical significance determined by Mann-Whitney test (A, B).

Interestingly, subset-specific differences were also observed with regard to the course of CLD progression. Using the model for end-stage liver disease- (MELD-) score as surrogate for disease severity, the frequency of intrahepatic CRTH2+ ILC2 was found to negatively correlate with CLD staging (**Fig. 3.15A**). CRTH2-CD117+ ILC3 on the other hand, as well as the proportion of IL-13+ ILC3-like cells (**Fig. 3.15A, B**) increased with ongoing hepatic fibrogenesis, further suggesting that the two ILC subsets might be differentially involved at distinct time points of CLD progression.

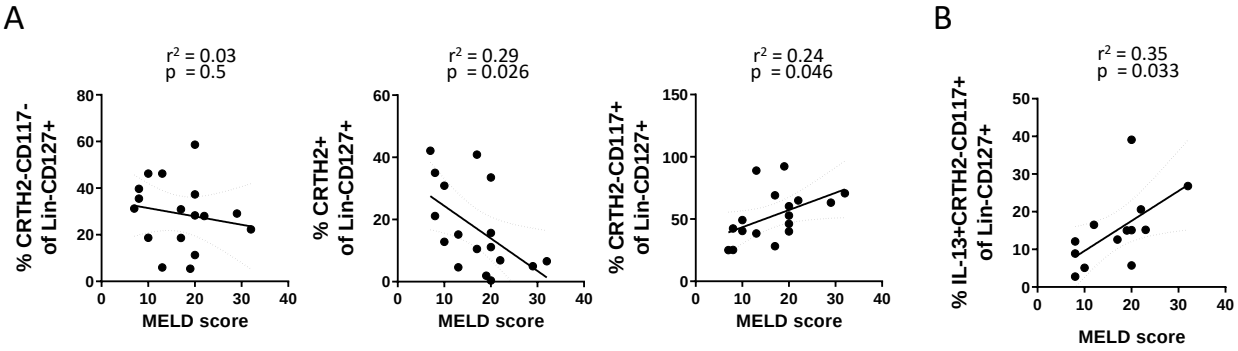

Fig. 3.15 Frequency of intrahepatic ILC subsets in course of CLD progression

(A, B) Pearson correlation of indicated ILC subset frequencies in CLD patients with corresponding MELD score, used as surrogate for disease severity.

3.5 Functional impact of IL-13-producing ILC3 on HSCs

Given the general involvement of ILCs and IL-13-expressing ILC3 in hepatic fibrogenesis, further analyses were performed to assess the functional impact of IL-13 producing cells in a pathological setting. For this purpose, an *in vitro* culture system of primary human HSCs was utilized, as the influence of ILCs in this context has typically been attributed to the modulation of these cells (Fabre et al., 2018; Liu and Zhang, 2017; Wang et al., 2018; Wang and Zhang, 2019).

In the first step, HSCs were treated with recombinant human IL-13 (rhIL-13) in order to assess the overall effects of this cytokine in the chosen setting. After 48 h of stimulation, changes in gene expression were analysed and evaluated in comparison to cells treated with TGFβ, which served as a positive control for the induction of a pro-fibrotic phenotype in HSCs. In contrast to the previously described direct pro-fibrotic effects of IL-13 (Liu et al., 2011; Mchedlidze et al., 2013; Sugimoto et al., 2005), treatment of HSCs with rhIL-13 did not result in the upregulation of fibrosis-associated markers, such as *COL1A1*, *ACTA2*, *ACTG2* or *MMP2* (**Fig. 3.16A**). This was also observed when rhIL-13 was administered in combination with TGFβ, which for itself significantly increased expression of these genes. In return, IL-13 caused a significantly increased expression of pro-inflammatory genes such as *CXCL8* and *CXCL1*, revealing a functional impact which has not been reported for this cytokine and cell type up to date (**Fig. 3.16B**).

The increased gene expression of *CXCL8* in IL-13-treated HSCs, also translated into increased protein expression and secretion as detected in the supernatant after 48 h by ELISA (**Fig. 3.17A**). Overall, this functional impact appeared to be specific for IL-13 in the established setting, since neither the pro-fibrotic agent TGFβ nor the typical ILC3-specific cytokine IL-22 induced similar effects. Of note, a combination of IL-13 and TGFβ synergistically enhanced the observed induction of CXCL8 secretion, indicating that this IL-13-mediated effect might be even more pronounced in pre-activated HSCs. Importantly, the increase in CXCL8 expression in HSCs was not only observed after treatment with rhIL-13 but also after co-culture with purified, pre-stimulated liver ILC3 (**Fig. 3.17B, C**).

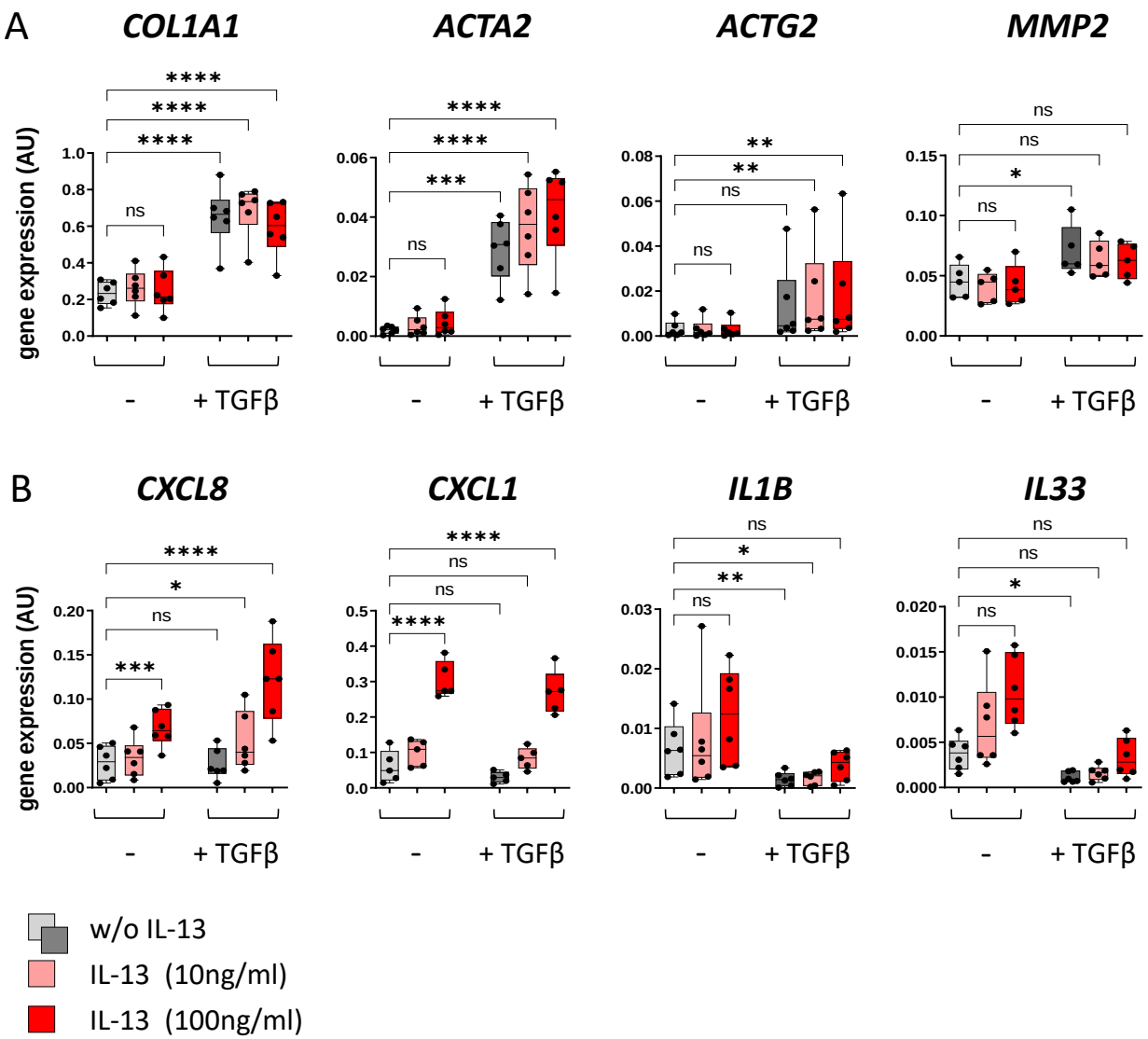

Fig. 3.16 Functional impact of rhIL-13-treatment on HSCs (A) Boxplots displaying mRNA expression levels of pro-fibrotic and **(B)** pro-inflammatory marker genes in HSCs after 48 h of treatment with indicated doses and combinations of rhIL-13 and TGFβ. Statistical significance determined by ANOVA (A: *COL1A1*, *ACTA2*; B: *CXCL8*, *CXCL1*) or Friedman test (A: *ACTG2*, *MMP2*; B: *IL1B*, *IL33*) corrected for multiple comparisons by controlling FDR.

In the next step, the chemotactic potential of IL-13-stimulated HSCs was assessed, in order to evaluate if the observed changes in gene expression were sufficient to induce an effective pro-inflammatory phenotype in stellate cells. For this purpose, the migration of isolated peripheral blood monocytes towards supernatants of pre-treated HSCs was measured. Here, a dose-dependent increase in myeloid cell chemotaxis could be

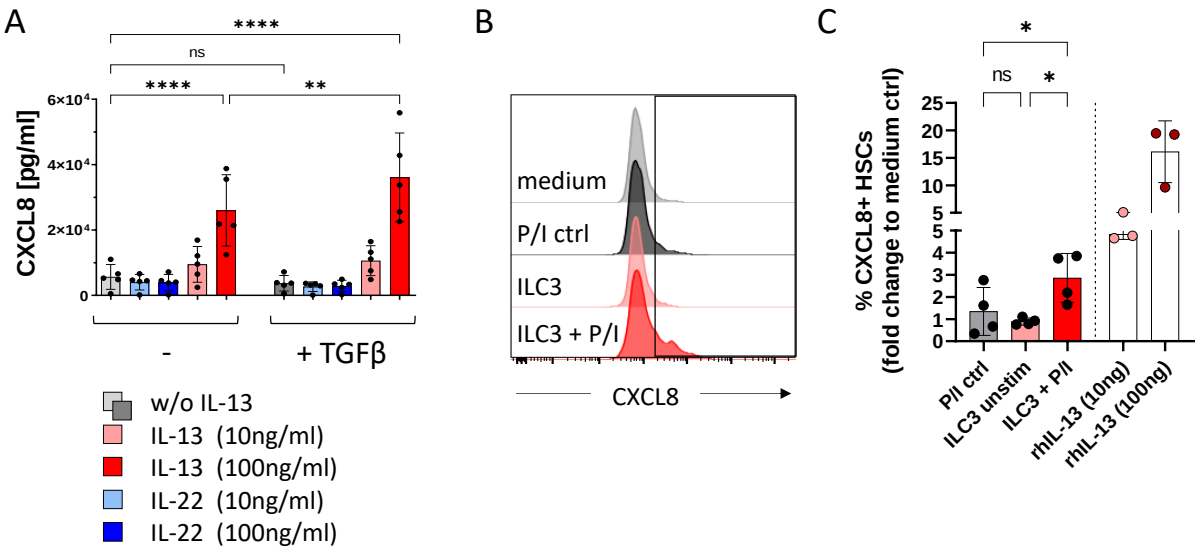

Fig. 3.17 Induction of CXCL8 in HSCs by IL-13 and stimulated liver ILC3 (A) Concentration of CXCL8 in supernatant of HSCs after 48 h of treatment with indicated doses and combinations of rhIL-13, rhIL-22 and TGFβ. **(B, C)** Proportion of CXCL8 expressing HSCs after 24 h of co-culture with sort-purified, PMA/Ionomycin (P/I) pre-stimulated CRTH2-CD117+ liver ILCs or treatment with rhIL-13. Statistical significance determined by ANOVA (A, C) corrected for multiple comparisons by controlling FDR. Error bars showing SD.

observed, which was dependent on the IL-13-mediated upregulation of CXCL8 and not caused by rhIL-13 alone (**Fig. 3.18A, B**). These findings indicate that IL-13-producing liver ILCs may promote an inflammatory signaling in HSCs and therefore might be linked to reported hallmarks of liver fibrogenesis such as the accumulation of myeloid cells (Zimmermann et al., 2011).

Taken together, these observations suggested that the progression of fibrotic liver disease can be characterized by an accumulation of intrahepatic ILCs and IL-13-producing ILC3 in particular. Mechanistically, these might contribute to a pro-inflammatory modulation of HSCs and, as such, display the capacity to critically influence an acknowledged driver of hepatic fibrogenesis.

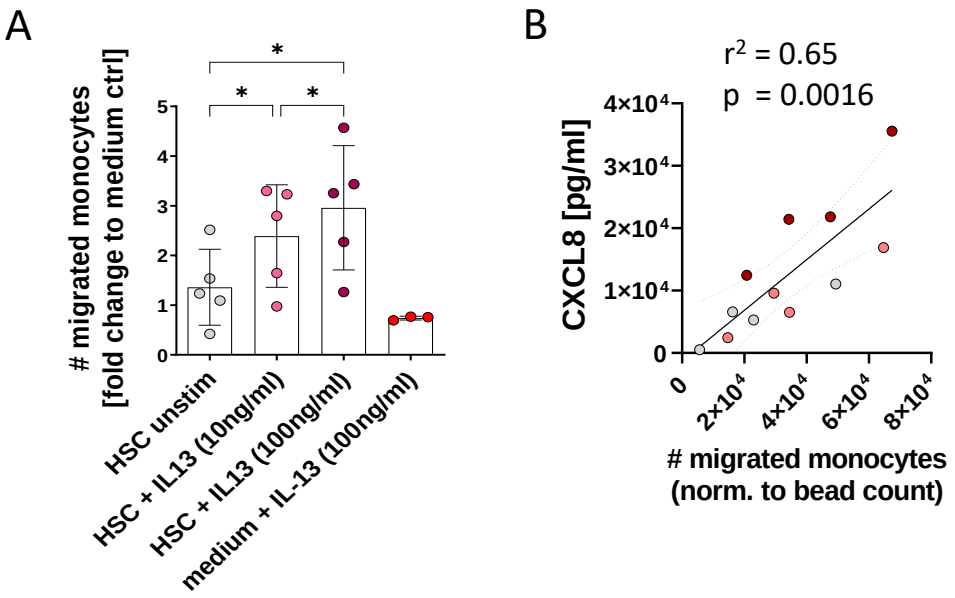

Fig. 3.18 Mechanistic impact of CXCL8 secretion by HSCs on monocyte migration **(A)** Number of monocytes migrated through 5µm transwell pores towards indicated HSC supernatant after 4 h of incubation. Indicated fold change calculated by normalization to medium control without HSCs. **(B)** Pearson correlation of number of transmigrated monocytes and CXCL8 concentration in corresponding HSC supernatants. Statistical significance determined by ANOVA (A) corrected for multiple comparisons by controlling FDR. Error bars showing SD.

3.6 Investigation of the emergence of IL-13+ liver ILC3

Given the tissue-specific enrichment of IL-13-producing liver ILC3 and their implications for the progression of fibrotic liver disease, subsequent research was focussed on the investigation of the mechanisms and circumstances, under which these newly characterized cells arise. A better understanding of these processes could provide insights on multiple hepatic diseases, in which an involvement of IL-13-mediated signaling has been reported (Gieseck et al., 2016; Liu et al., 2012; Shimamura et al., 2008).

As recently described, chimeric expression signatures with combined ILC3- and ILC2-like features can be observed when mature CRTH2+ ILC2 or CRTH2-CD117+ ILC progenitors are exposed to prolonged stimulation with IL-1β, IL-23 and TGFβ (Bernink et al., 2019; Golebski et al., 2019; Lim et al., 2017; Nagasawa et al., 2019). Of note, expression of all these ILC3-priming factors could be detected in the intrahepatic microenvironment, with increased levels of TGFβ in fibrotic or cirrhotic tissue (**Fig. 3.19A**). In addition, *IL13*+ ILC3

displayed elevated expression of the corresponding cytokine receptors when compared to *IL13*- ILC3 (**Fig. 3.19B**), indicating that this specific signaling potentially contributes to the differential properties of both cell types.

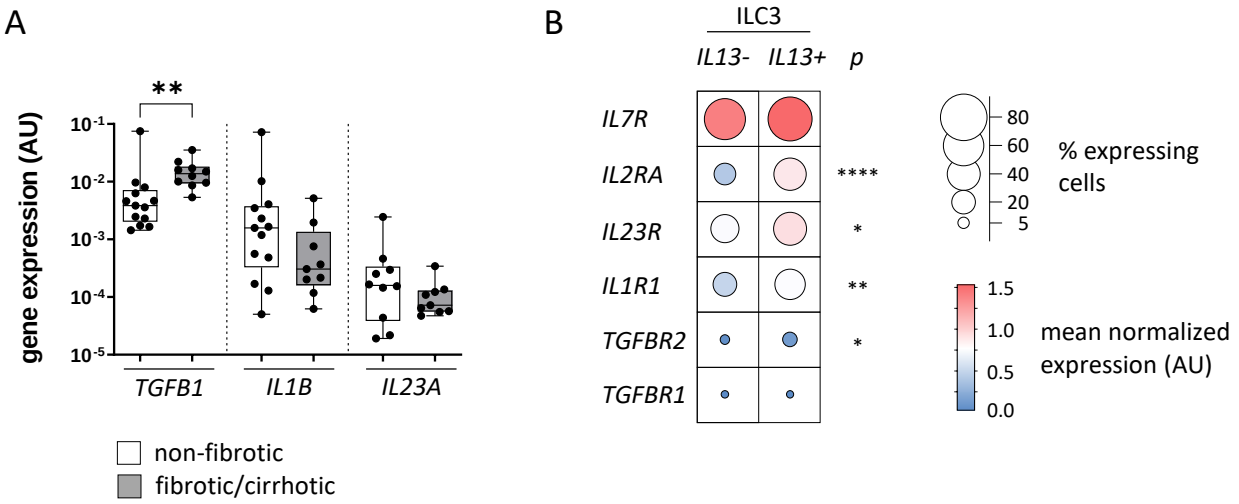

Fig. 3.19 Involvement of ILC3-priming signaling in hepatic tissue and *IL13*+ ILC3 (A) mRNA expression levels of indicated genes in tissue lysates from non-fibrotic vs fibrotic or cirrhotic liver specimen. **(B)** Expression of indicated cytokine receptors in *IL13*- and *IL13*+ liver ILC3, extracted from cleansed ILC scRNA-seq dataset. Bubble chart depicting percentage of expressing cells (area) and mean expression level (colour) in each cluster. Statistical significance determined by Mann-Whitney test (A, B).

In order to evaluate whether such a mechanism might be involved in the emergence of IL-13+ ILC3 in the human liver, the plasticity of intrahepatic ILCs was studied using an OP9-DL4 stromal cell-based *in vitro* culture system. OP9-DL4 feeder cells, which express the Notch ligands DLL1 and DLL4, are routinely employed in ILC plasticity studies (Klose et al., 2014; Lim et al., 2017; Scoville et al., 2016), given the critical requirement of Notch signaling for ILC differentiation (Chea et al., 2016; Golub, 2021; Zhang et al., 2017).

In this setting, sort-purified bulks of CRTH2+ and CRTH2-CD117+ liver ILCs were cultured in presence of IL-2, IL-7, IL-1β and IL-23 with or without TGFβ for 14 days, as described in previous reports (**Fig. 3.20A**) (Golebski et al., 2019). In CRTH2+ ILCs, exposure to this cytokine combination resulted in increased expression of CD117 but decreased expression of the ILC2-specific markers CRTH2 and KLRG1 and, thus, the induction of a prominent CRTH2-CD117+ ILC3-like subpopulation (**Fig. 3.20B**). This effect was particularly pronounced when TGFβ was added to the culture. Similar observations were

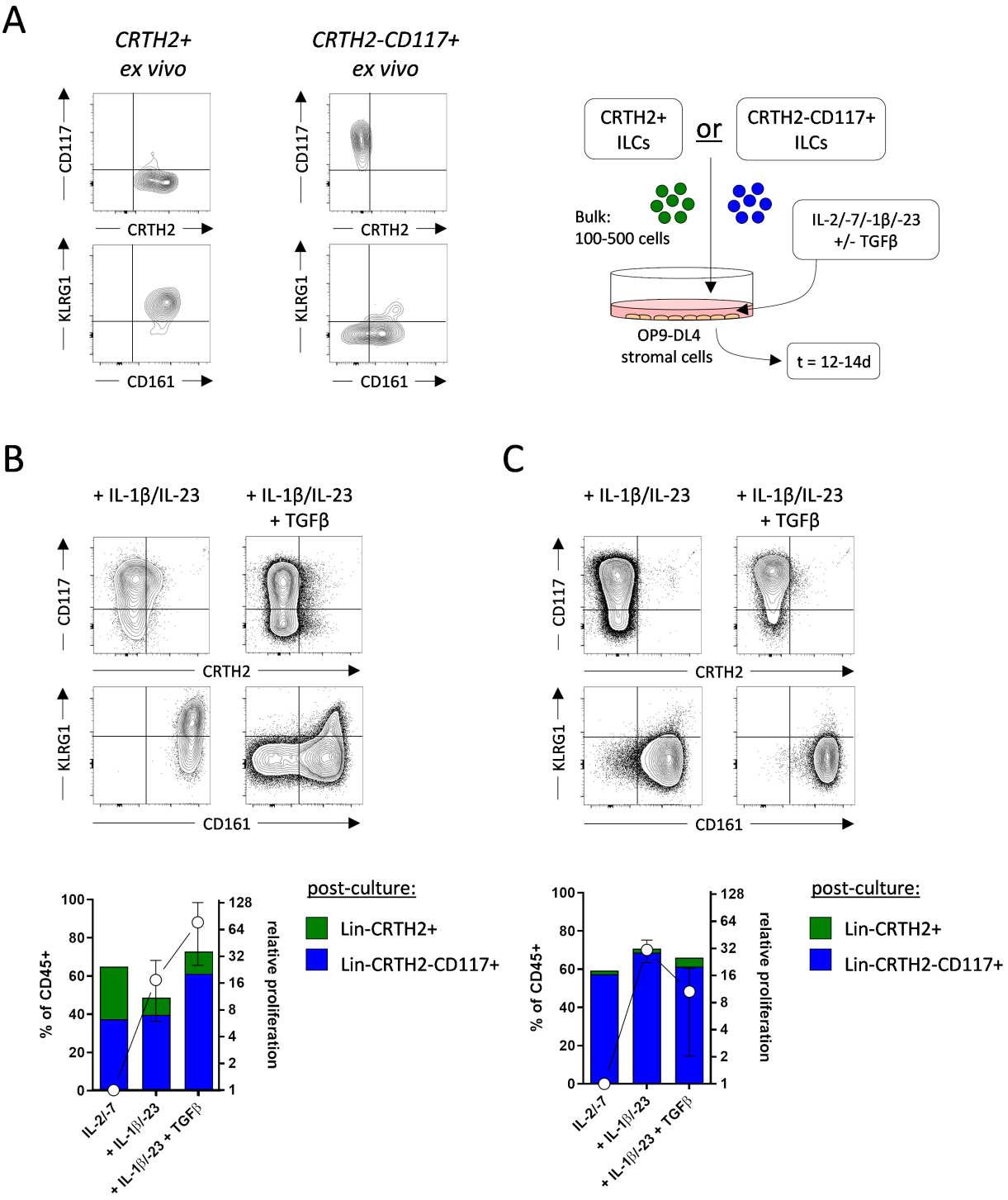

Fig. 3.20 Phenotypical analysis of bulk ILCs cultured under ILC3-priming conditions
(A) *Ex vivo* phenotype of sort-purified CRTH2+ (*left*) and CRTH2-CD117+ (*right*) liver ILCs and experimental design for subsequent bulk culture expansion assay. **(B)** Analysis of surface marker expression in expanded CRTH2+ and **(C)** CRTH2-CD117+ bulk ILCs after 14 d of culture in presence of indicated stimuli. Columns showing mean percentages of Lin-CRTH2+ and Lin-CRTH2-CD117+ cells identified post-culture (N = 7). Symbols and

lines indicate fold change in proliferation as relative to basal maintenance condition (IL-2, IL-7). Error bars showing SD.

made for cultured CRTH2-CD117+ ILCs, yet here CRTH2- and KLRG1-expressing cells were virtually absent post-culture (**Fig. 3.20C**). Overall, administration of the ILC3-priming cytokines IL-1β, IL-23 and TGFβ resulted in a marked increase of proliferation in comparison to basally maintained IL-2/IL-7-treated cells.

Supporting the concept of an ILC3-directed conversion, ILC2-derived CRTH2-CD117+ cells displayed decreased GATA3 expression in comparison to post-culture identified CRTH2+ cells, while in parallel RORγt expression was found to be increased (**Fig. 3.21A**). While the upregulation of RORγt even surpassed the level of expression observed in ILC3-derived CRTH2-CD117+ cells, GATA3 expression remained to be significantly higher in ILC2-derived cells. This finding indicated that, while cultured ILC2 are converting towards an ILC3-like phenotype, they might retain “ex-ILC2”-like properties.

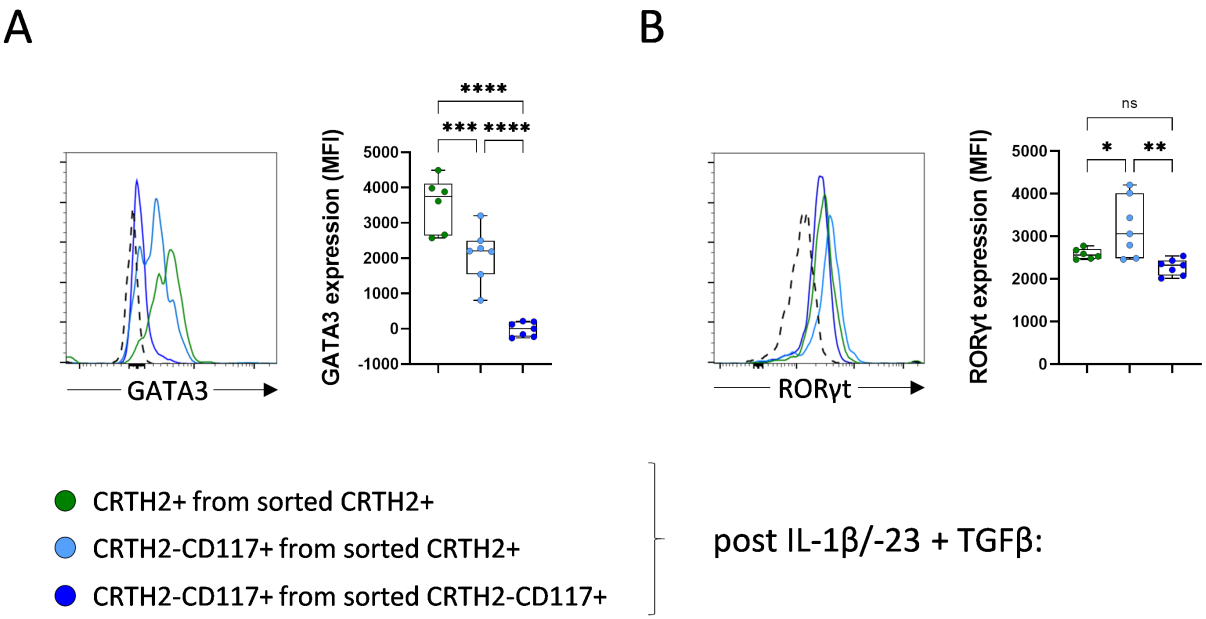

Fig. 3.21 Transcription factor profile of bulk cultured ILCs (A) Expression level (MFI) of GATA3 and **(B)** RORγt in post-culture identified subsets arising from indicated precursor cell type under influence of IL-2, IL-7, IL-1β, IL-23 and TGFβ. Statistical significance determined by ANOVA (A, B) corrected for multiple comparisons by controlling FDR.

Despite this ILC3-directed conversion of cultured CRTH2+ and CRTH2-CD117+ ILCs, elevated levels of IL-13 could be detected in the supernatant of both cell types, when expanded in presence of IL-1β, IL-23 and TGFβ (**Fig. 3.22A**). To analyse the functional capacities of differentiated bulk ILCs in more detail, cells were re-stimulated with PMA/Ionomycin upon culture harvest and the frequency of cytokine-producing cells among gated subsets was determined by flow cytometry (**Fig. 3.22B**). While most of the

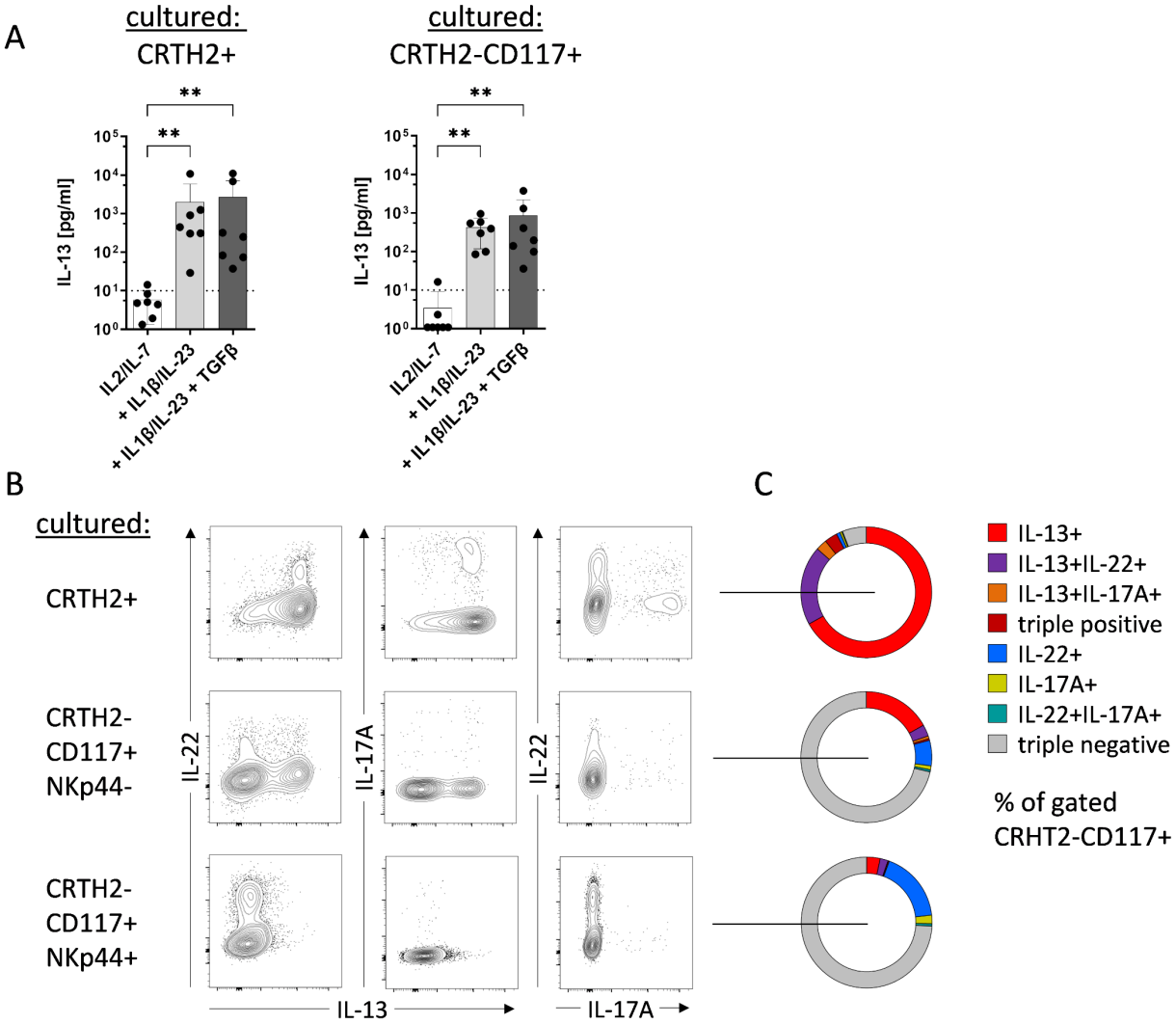

Fig. 3.22 Cytokine production profile of bulk cultured ILCs (A) Concentration of IL-13 in supernatant of indicated bulk ILC cultures after 10 d of treatment (N = 7). **(B)** Analysis of cytokine production in Lin- progeny of indicated ILC subset after culture in presence of IL-2, IL-7, IL-1β, IL-23 and TGFβ and subsequent re-stimulation with PMA/Ionomycin. **(C)** Percentage of IL-13, IL-17A and IL-22 (co-) expressing cells detected among post-culture identified Lin-CRTH2-CD117+ cells of analysed bulks of CRTH2+ (N = 4), NKp44-CRTH2-

CD117+ (N = 5) or NKp44+CRTH2-CD117+ (N = 3) ILCs. Statistical significance determined by Kruskal-Wallis test (A) corrected for multiple comparisons by controlling FDR. Error bars showing SD.

ILC2-derived ILC3-like cells displayed a robust induction of IL-13 production, this capacity could only be observed in the progeny of the NCR- subset of cultured CRTH2-CD117+ ILCs (**Fig. 3.22C**). Cultured NKp44+ ILC3 on the other hand mainly gave rise to IL-22-producing cells, outlining potential subset-specific limitations of ILC plasticity.

To further dissect these differences in the potential to generate IL-13+ ILC3-like cells and to exclude any bias due to bulk contaminations, CRTH2+ ILC2 and NCR-CRTH2-CD117+ ILC3 were subsequently cultured and studied in clonal assays. To avoid cultivation of pre-differentiated *ex vivo* IL-13+CRTH2-CD117+ ILCs, cells were sort-purified from peripheral blood, where only marginal numbers of this cell type had been observed (**Fig. 3.7A**).

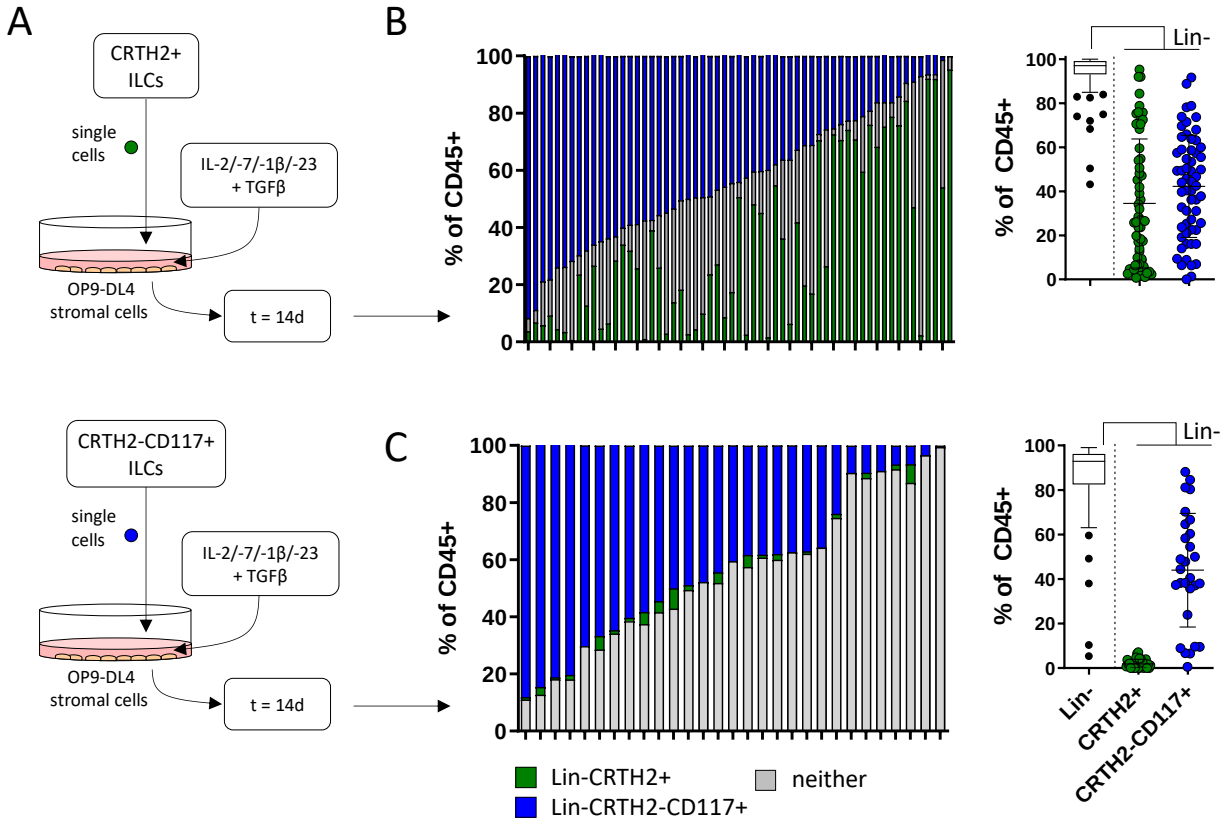

Fig. 3.23 Phenotypical analysis of clonally expanded ILCs (A) Experimental design for clonal expansion of single CRTH2+ (*top*) or CRTH2-CD117+ (*bottom*) ILCs under influence of IL-2, IL-7, IL-1β, IL-23 and TGFβ. **(B, C)** Percentage of Lin-CRTH2+ and Lin-

CRTH2-CD117+ cells identified post-culture among total CD45+ cells in indicated subset. Error bars showing SD.

Phenotypic analysis of the clonal progeny confirmed the observations made in bulk culture experiments, indicating an equally distributed potential for the generation of Lin-CRTH2-CD117+ among cultured CRTH2+ and CRTH2-CD117+ ILCs upon exposure to IL-1β, IL-23 and TGFβ (**Fig. 3.23A, B**).

IL-13 production appeared to be preserved in virtually all cultured CRTH2+ clones, whereas among NCR-ILC3-derived clones only some acquired this capacity (**Fig. 3.24A**).

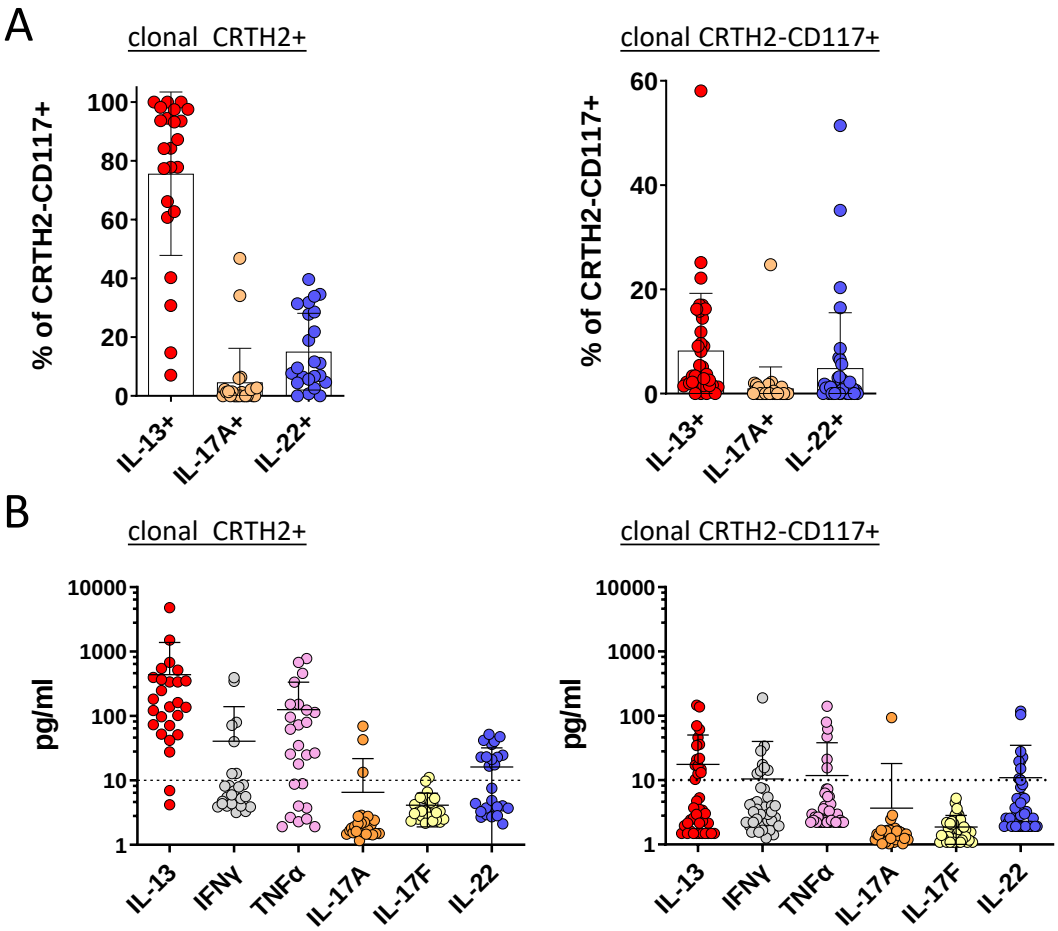

Fig. 3.24 Cytokine production and secretion in clonally expanded ILCs (A) Percentage of cytokine-positive cells among post-culture identified CRHT2-CD117+ cells arising from indicated cell type. **(B)** Concentration of indicated cytokines in supernatant of clonally expanded CRTH2+ or CRTH2-CD117+ ILCs. Assessment of cytokine production and secretion performed after re-stimulation with PMA/Ionomycin. Error bars showing SD.

In addition, both frequency of IL-13+ cells as well as their quantitative output was found to be distinctively higher in clonally expanded ILC2 (**Fig. 3.24B**). The extended cytokine profile on the other hand was found to be qualitatively similar among CRTH2+ and NCR- ILC3-derived clones, including secretion of TNFα, IL-22 and IFNγ but almost no IL-17, which was in contrast to observations from previous reports (Golebski et al., 2019).

Although the progeny of both cultured cell types displayed certain similarities to IL-13-producing intrahepatic ILC3, expression of critical ILC3-defining markers such as NKp44 and CD56 was lacking (**Fig. 3.25A**). While cultured NCR-ILC3 did at least show expression of these markers, no co-expression with IL-13 could be observed (**Fig. 3.25B**).

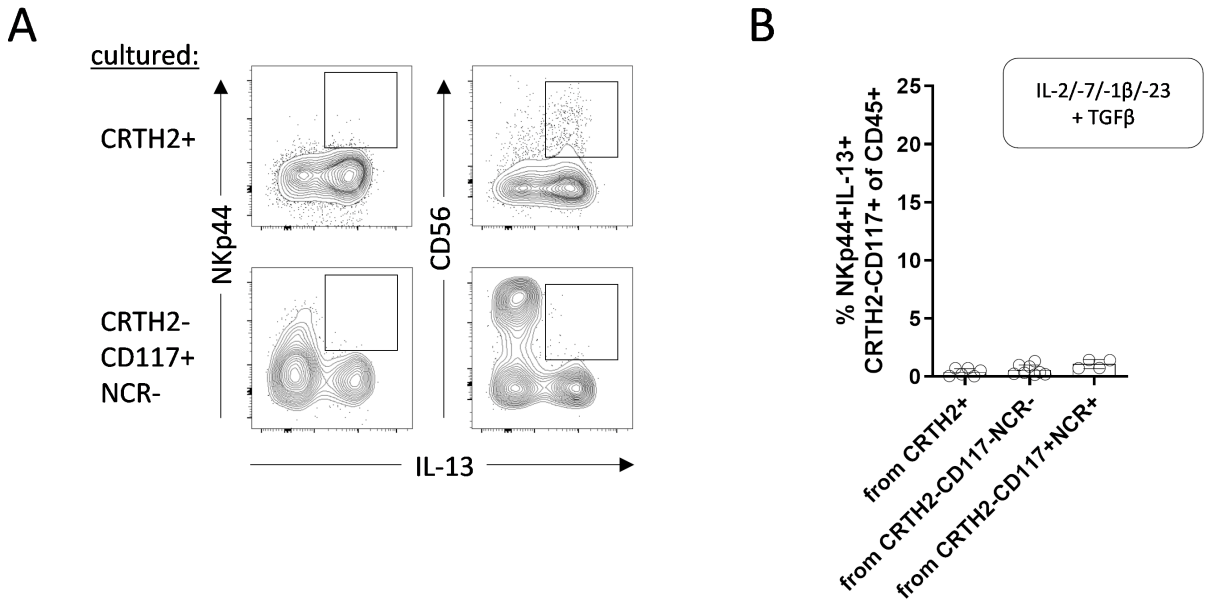

Fig. 3.25 Co-expression of IL-13 and ILC3-restricted markers in bulk cultured ILCs
(A) Co-expression of IL-13 with NKp44 or CD56 among Lin- cells arising from IL-2/IL-7/IL-1β/IL-23/TGFβ-cultured bulk ILCs after re-stimulation with PMA/Ionomycin. **(B)** Percentage of IL-13+NKp44+ double-positive ILC3-like cells detected among progeny of indicated subsets. Error bars showing SD.

Therefore, the initial experimental set-up was modified in order to enhance the ILC3-directed conversion of CRTH2+ and NCR-CRTH2-CD117+ ILCs and to achieve a more consistent phenotypical reflection of IL-13+ liver ILC3. Given the acknowledged role of AhR receptor signaling in the stabilization of ILC3 identity and regulation of NKp44 expression (Hughes et al., 2014; Li et al., 2018; Moreno-Nieves et al., 2018), culture

conditions were expanded for the well-studied AhR agonist 6-formylindolo[3,2-b]carbazole (FICZ) for this purpose.

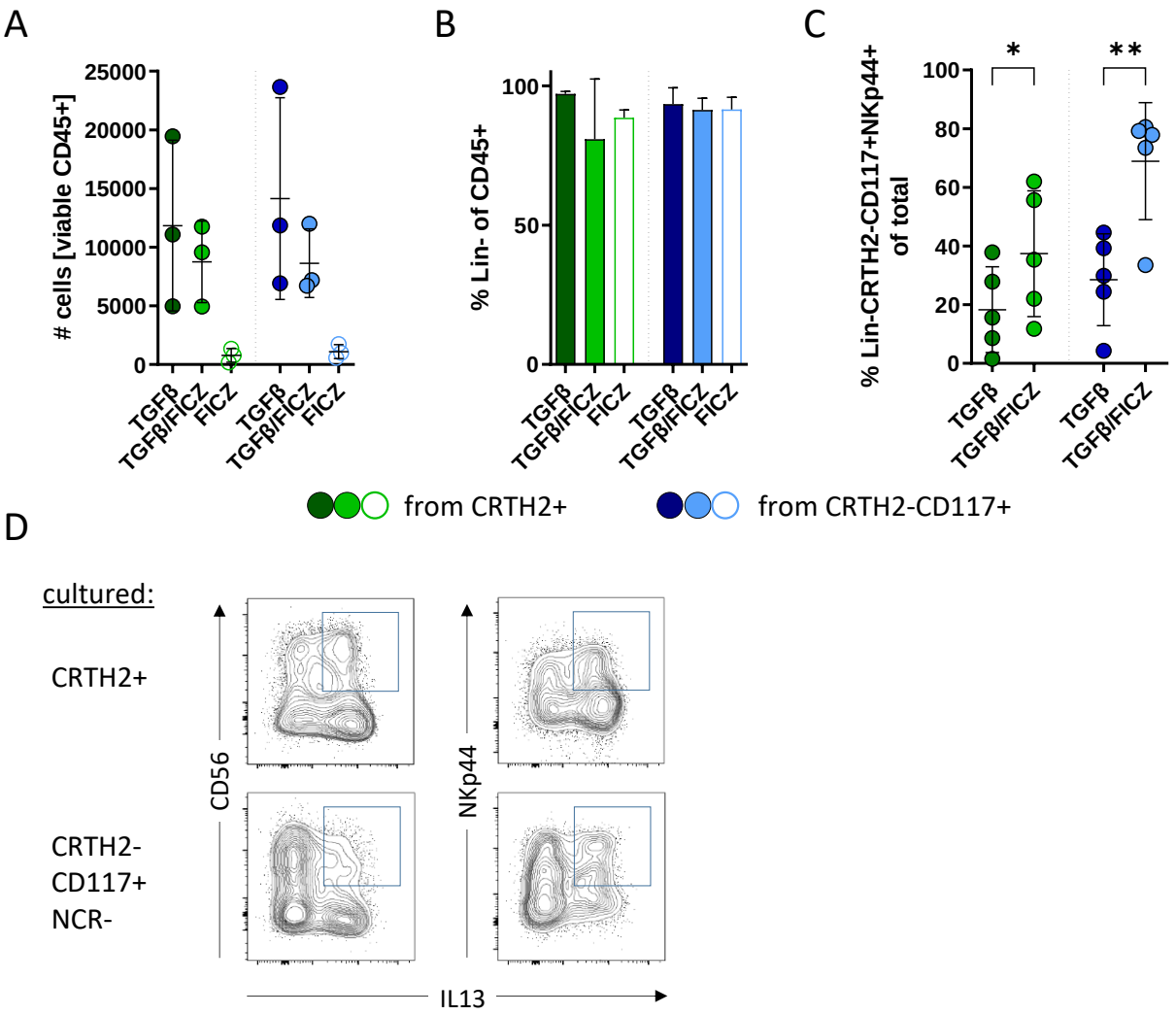

Fig. 3.26 Impact of FICZ supplementation on phenotype of bulk cultured ILCs (A) Number of viable CD45+ lymphocytes detected in bulk cultures of indicated subset after treatment with original stimuli ("TGFβ"), TGFβ substitution by FICZ at D7 ("TGFβ/FICZ") or full replacement of TGFβ with FICZ ("FICZ"). **(B)** Percentage of Lin- cells among CD45+ progeny of analysed culture samples. **(C)** Percentage of ILC3-like cells (Lin-CRTH2-CD117+NKp44+) arising from TGFβ- or TGFβ/FICZ-cultured indicated ILC subsets. **(D)** Co-expression of IL-13 with NKp44 or CD56 among Lin- cells arising from TGFβ/FICZ-cultured bulk ILCs after re-stimulation with PMA/Ionomycin. Statistical significance determined by ANOVA (C) corrected for multiple testing by controlling FDR. Error bars showing SD.

Since mere addition of FICZ drastically impaired cell proliferation of bulk cultured CRTH2+ and NCR-CRTH2-CD117+ ILCs (**Fig. 3.26A**), a primary expansion period with the initial stimuli was maintained, before substituting TGFβ with FICZ for the second half of the culture. The proportion of Lin- cells arising from these culture conditions remained unaltered by the addition of FICZ, indicating an unchanged stable generation of non-NK ILCs (**Fig. 3.26B**). As intended TGFβ/FICZ-treated ILC bulks did not only display increased proportions of NKp44+CRTH2-CD117+ cells after culture (**Fig. 3.26C)**, but also gave rise to IL-13+NKp44+/CD56+ ILC3-like cells (**Fig. 3.26D**), thus more closely resembling intrahepatic IL-13+ ILC3.

In order to specifically evaluate the effects of FICZ in comparison to TGFβ-only cultures, clone-splitting experiments were performed next, enabling a setting-dependent comparison of individual clones. In this setting, the progeny of single clones was divided

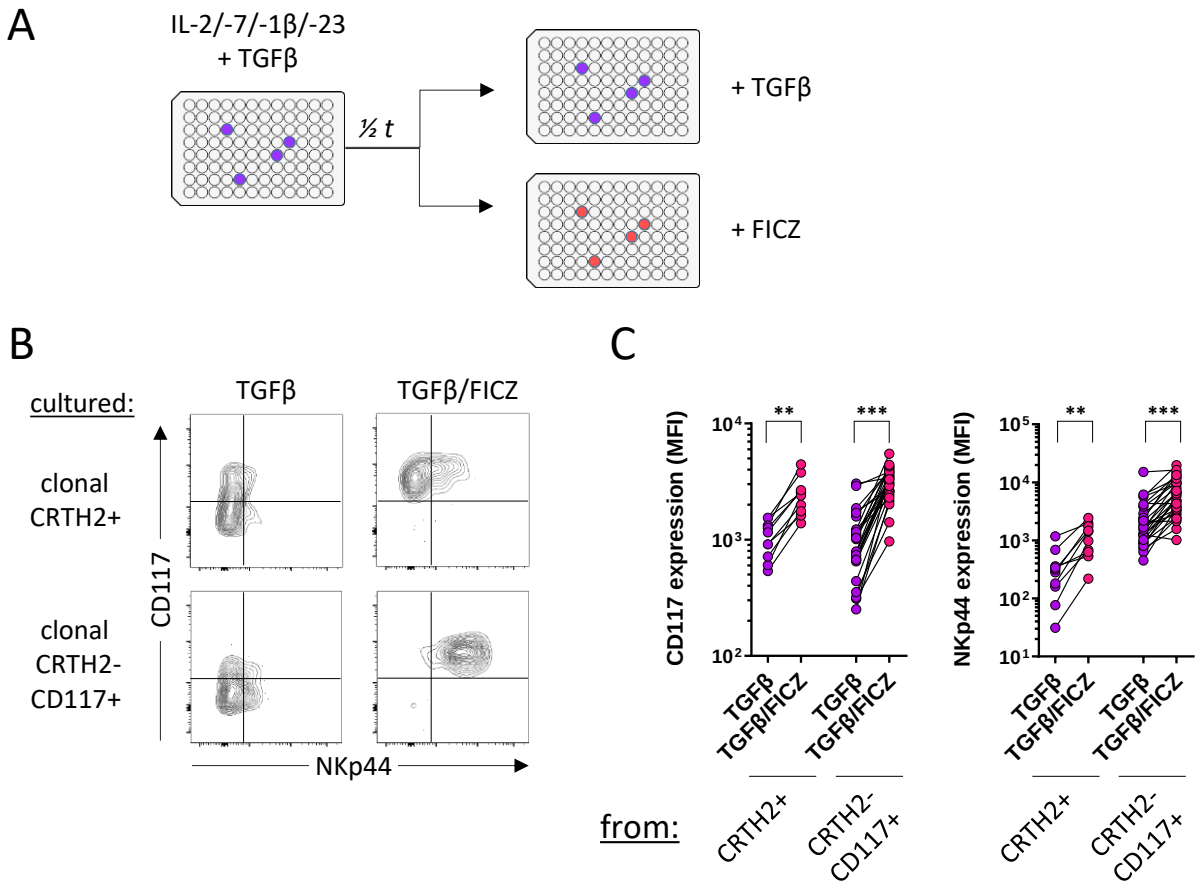

Fig. 3.27 Analysis of FICZ-specific effects in clone splitting experiments (A) Experimental design for the paired analysis of setting-dependent effects on the

development of individual clones. **(B)** Co-expression of CD117 and NKp44 in matched clones treated with TGFβ or TGFβ/FICZ. (C) Paired analysis of CD117 and NKp44 expression levels (MFI) in clones derived from indicated ILC subset and culture setting. Statistical analysis determined by Wilcoxon test (C).

after 7 days of the primary expansion period and the two batches were subsequently treated either with TGFβ or FICZ for the following culture time (**Fig. 3.27A**). This paired analysis precisely revealed that ligation of the AhR caused the significant upregulation of CD117 and NKp44 in TGFβ/FICZ-cultured clones (**Fig. 3.27B, C**).

Accordingly, the enhanced generation of CRTH2-CD117+ ILC3-like cells observed in TGFβ/FICZ-treated bulks was also found among clonally expanded single CRTH2+ and

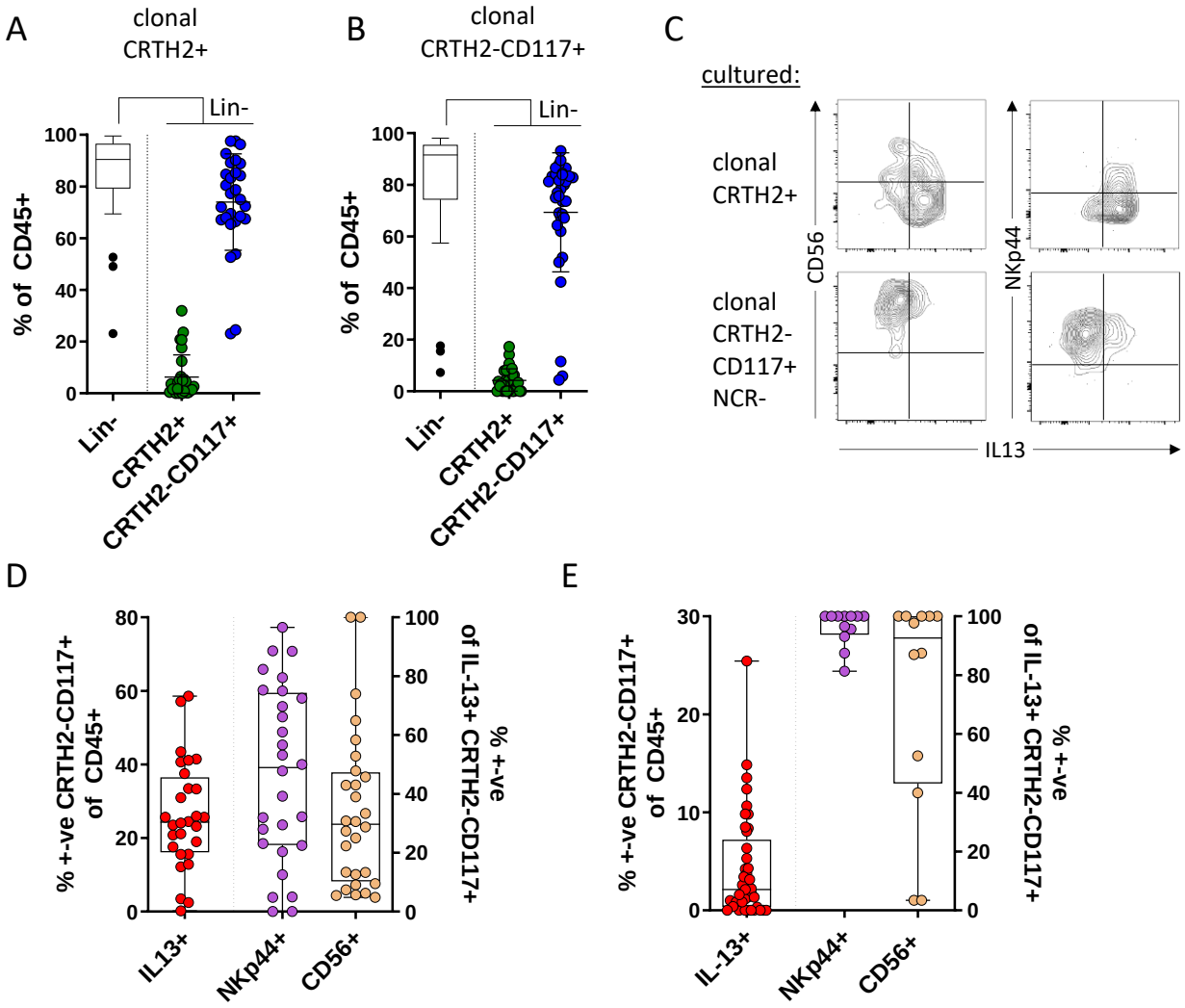

Fig. 3.28 Phenotypical and functional analysis of TGFβ/FICZ-cultured clonal ILCs

(A) Percentage of Lin-, Lin-CRTH2+ and Lin-CRTH2-CD117+ cells identified post-culture among total CD45+ cells arising from TGFβ/FICZ-treated clonal CRTH2+ and **(B)** CRTH2-CD117+ ILCs. **(C)** Co-expression of IL-13 with NKp44 or CD56 among Lin- cells arising from analysed clones after re-stimulation with PMA/Ionomycin. **(D)** Percentage of IL-13+ CRTH2-CD117+ cells among progeny of clonal CRTH2+ and **(E)** CRTH2-117+ ILCs and corresponding percentages of NKp44+ and CD56+ cells. Error bars showing SD.

CRTH2-CD117+ ILCs (**Fig. 3.28A, B**), as was the emergence of IL-13+NKp44+/CD56+ co-expressing cells (**Fig. 3.28C**). Of note, cultured CRTH2+ ILCs appeared to be more potent in generating IL-13-producing cells, whereas among cultured CRTH2-CD117+ ILCs a stronger induction of NKp44 and CD56 could be detected (**Fig. 3.28.D, E**), once again outlining the differential plastic capacities of both cell types.

In contrast to the TGFβ/FICZ-cultured single CRTH2+ ILC2, only some CRTH2-CD117+ ILC clones acquired the capacity to produce IL-13, which reflected the observations made in culture settings without FICZ supplementation (**Fig. 3.24A, B**). In order to evaluate if this variability was due to the acknowledged subset-intrinsic heterogeneity of CRTH2-CD117+ ILCs (Lim et al., 2017), a retrospective phenotypical analysis of the cultured precursor cells was conducted. By indexing of single cells upon sort-purification, these could be stratified for the expression of specific surface markers afterwards. Using this approach, IL-13-expressing cells were found to predominantly arise from KLRG1-expressing CRTH2-CD117+ ILCs (**Fig. 3.29A**), a cell type, which has been previously described to comprise ILC2-skewed progenitors (Nagasawa et al., 2019).

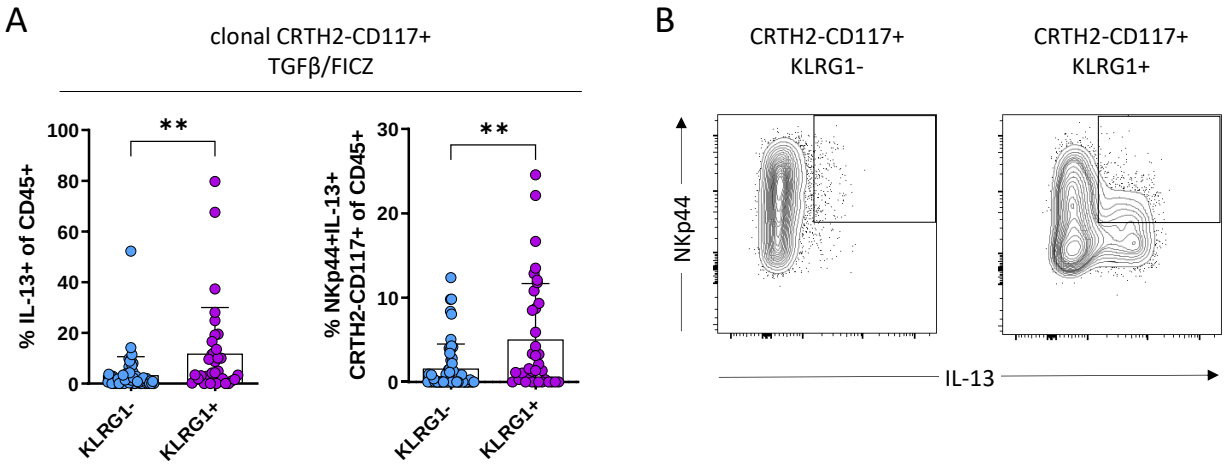

Fig. 3.29 Retrospective profiling of IL-13+ cells arising from CRTH2-CD117+ ILCs **(A)** Percentage of Lin-IL-13+ (*left*) and IL-13+ ILC3-like cells (*right*) detected among

TGFβ/FICZ-cultured CRTH2-CD117+ ILC clones after re-stimulation with PMA/Ionomycin, stratified for KLRG1 expression. **(B)** Co-expression of IL-13 and NKp44 among Lin- progeny of indicated ILC subset cultured under TGFβ/FICZ. Statistical significance determined by Mann-Whitney test (A). Error bar showing SD.

This finding could also be observed in a comparative bulk culture analysis of sort-purified KLRG1+ versus KLRG1- CRTH2-CD117+ ILCs (**Fig. 3.29B**), validating the retrospective identification of cultured clones.

Since KLRG1 expression is predominantly, albeit not exclusively, observed in mature ILC2, further post-culture analyses were performed to exclude a potential inclusion of misidentified ILC2 among sort-purified clonal KLRG1+CRTH2-CD117+ ILCs. For this purpose, the expression of GATA3 by cultured clonal CRTH2+ and CRTH2-CD117+ ILCs was analysed, given the significant differences previously observed between both cell types (**Fig. 3.21A**). Here, the progeny of KLRG1-expressing CRTH2-CD117+ ILCs could be clearly distinguished from ILC2-derived cells and instead displayed a similar pattern as observed in cultured KLRG1-CRTH2-CD117+ ILCs (**Fig. 3.30A**).

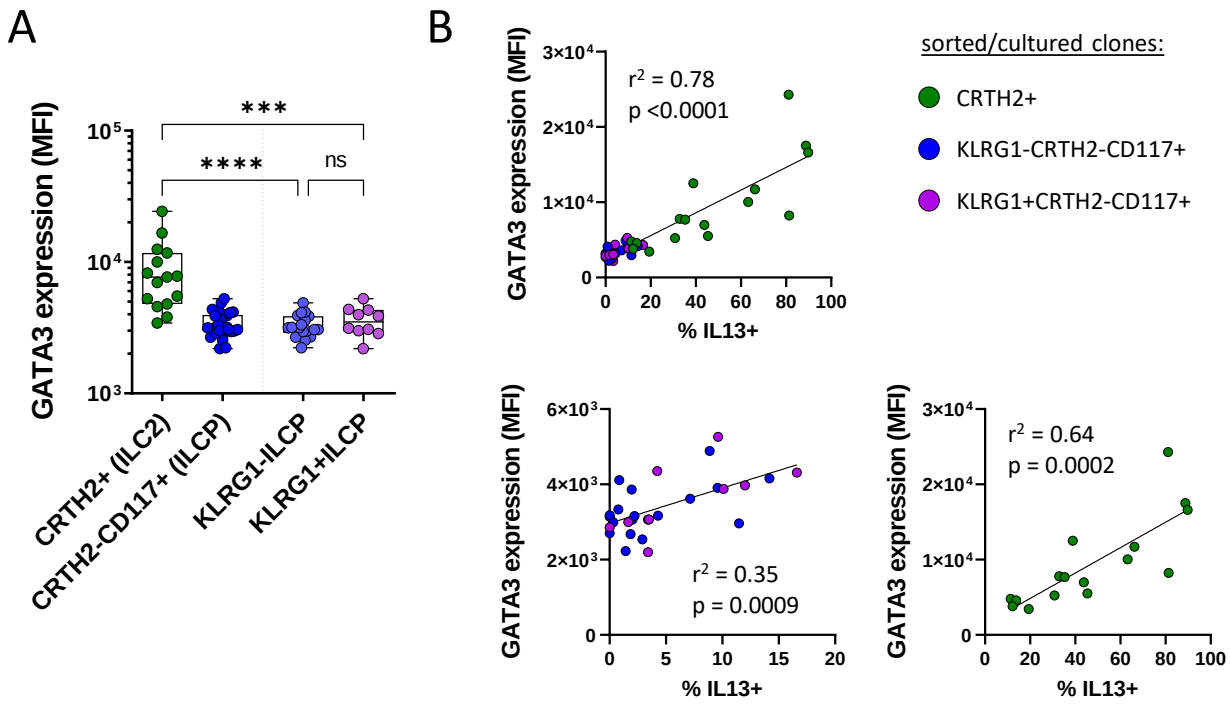

Fig. 3.30 Transcription factor analysis in TGFβ/FICZ-cultured ILC subsets (A) Expression level (MFI) of GATA3 in progeny of indicated clonal ILCs after TGFβ/FICZ culture. **(B)** Pearson correlation of GATA3 expression level and percentage of IL-13+

among total CD45+ cells in indicated cultured ILC subsets. Statistical significance determined by Kruskal-Wallis test (A) corrected for multiple testing by controlling FDR.

This finding supported the progenitor-like phenotype of KLRG1+CRTH2-CD117+ ILCs as well as their distinction from CRTH2+ ILC2. Interestingly, GATA3 expression correlated with the percentage of IL-13+ cells arising from all cultured subsets, indicating a general role of this transcription factor in the regulation of IL-13 production by ILCs (**Fig. 3.30B**). Taken together, these data obtained in culture experiments suggested that a balanced engagement of ILC2-specific (GATA3) and ILC3-stabilizing (AhR) transcription factors might be important for the development of IL-13+ ILC3-like cells.

Given the observed differences between IL-13+NKp44+CRTH2-CD117+ cells originating from CRTH2+ and KLRG1+CRTH2-CD117+ ILCs, a detailed transcriptional analysis was performed next, to evaluate if any or both cultured cell types in fact reflected the transcriptional signature of intrahepatic *IL13*+ ILC3. Isolation of viable IL-13+ cells for mRNA analysis was achieved by the use of an IL-13-secretion detection and enrichment assay after sort-purifying Lin-CRTH2-CD117+NKp44+ cells from TGFβ/FICZ-cultured bulks of CRTH2+ or KLRG1+CRTH2-CD117+ ILCs (**Fig. 3.31A,** *also see* **2.2.12**). Multiple ILC2- and ILC3-specific signature genes (Björklund et al., 2016) were selected for analysis and their expression was compared to the transcriptional profile of stimulated *ex vivo* CRTH2+ ILC2, *ex vivo* CRTH2-CD117+ ILC3 and the intrahepatic *IL13*+ ILC2 and ILC3 (**Fig. 3.31B**). Cells derived from CRTH2+-progenitors indeed showed a decreased expression of some ILC2-related genes, however their mean score of expression was significantly higher than in *ex vivo* ILC3 or cultured KLRG1+CRTH2-CD117+ ILCs (**Fig. 3.31C**, *upper panel*). In parallel, only a minor upregulation of single ILC3-related genes was detected in these cells (*lower panel*). This was in strong contrast to cells derived from KLRG1+CRTH2-CD117+ ILCs, which displayed a consistent ILC3-like expression pattern, thus resembling the molecular phenotype of intrahepatic *IL13*+ ILC3.

In summary, these findings indicated that intrahepatic IL-13-producing ILC3 most likely arise from KLRG1-expressing CRTH2-CD117+ ILC precursors under the given environmental conditions and not from converted mature ILC2.

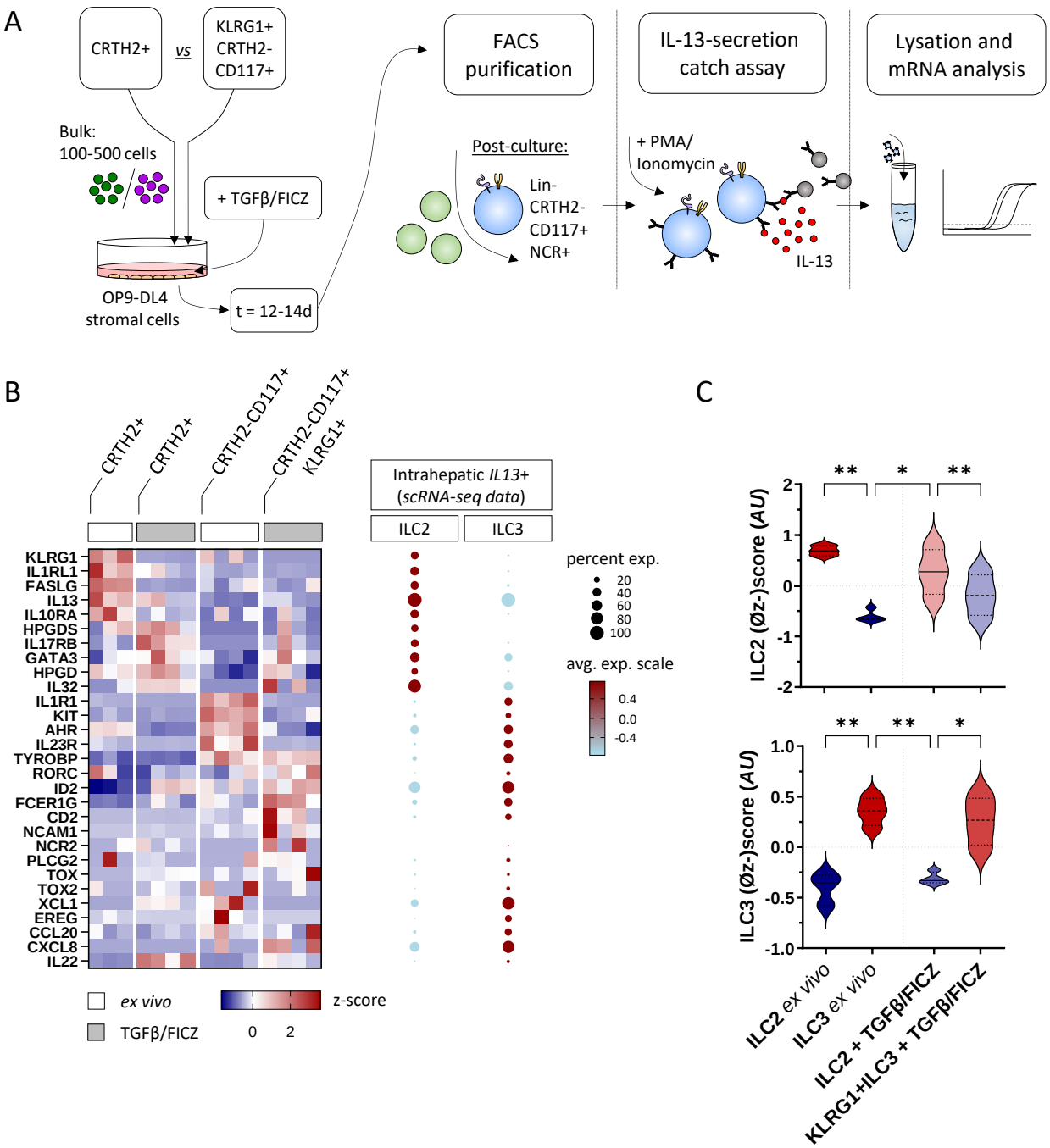

Fig. 3.31 Transcriptional profiling of IL-13+ ILC3-like cells derived from different ILC subsets (A) Experimental design for the isolation of viable IL-13-secreting ILC3-like cells arising from indicated bulk ILC subset after TGFβ/FICZ culture. **(B)** Heatmap depicting mRNA expression levels of indicated genes (z-score normalized) in *ex vivo* stimulated CRTH2+ or CRTH2-CD117+ ILCs (*white blocks*) or post-culture isolated IL-13+ ILC3-like cells (see A) derived from CRTH2+ or KLRG1+CRTH2-CD117+ ILCs (*grey blocks*). Bubble Chart showing corresponding expression signature of intrahepatic *IL13*+ ILC subset, indicating percentage of expressing cells (area) and mean expression (colour). **(C)** Mean expression of z-scores of all ILC2-related (*top*) and ILC3-related (*bottom*)

transcripts in analysed *ex vivo* or post-culture purified ILC subsets. Statistical significance determined by mixed effects analysis (C) corrected for multiple testing by controlling FDR.

Finally, this hypothesis was in line with the tissue-specific enrichment of KLRG1+ ILC precursors in the human liver in comparison to tonsils or colon mucosa (**Fig. 3.32A, B**). Among circulating ILCs even higher proportions were detectable, potentially corresponding to the large reservoir of progenitor ILCs in peripheral blood (Lim et al., 2017).

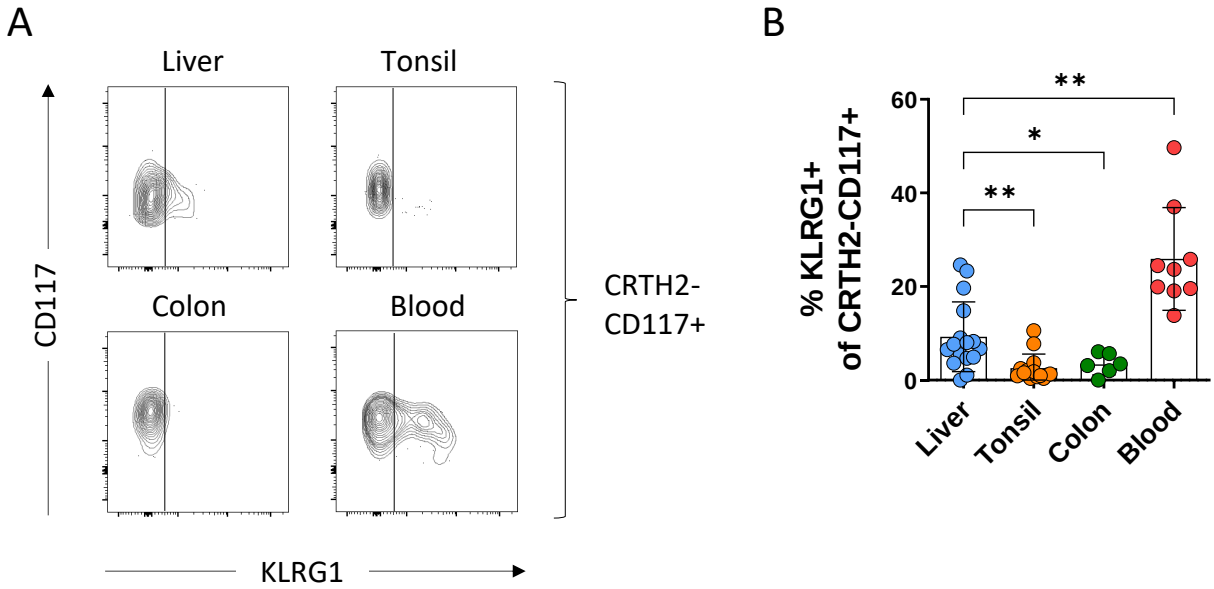

Fig. 3.32 Frequency of KLRG1-expressing progenitors in different human tissues (A, B) Percentage of KLRG1+ cells among CRTH2-CD117+ ILCs in liver, tonsil, colon and peripheral blood. Statistical significance determined by Kruskal-Wallis test (B), corrected for multiple comparisons by controlling FDR if applicable. Error bars showing SD.

4. Discussion

Over the past decade, the appreciation of innate lymphoid cells as important regulators of homeostatic and immunologic processes has steadily increased alongside the accumulating evidence for their involvement in numerous inflammatory diseases (Castellanos and Longman, 2019; Ebbo et al., 2017). Their extensive investigation has led to a better understanding of a wide variety of elusive pathologies, which are typically characterized by persistent, dysregulated immune responses, such as Crohn's disease, asthma or psoriasis (Bartemes et al., 2012; Bernink et al., 2013; Forkel et al., 2019; Fuchs et al., 2013; Smith et al., 2016; Teunissen et al., 2014).
In the human liver however, the overall involvement of ILCs in physiological and pathological settings has remained scarcely studied and poorly understood, despite the importance of inflammatory processes in hepatic fibrogenesis and the predominant role of the local innate immune system (Chen and Tian, 2021). Data obtained in mouse models strongly suggest that ILCs contribute to the progression of liver fibrosis (Marvie et al., 2009; Mchedlidze et al., 2013), yet human studies have reported inconsistent results and were primarily focussed on minor subsets (Forkel et al., 2017; Jeffery et al., 2017).

The aim of this project was to significantly extend the current knowledge of human intrahepatic ILCs, to resolve existing conflicts in the published literature and to assess potential tissue-specific features as well as implications of ILCs in chronic fibrotic liver disease.

The present study demonstrates that the human intrahepatic ILC pool is characterized by a predominance of tissue-resident ILC3 and in addition identifies a so far unrecognized cell type with an ILC3-like phenotype and the capacity to produce the ILC2-specific cytokine IL-13. These cells were specifically enriched in the human liver where they represented the dominant fraction of IL-13-producing ILCs, whose abundance and influence might have been drastically underestimated up to date. Furthermore, this study provides first evidence for an involvement of this cell type in hepatic fibrogenesis and additionally outlines its functional impact on the liver microenvironment by characterizing its pro-inflammatory influence on HSCs. Moreover, the identification of KLRG1-expressing ILCPs as putative progenitors of intrahepatic IL-13+ ILC3-like cells marks a novel

developmental trajectory, reinforcing our understanding of ILCs as highly versatile branch of the innate immune system.

These key findings will be discussed in the following section, addressing their significance and implications in the context of our current knowledge, limitations as well as future directions for further research.

4.1 Characterization of human intrahepatic ILCs

4.1.1 The human intrahepatic ILC pool is dominated by tissue-resident NCR- ILC3

Although several reports have previously addressed the composition and functionality of the intrahepatic ILC pool, its overall characterization remained an important aspect of this project. This is primarily due to the limited availability of studies which have investigated human liver-resident ILCs and the conflicting findings they have reported.
This study demonstrates that a majority of over 70 % of ILCs in the human liver belong to the subset of CRTH2-CD117+ ILC3, supporting one of the first reports on this subject by Forkel et al. (2017). This finding had been questioned by another study, in which Jefferey et al. (2017) have described a predominance of CRHT2-CD117- ILC1 among intrahepatic ILCs. In their work however, Jefferey et al. did not include any markers to identify $CD3^{low/-}$ T cells in their lineage definition, as for example TCRαβ or TCRγδ. This renders their identification of ILC1, which were merely characterized by the lack of CRTH2 and CD117 expression, prone to contamination with CD127-expressing T cells, potentially causing an artificial inflation of the ILC1 population. Flow cytometric analyses, which can only account for a limited number of markers, are particularly affected by this bias as it has been demonstrated in detailed transcriptional studies (Simoni et al., 2017). Given the low frequency of ILCs and their similarity to T cells, even slight contaminations can result in a drastic distortion of the assessed ILC frequencies. Consequently, the present study as well as the work of Forkel and colleagues have most likely provided a more accurate depiction of the intrahepatic ILC pool, due to a more comprehensive exclusion of non-ILC contaminants.

Despite these relations in ILC frequency, previous reports on liver ILCs have been mainly focussed on phenotype and function of IL-33-responsive ILC2 (Forkel et al., 2017; Jeffery

et al., 2017; Marvie et al., 2009; Mchedlidze et al., 2013). As these and the current study have shown, such analyses are neglecting over 90 % of tissue-resident non-NK ILCs since ILC2 account for only 7 % of them on average in the human liver. In contrast, the comparative compartment analysis conducted in this project indicates that one of the most prominent and major distinguishing features of the intrahepatic ILC pool is the characteristic enrichment of tissue-resident NCR-negative ILC3. In their report, Forkel et al. speculate that these NCR- ILC3 mainly constitute a pool of immature ILC progenitors, similar to their circulating counterparts in peripheral blood (Lim et al., 2017). Accordingly, this hypothesis suggests that the main ILC subset in the human liver does not convey any primary functional influence, which might be supported by its low production of proto-typical ILC3-specific cytokines such as IL-22 and IL-17A.

However, this perception is contradicted by one of the major findings of the present study, the identification of intrahepatic ILC3-like cells as a substantial source of IL-13.

4.1.2 The human intrahepatic ILC pool contains an IL-13-producing ILC3-like cell

Given the predominance of ILC3 in the liver ILC pool, the previously unrecognized IL-13+ ILC3-like cells comprise the majority of IL-13-producing ILCs in the human liver. Considering the comparably low amounts of other cytokine-producing cells among intrahepatic ILCs, this implies that the functional impact of both ILC3 and ILC-derived IL-13 in the hepatic compartment might have been drastically underestimated up to date. Consequently, a central part of this study has been dedicated to further investigate this newly characterized subset and to enable a reliable classification within the ILC family.

Several lines of evidence indicate that the intrahepatic IL-13+ ILC3-like cells are profoundly different from conventional ILC2 and do not reflect any transitional or activated stage of ILC2 or even misidentified ILC2 with downregulated CRTH2 expression. This could be demonstrated on the basis of detailed proteomic and transcriptional analyses, which show that IL-13+ ILC3-like cells do not share the expressional pattern of IL-13+ ILC2 with regard to multiple reported ILC2-specific markers (Björklund et al., 2016). Of note, this also applies to transcription factors which are critically required for the ILC2-directed development of ILCs, such as GATA3 and RORα (Ferreira et al., 2021; Klein

Wolterink et al., 2013; Mjösberg et al., 2012). In addition, IL-13+ ILC3-like cells partially express CD56, which has been shown to be absent on ILC2 and ILC2-skewed progenitors and marks a delineating feature in the development of ILC precursors (Chen et al., 2018; Nagasawa et al., 2019). Hence, these data indicate an early divergence of IL-13+ ILC3-like cells from an ILC2-directed developmental pathway.
In return, they reflect a consistent ILC3-specific gene expression signature which supports their classification as ILC3-like cells. This transcriptional profile includes expression of important ILC3-defining features such as the key transcription factor *RORC*/RORγt (Lim and Di Santo, 2019), the maturation-associated marker NKp44 as well as functionally relevant genes such as *IL1R1*, *IL23R* and *AHR* (Sonnenberg, 2016). Of note, the presence of IL-13+ cells among both the NKp44- and NKp44+ subset indicates that IL-13 expression persists during several stages of maturation of liver ILC3. This is in contrast to other ILC3-specific cytokines such as IL-22, which is predominantly produced by the maturated subsets but undetectable in immature NKp44- ILC3 (Hoorweg et al., 2012; Lim et al., 2017).

Taken together, these data suggest that the capacity of ILCs to produce IL-13 might arise along several distinct developmental trajectories and is not solely restricted to ILC2, unlike currently assumed (Vivier et al., 2018). While this finding indicates a higher versatility of ILC3 in general, it also fundamentally affects the functional impact of liver ILCs in particular.

4.1.3 Intrahepatic IL-13-producing ILC2 and ILC3-like cells are functionally different

In this context, the functional differences between intrahepatic IL-13+ ILC2 and IL-13+ ILC3 mark another important aspect, as they imply distinct modes of activation for each cell type. Human liver ILC2 produce IL-13 in response to the ILC2-specific (Barlow et al., 2013; Han et al., 2017) stimuli IL-33 and TSLP, whereas intrahepatic ILC3 were unresponsive to this treatment, which is in line with their lack of *IL1RL1* (encoding IL-33R) expression. Of note, the ILC3-specific stimuli IL-1β and IL-23 also failed to induce IL-13 expression in ILC3 after overnight treatment. However, elevated levels of IL-13 could be detected in the supernatant of ILC3 cultured in presence of IL-1β and IL-23 together with

IL-2, IL-7 as well as Notch ligand-expressing feeder cells after 10 days of stimulation, indicating that a longer exposure or additional stimuli were required for this.
These findings suggest that the ILC-mediated secretion of IL-13 in the human liver can occur in response to different environmental stimuli and consequently in differential physiologic or pathologic settings. In addition to the alarmin-driven induction of IL-13 in ILC2, a persisting pro-inflammatory environment, which is a characteristic feature of chronic liver disease (Barbier et al., 2019; Koyama and Brenner, 2017; Tanwar et al., 2020), might trigger IL-13 production in intrahepatic ILC3.

Beyond that, the identification of a physiological stimulus of intrahepatic IL-13+ ILC3 supports the hypothesis that these in fact represent a functional cell type which are effectively engaged *in vivo* instead of a developmental artefact, which can only be induced upon pharmacological stimulation.

Of note, the combination of IL-2, IL-7, IL-1β, IL-23 and Notch ligands also triggers IL-13 production in ILC2 upon prolonged treatment, resulting in even higher quantities of secreted IL-13. While this is supporting reports about an additional mode of activation for ILC2 (Ohne et al., 2016), it also corresponds to the higher frequency of IL-13+ cells observed among CRTH2+ liver ILCs after PMA/Ionomycin treatment. This relatively higher IL-13 production capacity of ILC2 might be explained by their significantly increased expression of GATA3, which is one of the main regulatory elements of IL-13 expression (Kozuka et al., 2011; Lavenu-Bombled et al., 2002). Yet more importantly, it might also explain why previous studies have failed to identify the atypical IL-13+ ILC3. While in the work of Jefferey et al. (2017) the detection of IL-13-producing ILC3 might have been merely obscured by the analysis of a presumably inflated pool of CRTH2- ILCs, Forkel et al. (2017) in fact describe a minor secretion of IL-13 by ILC3. However, the authors neglect this finding since they observe that an equal number of isolated ILC2 produces significantly higher amounts of IL-13. Yet, such an experimental set-up does not reflect the actual composition of the intrahepatic ILC pool where the number of ILC3 exceeds that of ILC2 by the factor of ten. Further analyses would be required to evaluate the exact quantitative output of intrahepatic ILC2 and ILC3 with regard to the ratios found *in situ*. These however remain challenging since they either require large quantities of the rare

liver ILCs or highly sensitive assays to detect cytokine levels secreted by a small number of cells.

Further functional differences between IL-13+ ILC2 and ILC3 might be shaped by their extended cytokine production profiles. The transcriptional data presented in this work provides first insights at this point, showing that expression of cytokines such as *IL4* in ILC2 as well as *CXCL8* and *CCL20* in ILC3 in fact constitute major discriminating factors of both cell types. More functional analyses would be required to evaluate the contribution of these cytokines to the overall functional profile of intrahepatic ILCs. At this point, the acquired scRNA-seq data may present a valuable option for future investigation, as it represents one of the largest transcriptional datasets on single human liver ILCs currently available. Moreover, it allows for an effective evaluation of cytokine expression, due to the applied experimental approach which includes prior stimulation. This is in contrast to previously published studies, which have focussed on *ex vivo* characterizations with minimal pre-treatment (Heinrich et al., 2021) and may provide only a limited overview of such activation-dependent expression features.

With regard to this project, the analytical focus on IL-13-producing ILC3 certainly represents one of its major limitations, since it is associated with a neglect of other intrahepatic ILC subsets and their cytokine output. Given the general functional versatility of tissue-resident ILCs (Meininger et al., 2020; Simoni and Newell, 2018), it is reasonable to assume that the full spectrum of ILC-mediated effects in the human liver is conveyed by additional factors.

Nevertheless, the influence of IL-13-producing ILC3 in the human liver might be of central importance and particularly relevant in chronic liver disease given the following aspects: First, IL-13+ ILC3 make up a substantial fraction of all cytokine-producing intrahepatic ILCs, due to the local predominance of ILC3 and their sparse production of other ILC3-specific cytokines. Second, their inducibility by pro-inflammatory stimuli suggests an involvement in hepatic fibrogenesis, which is often characterized by the presence of these factors (Barbier et al., 2019; Koyama and Brenner, 2017). And third, IL-13 itself has been described as an important modulator of liver fibrosis in multiple settings (Gieseck et al., 2016; Liu et al., 2012; Shimamura et al., 2008), thus implying a concomitant involvement of IL-13-producing ILCs.

4.2 Involvement of human intrahepatic ILCs in chronic fibrotic liver disease

4.2.1 Frequencies of ILCs and IL-13+ ILC3 are increased in fibrotic or cirrhotic livers

These indications for IL-13-producing ILCs, together with previously published reports on murine or human ILCs (Forkel et al., 2017; Marvie et al., 2009; Mchedlidze et al., 2013), support the hypothesis that ILCs in general and IL-13+ ILCs in particular may significantly contribute to fibrotic liver disease.

In this context, the increased frequencies of ILCs observed in fibrotic or cirrhotic livers provide further evidence for this assumption. The expansion of ILCs in CLD patients appears to be liver-specific, thus suggesting that the pathological changes of the liver microenvironment are driving this enrichment. Accordingly, no increase of ILC numbers could be detected in physiologically connected compartments such as the colon or circulating bloodstream. In contrast, the frequency of ILCs in the colon of some CLD patients was even markedly decreased. Since ILCs critically contribute to the maintenance of the intestinal barrier (Fan et al., 2019; Sonnenberg et al., 2012), a loss of colon ILCs could contribute to liver inflammation and disease progression due to increased translocation of microbial products to the hepatic compartment (Ohtani and Kawada, 2019; Pinzone et al., 2012). Although in total, the decrease of colon ILCs did not reach statistical significance, the high standard deviation within the diseased colon cohort might indicate etiology-related differences. Thus, more patient material should be collected in order to allow for a stratification analysis of the CLD cohort and the investigation of this topic.

While it remains unclear if the enrichment of intrahepatic ILCs is a cause or an effect of CLD, this finding suggests an increasing influence of ILCs and ILC-derived cytokines in hepatic fibrogenesis.

In accordance with previous reports, an accumulation of intrahepatic ILC2, on which human studies have been primarily focused so far (Forkel et al., 2017; Jeffery et al., 2017), could be observed in this study. Given the unaltered percentages of IL-13+ ILC2 among liver-infiltrating lymphocytes however, the functional relevance of the numerical increase of ILC2 remains questionable. Moreover, the comparably higher frequency of IL-13+ ILC3, which could also be observed in fibrotic or cirrhotic livers, suggests that the major source

of ILC-derived IL-13 in chronic liver disease has been overlooked so far. In addition, the increase of IL-13-producing ILC3 in fibrotic or cirrhotic livers, as well as their correlation with the MELD score further support the implications of this cell type in CLD.

Of note, the MELD score, which is commonly used to predict the three-month survival of patients enlisted for liver transplantation, primarily assesses the severity of liver disease in its final stages. The investigation of ILCs at earlier stages of liver disease was beyond the scope of this project, although insights at these time points might be highly valuable for the evaluation of the contribution of ILCs over the course of CLD. In this study, patient material was derived from explanted organs, and thus at an advanced point of disease progression. Future studies addressing this subject, would require the collection of hepatic tissue prior to transplantation, ideally at several stages of disease, monitoring the clinical course of individual patients. The low frequency of ILCs however, will remain a major burden to such investigations, as the amount of tissue collected - for instance - during liver biopsies is often insufficient to enable a reliable assessment of ILCs. Advances in highly multiplexed imaging technologies, which enable detailed cytometric analysis of single cells in histological sections, might facilitate research at this point in future (Black et al., 2021).

4.2.2 IL-13 secretion of liver ILCs mediates pro-inflammatory imprinting of HSCs

Nevertheless, mechanistic studies can already provide the basis for a better understanding of the increasing ILC-mediated influence in the progression of hepatic fibrogenesis. In this context, previous reports have mainly described upstream events of ILC activation (Forkel et al., 2017) or investigated related systemic effects (Marvie et al., 2009; Mchedlidze et al., 2013), but did not address the specific downstream effects of intrahepatic ILCs.

In this study, a direct modulatory influence of intrahepatic ILC3 on HSCs could be identified, revealing that, via IL-13, ILC3 mediate the pro-inflammatory imprinting of a cell type, which is centrally involved in hepatic fibrogenesis (Higashi et al., 2017). Unexpectedly, these IL-13-mediated effects did not include upregulation of classic pro-fibrotic markers in HSCs, such as *COL1A1* or *ACTA2*, thus challenging the perception of IL-13 as a direct pro-fibrotic agent. Whereas this specific influence of IL-13 on HSCs has

been mainly described in murine models (Liu et al., 2011; Mchedlidze et al., 2013; Weng et al., 2009), observations made in human HSC cell lines (Forkel, 2017) support the findings presented in this study. These are further strengthened by the fact that, in this work, primary human hepatic stellate cells have been used instead of immortalized cell lines. Furthermore, the cells, which have been commercially obtained for this project, reflect the biological variability of six individual donors, in return underlining the reproducibility of the observed effects on human HSCs. At this point, more extensive comparative studies would be required to evaluate, if the observed differences of IL-13 signaling on murine and human HSCs are in fact due to inherent biological differences or rather arise from setting-dependent factors.

The upregulation of pro-inflammatory cytokines such as CXCL8 in HSCs indicates a so far unrecognized role for IL-13-producing ILCs in hepatic fibrogenesis. Consequently, the enrichment of IL-13+ ILC3 in the course of CLD might be linked to multiple hallmarks of chronic disease and inflammation, given the pleiotropic effects of CXCL8 in the liver.
As such, intrahepatic ILC3 might contribute to the accumulation of myeloid cells in fibrotic or cirrhotic livers (Zimmermann et al., 2011), which is supported by the increased myeloid chemotaxis observed towards supernatant of IL-13-treated HSCs. Given the implications of HSC-derived CXCL8 secretion in angiogenesis and formation of hepatocellular carcinomas (Zhu et al., 2015), they might also play a role in liver tumorigenesis, as indicated by a recent study (Heinrich et al., 2021). Furthermore, CXCL8 itself has been described to increase the expression of pro-fibrotic markers in HSCs (Clément et al., 2010), which might explain the described pro-fibrotic effects of IL-13 and IL-13-producing ILCs via an indirect mechanism, manifesting upon prolonged exposure.

On the other hand however, the induction of pro-inflammatory genes in HSCs might also mediate beneficial effects in CLD. As such, increased expression of CXCL8 and CXCL1 have been described to be associated with the reversion of HSCs to a more quiescent state and contained inflammatory responses are considered to contribute to liver regeneration (El Taghdouini et al., 2015; Gao and Tsukamoto, 2016). Furthermore, the pro-inflammatory imprinting of HSCs might also contribute to the defense against bacterial infections, which frequently occur in late-stage liver cirrhosis (Fernández and Gustot,

2012). Interestingly, this might correspond to the enrichment of IL-13+ ILC3, which is also most prominent in these stages of disease.

Of note, the IL-13-mediated upregulation of CXCL8 appears to be even more pronounced in activated, TGFβ-stimulated HSCs, which accumulate during disease progression (Dewidar et al., 2019; Fabregat et al., 2016; Tsuchida and Friedman, 2017). Thus, the enrichment of IL-13+ ILC3 in CLD may additionally be associated with an enhancement of their functional impact on HSCs.

Taken together, these findings indicate a complex role of human liver ILCs and, in particular, IL-13-producing ILC3 in regulating hepatic fibrogenesis. Although infrequent in comparison to other intrahepatic immune cells, the ability to modulate HSCs, the main drivers of hepatic fibrogenesis, supports the relevance of ILC-mediated effects in the human liver. Furthermore, the overall increase of intrahepatic ILCs in CLD also indicates the involvement of cell types which have not been addressed in this project, due to the analytical focus on the main intrahepatic ILC subset.
This study provides first evidence for the involvement and implications of ILC3 in CLD but the beneficial or detrimental nature of their mediated effects remains elusive. Overall, a better understanding of the factors and mechanisms which drive the emergence and accumulation of IL-13-producing ILC3 would be required to elucidate how these cells are or can be regulated in the human liver. To provide additional insights at this point, the final part of this work examined the potential origin of IL-13+ ILC3.

4.3 Investigation of the emergence of IL-13+ ILC3 in the human liver

4.3.1 IL-13+ ILC3-like cells arise from KLRG1-expressing ILC precursors

Diversity and versatility of tissue-specific ILC pools are centrally facilitated by the plasticity of mature ILC subsets as well as the multipotency of developing ILC precursors (Bal et al., 2020; Lim and Di Santo, 2019). The generation of chimeric ILCs with ILC3- and ILC2-like features has been previously described to occur under the influence of ILC3-priming stimuli on cells developing along an ILC2-directed pathway (Bernink et al., 2019; Golebski et al., 2019; Lim et al., 2017; Nagasawa et al., 2019).

In line with these reports, the present study indicates that intrahepatic IL-13+ ILC3 predominantly emerge from KLRG1-expressing ILC precursors (ILCP). These have been described as ILC2-skewed, but not fully committed progenitors, which can develop into functionally different cells depending on the environmental cues they encounter (Nagasawa et al., 2019). As demonstrated in this work, they primarily account for the IL-13-producing cells arising from the heterogeneous pool of ILCP, and furthermore acquire a transcriptional profile similar to that observed in IL-13-producing liver ILC3.

In line with this finding, increased frequencies of KLRG1+ ILCP can be found in the human liver when compared to tonsils or colon, corresponding to the tissue-specific accumulation of intrahepatic IL-13+ ILC3. While it remains unclear if KLRG1+ ILCP are recruited to the liver or proliferate locally, the development of IL-13+ ILC3 appears to be specifically driven by the liver microenvironment, given their absence in peripheral blood or other physiologically connected compartments such as the gut.

In the liver, several factors centrally contribute to the development of IL-13+ ILC3. The ILC3-priming effects of IL-1β, IL-23 and TGFβ have been well-described in the context of ILC plasticity and development (Golebski et al., 2019; Lim et al., 2017) and also have been shown to play a role in liver physiology and hepatic fibrogenesis (Barbier et al., 2019; Fabregat et al., 2016; Zang et al., 2018). The increased expression of *IL1R1*, *IL23R* and *TGFBR2* on IL-13+ ILC3 additionally supports the relevance of this specific signaling in shaping this subset.

Apart from these extensively characterized factors, the data obtained in this project also indicates that the development of important ILC3-defining features in IL-13-producing ILCs, such as NKp44 expression, requires the additional influence of AhR-mediated signaling. The abundance of AhR ligands in the human liver, from tryptophan metabolites and bilirubin to modified low-density lipoprotein (McMillan and Bradfield, 2007; Tian et al., 2015), might contribute to make the liver a privileged site for the enrichment of IL-13+ ILC3. The same applies to Notch ligands, which are highly expressed by various cell types in the liver, such as liver sinusoidal endothelial cells (LSECs) (Adams and Jafar-Nejad, 2019; Neumann et al., 2015).

Of note, the aforementioned factors have also been reported to influence the microenvironment of other compartments, such as the intestinal tract (Pellegrinet et al.,

2011; Seo et al., 2015; Stockinger et al., 2021). However, virtually no IL-13+ ILC3 could be observed in colon tissue, raising the question if either the complex interplay of these factors or additional mechanisms facilitate the liver-specific emergence of IL-13-producing ILC3.

In this context, the opposing roles of Notch- and TGFβ-mediated signaling might contribute to the distinction of liver and colon microenvironment. While Notch ligands promote the stabilization of NCR+ ILC3, TGFβ has been shown to antagonize this mechanism and instead contributes to the development of ILC2 (Viant et al., 2016; Wang et al., 2020). Thus, their balanced engagement appears to be of vital importance in the generation of ILCs with mixed ILC2- and ILC3-like features such as intrahepatic IL-13+ ILC3. In this context, it is worth noting that the ILC pool in the colon is characterized by an absence of ILC2 and ILC2-skewed KLRG1-expressing progenitors, but in return predominantly populated by NCR+ ILC3. These findings support the hypothesis that, unlike in the human liver, the colon microenvironment does not promote a fine balance between both cell types, which consequently might inhibit the developmental pathway of IL-13-producing ILC3.

Given the plethora of developmental and plastic trajectories of ILCs, further pathways and stimuli might additionally contribute to the emergence of IL-13+ ILC3-like cells in the human liver.

However, the emergence of intrahepatic IL-13+ ILC3 from a conversion of mature ILC2, as it has been previously described in nasal or dermal tissue (Bernink et al., 2019; Golebski et al., 2019), appears to be less likely, given their inconsistent reflection of an ILC3-specific expression signature. Moreover, the minor expression of further ILC2-related features by IL-13+ liver ILC3, as well as the expression of factors indicating an early divergence from an ILC2-directed developmental trajectory argue against this hypothesis.

The upregulation of some genes such as *NCR2*/NKp44 and *IL22* in cultured ILC2 seem to indicate a certain degree of ILC3-directed conversion, as it has been reported in the aforementioned studies (Bernink et al., 2019; Golebski et al., 2019). However, with regard to the comprehensive transcriptional profile of ILC3, the differences between mature ILC2 and KLRG1+ ILCP become apparent, outlining the differential transdifferentiation capacities of both ILC subsets. In this context, the present study provides detailed insights,

which might also be useful to further assess the stage-dependent limits of ILC plasticity in future research.

Of note, cultured ex-ILC2 display many features that suggest a similarity to the intrahepatic IL-13+ CRTH2-CD117+ liver ILCs observed in the flow cytometry data presented. As these data are not directly matched to the more profound scRNA-seq data, it cannot be fully excluded that the identified population might in fact encompass at least some converted mature ILC2, which cluster among conventional ILC2 in the transcriptional analysis. However, cultured ILC2 still preserve significantly higher levels of GATA3 than ILCP- or ILC3-derived ILC3-like cells, which should also manifest in the flow cytometry data, if IL-13+ liver ILC3 were composed of two distinct cell types. Yet no such pattern can be observed, instead the intrahepatic IL-13-producing ILC3-like cells display a uniform GATA3^{low} expression profile, reflecting that of conventional ILC3. This finding strongly argues against the possibility that cells of such differential developmental origins are present within this observed population. To fully clarify this aspect, a renewed scRNA-seq analysis could be performed, where purified IL-13+ ILC3 and IL-13+ ILC2 are examined separately.

Whether mature ILC3 can acquire ILC2-like features remains unclear up to date (Bal et al., 2020). The experimental data presented in this work however, do not support this hypothesis, as virtually no IL-13-producing cells arise from NKp44+ ILC3 under the described circumstances. The ILC3-directed development of ILC2-skewed cells, on the other hand, has been observed in several compartments so far and may therefore represent a more common and plausible mechanism.

To elucidate the disease-associated accumulation of IL-13+ ILC3, and ultimately allow for a potential targeting of this subset in CLD, further research would be required to investigate the factors which mediate this additional expansion in hepatic fibrogenesis.

On the one hand, changes in the pathological microenvironment might enhance the development of KLRG1+ ILCP to IL-13+ ILC3 in human liver disease. In line with this, most of the factors which have been identified in this study to mediate this process, have also been described to be affected by hepatopathy-associated perturbations, such as TGFβ, Notch ligands or IL-1β (Barbier et al., 2019; Fabregat et al., 2016; Nijjar et al., 2002). The increased percentage of NKp44-expressing ILC3 in fibrotic or cirrhotic livers

might further support this hypothesis, indicating that the overall composition of the liver ILC pool is subject to plastic or developmental changes in CLD.

On the other hand, the enrichment of IL-13+ ILC3 in diseased livers might also be facilitated by an enhanced recruitment of KLRG1-expressing progenitors to the hepatic compartment. Further phenotypic data should be acquired in subsequent studies, in order to assess the potential differences in the composition of the intrahepatic ILCP pool in steady-state and disease. In this regard, analysing the expression of liver homing receptors such as CXCR3 or CXCR6 on peripheral blood ILCP in patients with liver fibrosis or cirrhosis might additionally contribute to a better understanding of these potential processes.

4.4 Concluding remarks

Since their first discovery (Cella et al., 2009; Cupedo et al., 2009; Neill et al., 2010; Spits and Di Santo, 2011), the investigation of ILCs has experienced increasing attention over the past decade. Nevertheless, it remains a comparably young field of research and many perceptions regarding ILCs are constantly adapted and revised (Vivier et al., 2018).

Up to date, several aspects remain a constant hindrance to a better understanding of ILC-mediated immunity. As such, the transfer of knowledge from murine models to the human system is often impaired due to substantial differences between both species. Furthermore, the acknowledged variability of ILCs throughout the system emphasizes the importance of investigating tissue-specific cells, however limited availability of specific human tissue impedes the quantitatively demanding ILC research. In addition, despite the proposal for a uniform nomenclature, discrepancies regarding the very definition of ILCs, especially in humans, still exist, fuelling the inconsistency of findings.

The present study might make a small but significant contribution to a better understanding of the human, intrahepatic ILCs pool and its role in CLD. The identification of IL-13-producing ILC3 in the liver, their potential developmental origin as well as first evidence for their involvement in hepatic fibrogenesis provide insights to an ILC subset which has been rather neglected so far. While the presented findings specifically imply a nuanced role of IL-13-producing ILCs and ILC3 in the human liver, further research is

required to elucidate how the functional influence of the total intrahepatic ILC pool is balanced and regulated in liver physiology and pathology. Whether IL-13 production by liver ILC3 represents a mechanism of redundancy or whether it is associated with a unique functional impact remains uncertain. Moreover, the role of intrahepatic ILCs in the onset or the early stages of liver fibrosis still needs to be addressed by further research. Characterizing the potentially different interactions of the intrahepatic ILC subsets with critical players of immune-mediated signaling in the liver, such as HSCs, LSECs, macrophages or T cells would be a compelling approach for future investigation. The advances in spatial transcriptomics and multiplexed imaging technologies might prove to be highly valuable for resolving the spatio-temporally confined effects of these rare immune cells.

5. Abstract

Innate lymphoid cells (ILCs) are a family of innate immune cells that mirror the functionality of T lymphocytes but do not express rearranged antigen receptors. As tissue-resident cells, ILCs primarily reside in peripheral organs and at mucosal surfaces where they engage in local immune responses as well as in homeostatic or metabolic processes. Accumulating evidence indicates that ILCs are critically involved in numerous inflammatory diseases affecting various tissues of the body. However, data on the composition and biological function of human liver-resident ILCs and their role in liver fibrosis are scarce and published studies have reported conflicting results.

The work in this thesis aimed to significantly improve our current knowledge by providing a detailed characterisation of the human intrahepatic ILC pool and by further assessing its involvement in hepatic fibrogenesis. For this purpose, tissue-resident ILCs were isolated from non-fibrotic and fibrotic or cirrhotic livers and analyzed using proteomic, transcriptional as well as functional assays. For comparative analyses, ILCs isolated from tonsillar and colon tissue, as well as from peripheral blood were additionally included in this project.

Intrahepatic ILC3, which are currently considered to mainly comprise immature ILC precursors, were found to display a liver-specific capacity to produce the ILC2-specific cytokine IL-13. Given their considerably high proportion among intrahepatic ILCs, they in fact constitute the major IL-13-producing ILC subset in the human liver. Fibrotic or cirrhotic liver samples were characterized by an accumulation of this cell type which correlated with disease severity. Mechanistically, both IL-13 and stimulated liver ILC3 induced a pro-inflammatory profile in hepatic stellate cells, revealing a modulatory impact of tissue-resident ILCs on one of the major profibrogenic cell types in liver fibrosis. Studies of ILC plasticity identified liver-specifically enriched KLRG1-expressing ILC precursors to acquire a similar molecular phenotype under ILC3-priming conditions, thereby constituting the putative progenitor of IL-13-expressing liver ILC3.

In summary, this study provides the first description of a so far unrecognized subset of IL-13+ ILC3 in the human liver, indicating that the pool of intrahepatic IL-13-producing ILCs is drastically underestimated up to date. The first evidence on their involvement in hepatic fibrogenesis and on their developmental trajectory might make a small but significant contribution to a better understanding of the biological role of human ILCs in the liver.

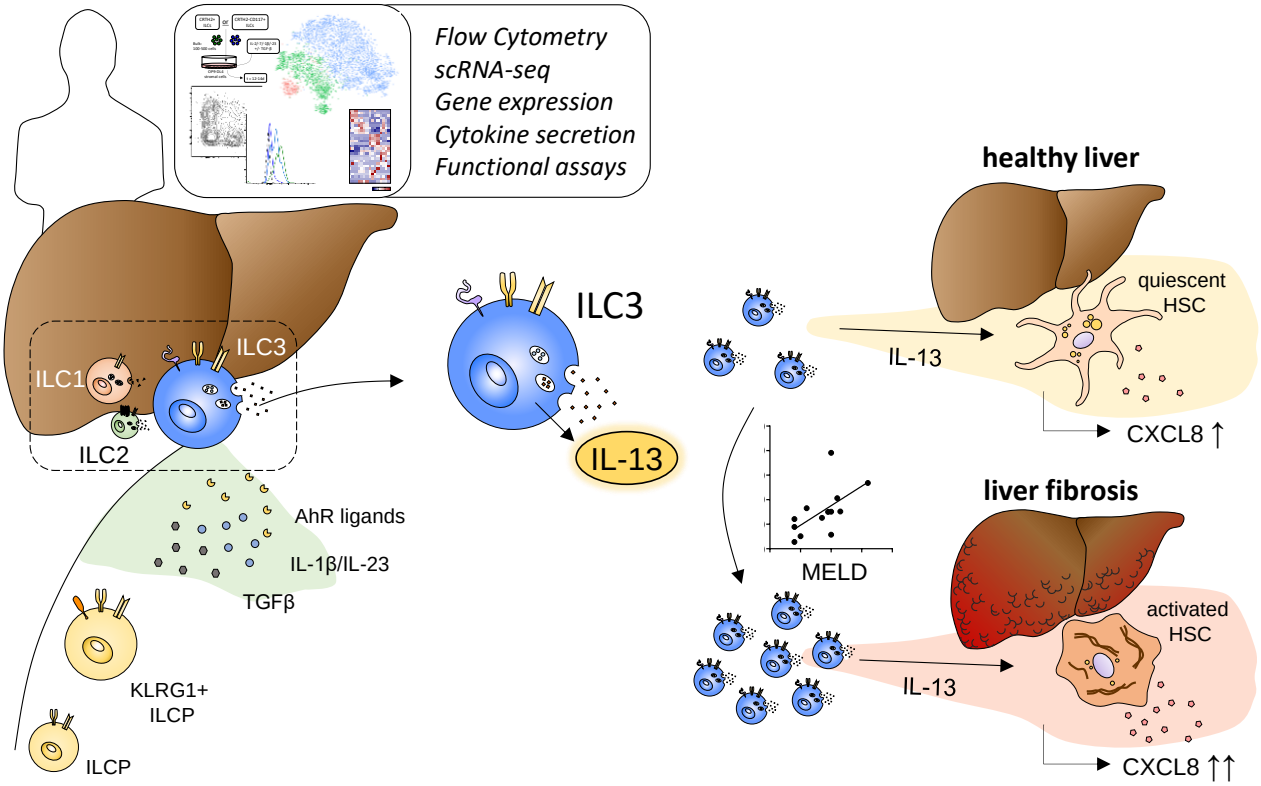

Fig. 5.1 Graphical abstract

6. List of figures

7. List of tables

8. References

8.1 Scientific Literature

Abt MC, Lewis BB, Caballero S, Xiong H, Carter RA, Sušac B, Ling L, Leiner I, Pamer EG. Innate Immune Defenses Mediated by Two ILC Subsets Are Critical for Protection against Acute Clostridium difficile Infection. Cell Host Microbe 2015;18:27–37

Adams J, Jafar-Nejad H. The Roles of Notch Signaling in Liver Development and Disease. Biomolecules 2019;9:608

Artis D, Spits H. The biology of innate lymphoid cells. Nature 2015;517:293–301.

Bal SM, Bernink JH, Nagasawa M, Groot J, Shikhagaie MM, Golebski K, van Drunen CM, Lutter R, Jonkers RE, Hombrink P, Bruchard M, Villaudy J, Munneke JM, Fokkens W, Erjefält JS, Spits H, Ros XR. IL-1β, IL-4 and IL-12 control the fate of group 2 innate lymphoid cells in human airway inflammation in the lungs. Nat Immunol 2016;17:636–45.

Bal SM, Golebski K, Spits H. Plasticity of innate lymphoid cell subsets. Nat Rev Immunol 2020;20:552–565

Barbier L, Ferhat M, Salamé E, Robin A, Herbelin A, Gombert J-M, Silvain C, Barbarin A. Interleukin-1 Family Cytokines: Keystones in Liver Inflammatory Diseases. Front Immunol 2019;10:2014

Bar-Ephraim YE, Koning JJ, Burniol Ruiz E, Konijn T, Mourits VP, Lakeman KA, Boon L, Bögels M, van Maanen JP, Den Haan JMM, van Egmond M, Bouma G, Reijmers RM, Mebius RE. CD62L Is a Functional and Phenotypic Marker for Circulating Innate Lymphoid Cell Precursors. J Immunol 2019;202:171–182

Barlow JL, Peel S, Fox J, Panova V, Hardman CS, Camelo A, Bucks C, Wu X, Kane CM, Neill DR, Flynn RJ, Sayers I, Hall IP, McKenzie ANJ. IL-33 is more potent than IL-25 in provoking IL-13–producing nuocytes (type 2 innate lymphoid cells) and airway contraction. J Allergy Clin Immunol 2013;132:933–941

Bartemes KR, Iijima K, Kobayashi T, Kephart GM, McKenzie AN, Kita H. IL-33–Responsive Lineage $^{-}$ CD25 $^{+}$ CD44 ^{hi} Lymphoid Cells Mediate Innate Type 2 Immunity and Allergic Inflammation in the Lungs. J Immunol 2012;188:1503–1513

Bataller R, Brenner DA. Liver fibrosis. J Clin Invest 2005;115:209–218

Benjamini Y, Krieger AM, Yekutieli D. Adaptive linear step-up procedures that control the false discovery rate. Biometrika 2006;93:491–507

Bernink JH, Krabbendam L, Germar K, de Jong E, Gronke K, Kofoed-Nielsen M, Munneke JM, Hazenberg MD, Villaudy J, Buskens CJ, Bemelman WA, Diefenbach A, Blom B, Spits H. Interleukin-12 and -23 Control Plasticity of CD127+ Group 1 and Group 3 Innate Lymphoid Cells in the Intestinal Lamina Propria. Immunity 2015;43:146–160

Bernink JH, Ohne Y, Teunissen MBM, Wang J, Wu J, Krabbendam L, Guntermann C, Volckmann R, Koster J, van Tol S, Ramirez I, Shrestha Y, de Rie MA, Spits H, Romero Ros X, Humbles AA. c-Kit-positive ILC2s exhibit an ILC3-like signature that may contribute to IL-17-mediated pathologies. Nat Immunol 2019;20:992–1003

Bernink JH, Peters CP, Munneke M, te Velde AA, Meijer SL, Weijer K, Hreggvidsdottir HS, Heinsbroek SE, Legrand N, Buskens CJ, Bemelman WA, Mjösberg JM, Spits H. Human type 1 innate lymphoid cells accumulate in inflamed mucosal tissues. Nat Immunol 2013;14:221–229

Björklund ÅK, Forkel M, Picelli S, Konya V, Theorell J, Friberg D, Sandberg R, Mjösberg J. The heterogeneity of human CD127+ innate lymphoid cells revealed by single-cell RNA sequencing. Nat Immunol 2016;17:451–460

Black S, Phillips D, Hickey JW, Kennedy-Darling J, Venkataraaman VG, Samusik N, Goltsev Y, Schürch CM, Nolan GP. CODEX multiplexed tissue imaging with DNA-conjugated antibodies. Nat Protoc 2021;16:3802–3835

Castellanos JG, Longman RS. The balance of power: innate lymphoid cells in tissue inflammation and repair. J Clin Invest 2019;129:2640–2650

Cella M, Fuchs A, Vermi W, Facchetti F, Otero K, Lennerz JKM, Doherty JM, Mills JC, Colonna M. A human natural killer cell subset provides an innate source of IL-22 for mucosal immunity. Nature 2009;457:722–725

Cella M, Otero K, Colonna M. Expansion of human NK-22 cells with IL-7, IL-2, and IL-1 reveals intrinsic functional plasticity. Proc Natl Acad Sci 2010;107:10961–10966

Chea S, Perchet T, Petit M, Verrier T, Guy-Grand D, Banchi E-G, Vosshenrich CAJ, Di Santo JP, Cumano A, Golub R. Notch signaling in group 3 innate lymphoid cells modulates their plasticity. Sci Signal 2016;9

Chen L, Youssef Y, Robinson C, Ernst GF, Carson MY, Young KA, Scoville SD, Zhang X, Harris R, Sekhri P, Mansour AG, Chan WK, Nalin AP, Mao HC, Hughes T, Mace EM, Pan Y, Rustagi N, Chatterjee SS, Gunaratne PH, Behbehani GK, Mundy-Bosse BL, Caligiuri MA, Freud AG. CD56 Expression Marks Human Group 2 Innate Lymphoid Cell Divergence from a Shared NK Cell and Group 3 Innate Lymphoid Cell Developmental Pathway. Immunity 2018;49:464-476.e4

Chen Y, Tian Z. Innate lymphocytes: pathogenesis and therapeutic targets of liver diseases and cancer. Cell Mol Immunol 2021;18:57–72

Chiaramonte MG, Donaldson DD, Cheever AW, Wynn TA. An IL-13 inhibitor blocks the development of hepatic fibrosis during a T-helper type 2–dominated inflammatory response. J Clin Invest 1999;104:777–785

Cichocki F, Miller JS. In Vitro Development of Human Killer–Immunoglobulin Receptor-Positive NK Cells. In: Campbell KS, editor. Nat. Kill. Cell Protoc 2010;vol. 612:15–26

Clément S, Pascarella S, Conzelmann S, Gonelle-Gispert C, Guilloux K, Negro F. The hepatitis C virus core protein indirectly induces alpha-smooth muscle actin expression in hepatic stellate cells via interleukin-8. J Hepatol 2010;52:635–643

Cooney LA, Towery K, Endres J, Fox DA. Sensitivity and Resistance to Regulation by IL-4 during Th17 Maturation. J Immunol 2011;187:4440–4450

Cupedo T, Crellin NK, Papazian N, Rombouts EJ, Weijer K, Grogan JL, Fibbe WE, Cornelissen JJ, Spits H. Human fetal lymphoid tissue–inducer cells are interleukin 17–producing precursors to RORC+ CD127+ natural killer–like cells. Nat Immunol 2009;10:66–74

Dewidar, Meyer, Dooley, Meindl-Beinker. TGF-β in Hepatic Stellate Cell Activation and Liver Fibrogenesis—Updated 2019. Cells 2019;8:1419

Diefenbach A, Colonna M, Koyasu S. Development, Differentiation, and Diversity of Innate Lymphoid Cells. Immunity 2014;41:354–365

van Dijk D, Sharma R, Nainys J, Yim K, Kathail P, Carr AJ, Burdziak C, Moon KR, Chaffer CL, Pattabiraman D, Bierie B, Mazutis L, Wolf G, Krishnaswamy S, Pe'er D. Recovering Gene Interactions from Single-Cell Data Using Data Diffusion. Cell 2018;174:716-729.e27

Ebbo M, Crinier A, Vély F, Vivier E. Innate lymphoid cells: major players in inflammatory diseases. Nat Rev Immunol 2017;17:665–678

El Taghdouini A, Najimi M, Sancho-Bru P, Sokal E, van Grunsven LA. In vitro reversion of activated primary human hepatic stellate cells. Fibrogenesis Tissue Repair 2015;8:14

Fabre T, Molina MF, Soucy G, Goulet J-P, Willems B, Villeneuve J-P, Bilodeau M, Shoukry NH. Type 3 cytokines IL-17A and IL-22 drive TGF-β–dependent liver fibrosis. Sci Immunol 2018;3:eaar7754

Fabregat I, Moreno-Càceres J, Sánchez A, Dooley S, Dewidar B, Giannelli G, ten Dijke P, the IT-LIVER Consortium. TGF-β signalling and liver disease. FEBS J 2016;283:2219–2232

Fan H, Wang A, Wang Y, Sun Y, Han J, Chen W, Wang S, Wu Y, Lu Y. Innate Lymphoid Cells: Regulators of Gut Barrier Function and Immune Homeostasis. J Immunol Res 2019;2019:1–15

Fernández J, Gustot T. Management of bacterial infections in cirrhosis. J Hepatol 2012;56 Suppl 1:S1-12

Ferreira ACF, Szeto ACH, Heycock MWD, Clark PA, Walker JA, Crisp A, Barlow JL, Kitching S, Lim A, Gogoi M, Berks R, Daly M, Jolin HE, McKenzie ANJ. RORα is a critical checkpoint for T cell and ILC2 commitment in the embryonic thymus. Nat Immunol 2021;22:166–78

Ficht X, Iannacone M. Immune surveillance of the liver by T cells. Sci Immunol 2020;5:eaba2351

Forkel M. Innate lymphoid cell heterogeneity in human tissues at steady state and during inflammation. Open WorldCat 2017

Forkel M, Berglin L, Kekäläinen E, Carlsson A, Svedin E, Michaëlsson J, Nagasawa M, Erjefält JS, Mori M, Flodström-Tullberg M, Bergquist A, Ljunggren H-G, Westgren M, Lindforss U, Friberg D, Jorns C, Ellis E, Björkström NK, Mjösberg J. Composition and functionality of the intrahepatic innate lymphoid cell-compartment in human nonfibrotic and fibrotic livers. Eur J Immunol 2017;47:1280–1294

Forkel M, van Tol S, Höög C, Michaëlsson J, Almer S, Mjösberg J. Distinct Alterations in the Composition of Mucosal Innate Lymphoid Cells in Newly Diagnosed and Established Crohn's Disease and Ulcerative Colitis. J Crohns Colitis 2019;13:67–78

Freud AG, Keller KA, Scoville SD, Mundy-Bosse BL, Cheng S, Youssef Y, Hughes T, Zhang X, Mo X, Porcu P, Baiocchi RA, Yu J, Carson WE, Caligiuri MA. NKp80 Defines a Critical Step during Human Natural Killer Cell Development. Cell Rep 2016;16:379–391

Fuchs A, Vermi W, Lee JS, Lonardi S, Gilfillan S, Newberry RD, Cella M, Colonna M. Intraepithelial Type 1 Innate Lymphoid Cells Are a Unique Subset of IL-12- and IL-15-Responsive IFN-γ-Producing Cells. Immunity 2013;38:769–781

Gao B, Jeong W-I, Tian Z. Liver: An organ with predominant innate immunity. Hepatology 2007;47:729–736

Gao B, Tsukamoto H. Inflammation in Alcoholic and Nonalcoholic Fatty Liver Disease: Friend or Foe? Gastroenterology 2016;150:1704–1709

Gieseck RL, Ramalingam TR, Hart KM, Vannella KM, Cantu DA, Lu W-Y, Ferreira-González S, Forbes SJ, Vallier L, Wynn TA. Interleukin-13 Activates Distinct Cellular Pathways Leading to Ductular Reaction, Steatosis, and Fibrosis. Immunity 2016;45:145–158

Glässner A, Eisenhardt M, Krämer B, Körner C, Coenen M, Sauerbruch T, Spengler U, Nattermann J. NK cells from HCV-infected patients effectively induce apoptosis of activated primary human hepatic stellate cells in a TRAIL-, FasL- and NKG2D-dependent manner. Lab Invest 2012;92:967–977

Glatzer T, Killig M, Meisig J, Ommert I, Luetke-Eversloh M, Babic M, Paclik D, Blüthgen N, Seidl R, Seifarth C, Gröne J, Lenarz M, Stölzel K, Fugmann D, Porgador A, Hauser A, Karlas A, Romagnani C. RORγt+ Innate Lymphoid Cells Acquire a Proinflammatory Program upon Engagement of the Activating Receptor NKp44. Immunity 2013;38:1223–1235

Golebski K, Ros XR, Nagasawa M, van Tol S, Heesters BA, Aglmous H, Kradolfer CMA, Shikhagaie MM, Seys S, Hellings PW, van Drunen CM, Fokkens WJ, Spits H, Bal SM. IL-1β, IL-23, and TGF-β drive plasticity of human ILC2s towards IL-17-producing ILCs in nasal inflammation. Nat Commun 2019;10:2162

Golub R. The Notch signaling pathway involvement in innate lymphoid cell biology. Biomed J 2021;44:133–143

Han M, Rajput C, Hong JY, Lei J, Hinde JL, Wu Q, Bentley JK, Hershenson MB. The Innate Cytokines IL-25, IL-33, and TSLP Cooperate in the Induction of Type 2 Innate Lymphoid Cell Expansion and Mucous Metaplasia in Rhinovirus-Infected Immature Mice. J Immunol 2017;199:1308–1318

Hazenberg MD, Spits H. Human innate lymphoid cells. Blood 2014;124:700–9.

Heinrich B, Gertz EM, Schäffer AA, Craig A, Ruf B, Subramanyam V, McVey JC, Diggs LP, Heinrich S, Rosato U, Ma C, Yan C, Hu Y, Zhao Y, Shen T-W, Kapoor V, Telford W, Kleiner DE, Stovroff MK, Dhani HS, Kang J, Fishbein T, Wang XW, Ruppin E, Kroemer A,

Greten TF, Korangy F. The tumour microenvironment shapes innate lymphoid cells in patients with hepatocellular carcinoma. Gut 2021:gutjnl-2021-325288

Herberman RB, Nunn ME, Holden HT, Lavrin DH. Natural cytotoxic reactivity of mouse lymphoid cells against syngeneic and allogeneic tumors. II. Characterization of effector cells. Int J Cancer 1975;16:230–239

Higashi T, Friedman SL, Hoshida Y. Hepatic stellate cells as key target in liver fibrosis. Adv Drug Deliv Rev 2017;121:27–42

Hoorweg K, Peters CP, Cornelissen F, Aparicio-Domingo P, Papazian N, Kazemier G, Mjösberg JM, Spits H, Cupedo T. Functional Differences between Human NKp44− and NKp44+ RORC+ Innate Lymphoid Cells. Front Immunol 2012;3

Hughes T, Briercheck EL, Freud AG, Trotta R, McClory S, Scoville SD, Keller K, Deng Y, Cole J, Harrison N, Mao C, Zhang J, Benson DM, Yu J, Caligiuri MA. The Transcription Factor AHR Prevents the Differentiation of a Stage 3 Innate Lymphoid Cell Subset to Natural Killer Cells. Cell Rep 2014;8:150–162

Jacquelot N, Luong K, Seillet C. Physiological Regulation of Innate Lymphoid Cells. Front Immunol 2019;10:405

Jeffery HC, McDowell P, Lutz P, Wawman RE, Roberts S, Bagnall C, Birtwistle J, Adams DH, Oo YH. Human intrahepatic ILC2 are IL-13positive amphiregulinpositive and their frequency correlates with model of end stage liver disease score. PLOS ONE 2017;12:e0188649

Jeong W, Park O, Gao B. Abrogation of the Antifibrotic Effects of Natural Killer Cells/Interferon-γ Contributes to Alcohol Acceleration of Liver Fibrosis. Gastroenterology 2008;134:248–258

Jeong W-I, Park O, Radaeva S, Gao B. STAT1 inhibits liver fibrosis in mice by inhibiting stellate cell proliferation and stimulating NK cell cytotoxicity. Hepatology 2006;44:1441–1451

Klein Wolterink RGJ, Serafini N, van Nimwegen M, Vosshenrich CAJ, de Bruijn MJW, Fonseca Pereira D, Veiga Fernandes H, Hendriks RW, Di Santo JP. Essential, dose-dependent role for the transcription factor Gata3 in the development of IL-5+ and IL-13+ type 2 innate lymphoid cells. Proc Natl Acad Sci 2013;110:10240–10245

Klose CSN, Flach M, Möhle L, Rogell L, Hoyler T, Ebert K, Fabiunke C, Pfeifer D, Sexl V, Fonseca-Pereira D, Domingues RG, Veiga-Fernandes H, Arnold SJ, Busslinger M, Dunay IR, Tanriver Y, Diefenbach A. Differentiation of Type 1 ILCs from a Common Progenitor to All Helper-like Innate Lymphoid Cell Lineages. Cell 2014;157:340–356

Kong X, Feng D, Wang H, Hong F, Bertola A, Wang F-S, Gao B. Interleukin-22 induces hepatic stellate cell senescence and restricts liver fibrosis in mice. Hepatology 2012;56:1150–1159

Kotas ME, Locksley RM. Why Innate Lymphoid Cells? Immunity 2018;48:1081–1090

Koyama Y, Brenner DA. Liver inflammation and fibrosis. J Clin Invest 2017;127:55–64

Kozuka T, Sugita M, Shetzline S, Gewirtz AM, Nakata Y. c-Myb and GATA-3 Cooperatively Regulate IL-13 Expression via Conserved GATA-3 Response Element and Recruit Mixed Lineage Leukemia (MLL) for Histone Modification of the IL-13 Locus. J Immunol 2011;187:5974–5982

Krämer B, Goeser F, Lutz P, Glässner A, Boesecke C, Schwarze-Zander C, Kaczmarek D, Nischalke HD, Branchi V, Manekeller S, Hüneburg R, van Bremen T, Weismüller T, Strassburg CP, Rockstroh JK, Spengler U, Nattermann J. Compartment-specific distribution of human intestinal innate lymphoid cells is altered in HIV patients under effective therapy. PLOS Pathog 2017;13:e1006373

Kronenberger B, Rudloff I, Bachmann M, Brunner F, Kapper L, Filmann N, Waidmann O, Herrmann E, Pfeilschifter J, Zeuzem S, Piiper A, Mühl H. Interleukin-22 predicts severity and death in advanced liver cirrhosis: a prospective cohort study. BMC Med 2012;10:102

Kubes P, Jenne C. Immune Responses in the Liver. Annu Rev Immunol 2018;36:247–277

Lavenu-Bombled C, Trainor CD, Makeh I, Romeo P-H, Max-Audit I. Interleukin-13 Gene Expression Is Regulated by GATA-3 in T Cells. J Biol Chem 2002;277:18313–18321

Lee CG, Homer RJ, Zhu Z, Lanone S, Wang X, Koteliansky V, Shipley JM, Gotwals P, Noble P, Chen Q, Senior RM, Elias JA. Interleukin-13 Induces Tissue Fibrosis by Selectively Stimulating and Activating Transforming Growth Factor β1. J Exp Med 2001;194:809–822

Lee UE, Friedman SL. Mechanisms of hepatic fibrogenesis. Best Pract Res Clin Gastroenterol 2011;25:195–206

Li J, Doty AL, Tang Y, Berrie D, Iqbal A, Tan SA, Clare-Salzler MJ, Wallet SM, Glover SC. Enrichment of IL-17A $^{+}$ IFN-γ $^{+}$ and IL-22 $^{+}$ IFN-γ $^{+}$ T cell subsets is associated with reduction of NKp44 $^{+}$ ILC3s in the terminal ileum of Crohn's disease patients: Crosstalk between ILCs and T cells in CD. Clin Exp Immunol 2017;190:143–153

Li S, Bostick JW, Ye J, Qiu J, Zhang B, Urban JF, Avram D, Zhou L. Aryl Hydrocarbon Receptor Signaling Cell Intrinsically Inhibits Intestinal Group 2 Innate Lymphoid Cell Function. Immunity 2018;49:915-928.e5

Lim AI, Di Santo JP. ILC-poiesis: Ensuring tissue ILC differentiation at the right place and time. Eur J Immunol 2019;49:11–8

Lim AI, Li Y, Lopez-Lastra S, Stadhouders R, Paul F, Casrouge A, Serafini N, Puel A, Bustamante J, Surace L, Masse-Ranson G, David E, Strick-Marchand H, Le Bourhis L, Cocchi R, Topazio D, Graziano P, Muscarella LA, Rogge L, Norel X, Sallenave J-M, Allez M, Graf T, Hendriks RW, Casanova J-L, Amit I, Yssel H, Di Santo JP. Systemic Human ILC Precursors Provide a Substrate for Tissue ILC Differentiation. Cell 2017;168:1086-1100.e10

Lim AI, Menegatti S, Bustamante J, Le Bourhis L, Allez M, Rogge L, Casanova J-L, Yssel H, Di Santo JP. IL-12 drives functional plasticity of human group 2 innate lymphoid cells. J Exp Med 2016;213:569–583

Liu M, Zhang C. The Role of Innate Lymphoid Cells in Immune-Mediated Liver Diseases. Front Immunol 2017;8:695

Liu Y, Meyer C, Müller A, Herweck F, Li Q, Müllenbach R, Mertens PR, Dooley S, Weng H-L. IL-13 Induces Connective Tissue Growth Factor in Rat Hepatic Stellate Cells via TGF-β–Independent Smad Signaling. J Immunol 2011;187:2814–2823

Liu Y, Munker S, Müllenbach R, Weng H-L. IL-13 Signaling in Liver Fibrogenesis. Front Immunol 2012;3:1-7

Mackay IR. Hepatoimmunology: A perspective. Immunol Cell Biol 2002;80:36–44

MacLean Scott E, Solomon LA, Davidson C, Storie J, Palikhe NS, Cameron L. Activation of Th2 cells downregulates CRTh2 through an NFAT1 mediated mechanism. PLOS ONE 2018;13:e0199156

Maric J, Ravindran A, Mazzurana L, Van Acker A, Rao A, Kokkinou E, Ekoff M, Thomas D, Fauland A, Nilsson G, Wheelock CE, Dahlén S-E, Ferreirós N, Geisslinger G, Friberg D, Heinemann A, Konya V, Mjösberg J. Cytokine-induced endogenous production of prostaglandin D2 is essential for human group 2 innate lymphoid cell activation. J Allergy Clin Immunol 2019;143:2202-2214.e5

Marvie P, Lisbonne M, L'Helgoualc'h A, Rauch M, Turlin B, Preisser L, Bourd-Boittin K, Théret N, Gascan H, Piquet-Pellorce C, Samson M. Interleukin-33 overexpression is associated with liver fibrosis in mice and humans. J Cell Mol Med 2009;14:1726–1739

Mazzurana L, Czarnewski P, Jonsson V, Wigge L, Ringnér M, Williams TC, Ravindran A, Björklund ÅK, Säfholm J, Nilsson G, Dahlén S-E, Orre A-C, Al-Ameri M, Höög C, Hedin C, Szczegielniak S, Almer S, Mjösberg J. Tissue-specific transcriptional imprinting and heterogeneity in human innate lymphoid cells revealed by full-length single-cell RNA-sequencing. Cell Res 2021;31:554–568

Mchedlidze T, Waldner M, Zopf S, Walker J, Rankin AL, Schuchmann M, Voehringer D, McKenzie ANJ, Neurath MF, Pflanz S, Wirtz S. Interleukin-33-Dependent Innate Lymphoid Cells Mediate Hepatic Fibrosis. Immunity 2013;39:357–371

McMillan BJ, Bradfield CA. The Aryl hydrocarbon receptor is activated by modified low-density lipoprotein. Proc Natl Acad Sci 2007;104:1412–1417

Mebius RE, Rennert P, Weissman IL. Developing Lymph Nodes Collect CD4 + CD3 − LTβ + Cells That Can Differentiate to APC, NK Cells, and Follicular Cells but Not T or B Cells. Immunity 1997;7:493–504

Meininger I, Carrasco A, Rao A, Soini T, Kokkinou E, Mjösberg J. Tissue-Specific Features of Innate Lymphoid Cells. Trends Immunol 2020;41:902–917

Mjösberg J, Bernink J, Golebski K, Karrich JJ, Peters CP, Blom B, te Velde AA, Fokkens WJ, van Drunen CM, Spits H. The Transcription Factor GATA3 Is Essential for the Function of Human Type 2 Innate Lymphoid Cells. Immunity 2012;37:649–659

Mjösberg JM, Trifari S, Crellin NK, Peters CP, van Drunen CM, Piet B, Fokkens WJ, Cupedo T, Spits H. Human IL-25- and IL-33-responsive type 2 innate lymphoid cells are defined by expression of CRTH2 and CD161. Nat Immunol 2011;12:1055–1062

Mohtashami M, Shah DK, Kianizad K, Awong G, Zúñiga-Pflücker JC. Induction of T-cell development by Delta-like 4-expressing fibroblasts. Int Immunol 2013;25:601–611

Moreno-Nieves UY, Mundy DC, Shin JH, Tam K, Sunwoo JB. The aryl hydrocarbon receptor modulates the function of human CD56 ^{bright} NK cells. Eur J Immunol 2018;48:771–776

Nagasawa M, Heesters BA, Kradolfer CMA, Krabbendam L, Martinez-Gonzalez I, de Bruijn MJW, Golebski K, Hendriks RW, Stadhouders R, Spits H, Bal SM. KLRG1 and NKp46 discriminate subpopulations of human CD117+CRTH2− ILCs biased toward ILC2 or ILC3. J Exp Med 2019;216:1762–1776

Nagasawa M, Spits H, Ros XR. Innate Lymphoid Cells (ILCs): Cytokine Hubs Regulating Immunity and Tissue Homeostasis. Cold Spring Harb Perspect Biol 2018;10:a030304

Neill DR, Wong SH, Bellosi A, Flynn RJ, Daly M, Langford TKA, Bucks C, Kane CM, Fallon PG, Pannell R, Jolin HE, McKenzie ANJ. Nuocytes represent a new innate effector leukocyte that mediates type-2 immunity. Nature 2010;464:1367–1370

Nemeth E, Baird AW, O'Farrelly C. Microanatomy of the liver immune system. Semin Immunopathol 2009;31:333–343

Neumann K, Rudolph C, Neumann C, Janke M, Amsen D, Scheffold A. Liver sinusoidal endothelial cells induce immunosuppressive IL-10-producing Th1 cells via the Notch pathway: Immunomodulation. Eur J Immunol 2015;45:2008–2016

Nijjar SS, Wallace L, Crosby HA, Hubscher SG, Strain AJ. Altered Notch Ligand Expression in Human Liver Disease. Am J Pathol 2002;160:1695–1703

Ohne Y, Silver JS, Thompson-Snipes L, Collet MA, Blanck JP, Cantarel BL, Copenhaver AM, Humbles AA, Liu Y-J. IL-1 is a critical regulator of group 2 innate lymphoid cell function and plasticity. Nat Immunol 2016;17:646–655

Ohtani N, Kawada N. Role of the Gut-Liver Axis in Liver Inflammation, Fibrosis, and Cancer: A Special Focus on the Gut Microbiota Relationship: Hepatology Communications. Hepatol Commun 2019;3:456–470

Oriente A, Fedarko NS, Pacocha SE, Huang SK, Lichtenstein LM, Essayan DM. Interleukin-13 modulates collagen homeostasis in human skin and keloid fibroblasts. J Pharmacol Exp Ther 2000;292:988–994

Panda SK, Colonna M. Innate Lymphoid Cells in Mucosal Immunity. Front Immunol 2019;10:861

Paquissi FC. Immunity and Fibrogenesis: The Role of Th17/IL-17 Axis in HBV and HCV-induced Chronic Hepatitis and Progression to Cirrhosis. Front Immunol 2017;8:1195

Pellegrinet L, Rodilla V, Liu Z, Chen S, Koch U, Espinosa L, Kaestner KH, Kopan R, Lewis J, Radtke F. Dll1- and Dll4-Mediated Notch Signaling Are Required for Homeostasis of Intestinal Stem Cells. Gastroenterology 2011;140:1230-1240.e7

Pinzone MR, Celesia BM, Di Rosa M, Cacopardo B, Nunnari G. Microbial Translocation in Chronic Liver Diseases. Int J Microbiol 2012;2012:1–12

Pross HF, Baines MG. Spontaneous human lymphocyte-mediated cytotoxicity againts tumour target cells. I. The effect of malignant disease. Int J Cancer 1976;18:593–604

Racanelli V, Rehermann B. The liver as an immunological organ. Hepatology 2006;43:S54–62

Robinson MW, Harmon C, O'Farrelly C. Liver immunology and its role in inflammation and homeostasis. Cell Mol Immunol 2016;13:267–276

Satija R, Farrell JA, Gennert D, Schier AF, Regev A. Spatial reconstruction of single-cell gene expression data. Nat Biotechnol 2015;33:495–502

Satoh-Takayama N, Vosshenrich CAJ, Lesjean-Pottier S, Sawa S, Lochner M, Rattis F, Mention J-J, Thiam K, Cerf-Bensussan N, Mandelboim O, Eberl G, Di Santo JP. Microbial Flora Drives Interleukin 22 Production in Intestinal NKp46+ Cells that Provide Innate Mucosal Immune Defense. Immunity 2008;29:958–970

Scoville SD, Mundy-Bosse BL, Zhang MH, Chen Li, Zhang X, Keller KA, Hughes T, Chen Luxi, Cheng S, Bergin SM, Mao HC, McClory S, Yu J, Carson WE, Caligiuri MA, Freud AG. A Progenitor Cell Expressing Transcription Factor RORγt Generates All Human Innate Lymphoid Cell Subsets. Immunity 2016;44:1140–1150

Seo S-U, Kamada N, Muñoz-Planillo R, Kim Y-G, Kim D, Koizumi Y, Hasegawa M, Himpsl SD, Browne HP, Lawley TD, Mobley HLT, Inohara N, Núñez G. Distinct Commensals Induce Interleukin-1β via NLRP3 Inflammasome in Inflammatory Monocytes to Promote Intestinal Inflammation in Response to Injury. Immunity 2015;42:744–755

Sepanlou SG, Safiri S, Bisignano C, Ikuta KS, Merat S, Saberifiroozi M, Poustchi H, Tsoi D, Colombara DV, Abdoli A, Adedoyin RA, Afarideh M, Agrawal S, Ahmad S, Ahmadian E, Ahmadpour E, Akinyemiju T, Akunna CJ, Alipour V, Almasi-Hashiani A, Almulhim AM, Al-Raddadi RM, Alvis-Guzman N, Anber NH, Angus C, Anoushiravani A, Arabloo J, Araya EM, Asmelash D, Ataeinia B, Ataro Z, Atout MMW, Ausloos F, Awasthi A, Badawi A, Banach M, Bejarano Ramirez DF, Bhagavathula AS, Bhala N, Bhattacharyya K, Biondi A, Bolla SR, Boloor A, Borzì AM, Butt ZA, Cámera LLA, Campos-Nonato IR, Carvalho F, Chu D-T, Chung S-C, Cortesi PA, Costa VM, Cowie BC, Daryani A, de Courten B, Demoz

GT, Desai R, Dharmaratne SD, Djalalinia S, Do HT, Dorostkar F, Drake TM, Dubey M, Duncan BB, Effiong A, Eftekhari A, Elsharkawy A, Etemadi A, Farahmand M, Farzadfar F, Fernandes E, Filip I, Fischer F, Gebremedhin KBB, Geta B, Gilani SA, Gill PS, Gutirrez RA, Haile MT, Haj-Mirzaian A, Hamid SS, Hasankhani M, Hasanzadeh A, Hashemian M, Hassen HY, Hay SI, Hayat K, Heidari B, Henok A, Hoang CL, Hostiuc M, Hostiuc S, Hsieh VC, Igumbor EU, Ilesanmi OS, Irvani SSN, Jafari Balalami N, James SL, et al. The global, regional, and national burden of cirrhosis by cause in 195 countries and territories, 1990–2017: a systematic analysis for the Global Burden of Disease Study 2017. Lancet Gastroenterol Hepatol 2020;5:245–266

Shih H-Y, Sciumè G, Mikami Y, Guo L, Sun H-W, Brooks SR, Urban JF, Davis FP, Kanno Y, O'Shea JJ. Developmental Acquisition of Regulomes Underlies Innate Lymphoid Cell Functionality. Cell 2016;165:1120–1133

Shimamura T, Fujisawa T, Husain SR, Kioi M, Nakajima A, Puri RK. Novel Role of IL-13 in Fibrosis Induced by Nonalcoholic Steatohepatitis and Its Amelioration by IL-13R-Directed Cytotoxin in a Rat Model. J Immunol 2008;181:4656–4665

Silver JS, Kearley J, Copenhaver AM, Sanden C, Mori M, Yu L, Pritchard GH, Berlin AA, Hunter CA, Bowler R, Erjefalt JS, Kolbeck R, Humbles AA. Inflammatory triggers associated with exacerbations of COPD orchestrate plasticity of group 2 innate lymphoid cells in the lungs. Nat Immunol 2016;17:626–635

Simoni Y, Fehlings M, Kløverpris HN, McGovern N, Koo S-L, Loh CY, Lim S, Kurioka A, Fergusson JR, Tang C-L, Kam MH, Dennis K, Lim TKH, Fui ACY, Hoong CW, Chan JKY, Curotto de Lafaille M, Narayanan S, Baig S, Shabeer M, Toh S-AES, Tan HKK, Anicete R, Tan E-H, Takano A, Klenerman P, Leslie A, Tan DSW, Tan IB, Ginhoux F, Newell EW. Human Innate Lymphoid Cell Subsets Possess Tissue-Type Based Heterogeneity in Phenotype and Frequency. Immunity 2017;46:148–161

Simoni Y, Newell EW. Dissecting human ILC heterogeneity: more than just three subsets. Immunology 2018;153:297–303

Smith SG, Chen R, Kjarsgaard M, Huang C, Oliveria J-P, O'Byrne PM, Gauvreau GM, Boulet L-P, Lemiere C, Martin J, Nair P, Sehmi R. Increased numbers of activated group

2 innate lymphoid cells in the airways of patients with severe asthma and persistent airway eosinophilia. J Allergy Clin Immunol 2016;137:75-86.e8

Sonnenberg GF. Transcriptionally defining ILC heterogeneity in humans. Nat Immunol 2016;17:351–352

Sonnenberg GF, Hepworth MR. Functional interactions between innate lymphoid cells and adaptive immunity. Nat Rev Immunol 2019;19:599–613

Sonnenberg GF, Monticelli LA, Alenghat T, Fung TC, Hutnick NA, Kunisawa J, Shibata N, Grunberg S, Sinha R, Zahm AM, Tardif MR, Sathaliyawala T, Kubota M, Farber DL, Collman RG, Shaked A, Fouser LA, Weiner DB, Tessier PA, Friedman JR, Kiyono H, Bushman FD, Chang K-M, Artis D. Innate Lymphoid Cells Promote Anatomical Containment of Lymphoid-Resident Commensal Bacteria. Science 2012;336:1321–1325

Spits H, Artis D, Colonna M, Diefenbach A, Di Santo JP, Eberl G, Koyasu S, Locksley RM, McKenzie ANJ, Mebius RE, Powrie F, Vivier E. Innate lymphoid cells — a proposal for uniform nomenclature. Nat Rev Immunol 2013;13:145–149

Spits H, Di Santo JP. The expanding family of innate lymphoid cells: regulators and effectors of immunity and tissue remodeling. Nat Immunol 2011;12:21–27

Stockinger B, Shah K, Wincent E. AHR in the intestinal microenvironment: safeguarding barrier function. Nat Rev Gastroenterol Hepatol 2021;18:559–570

Sugimoto R, Enjoji M, Nakamuta M, Ohta S, Kohjima M, Fukushima M, Kuniyoshi M, Arimura E, Morizono S, Kotoh K, Nawata H. Effect of IL-4 and IL-13 on collagen production in cultured LI90 human hepatic stellate cells. Liver Int 2005;25:420–428

Tan Z, Liu Q, Jiang R, Lv L, Shoto SS, Maillet I, Quesniaux V, Tang J, Zhang W, Sun B, Ryffel B. Interleukin-33 drives hepatic fibrosis through activation of hepatic stellate cells. Cell Mol Immunol 2018;15:388–398

Tan Z, Qian X, Jiang R, Liu Q, Wang Y, Chen C, Wang X, Ryffel B, Sun B. IL-17A Plays a Critical Role in the Pathogenesis of Liver Fibrosis through Hepatic Stellate Cell Activation. J Immunol 2013;191:1835–1844

Tanwar S, Rhodes F, Srivastava A, Trembling PM, Rosenberg WM. Inflammation and fibrosis in chronic liver diseases including non-alcoholic fatty liver disease and hepatitis C. World J Gastroenterol 2020;26:109–133

Teunissen MBM, Munneke JM, Bernink JH, Spuls PI, Res PCM, te Velde A, Cheuk S, Brouwer MWD, Menting SP, Eidsmo L, Spits H, Hazenberg MD, Mjösberg J. Composition of Innate Lymphoid Cell Subsets in the Human Skin: Enrichment of NCR + ILC3 in Lesional Skin and Blood of Psoriasis Patients. J Invest Dermatol 2014;134:2351–2360

Tian J, Feng Y, Fu H, Xie HQ, Jiang JX, Zhao B. The Aryl Hydrocarbon Receptor: A Key Bridging Molecule of External and Internal Chemical Signals. Environ Sci Technol 2015;49:9518–9531

Tsuchida T, Friedman SL. Mechanisms of hepatic stellate cell activation. Nat Rev Gastroenterol Hepatol 2017;14:397–411

Van Gassen S, Callebaut B, Van Helden MJ, Lambrecht BN, Demeester P, Dhaene T, Saeys Y. FlowSOM: Using self-organizing maps for visualization and interpretation of cytometry data: FlowSOM. Cytometry A 2015;87:636–645

Vély F, Barlogis V, Vallentin B, Neven B, Piperoglou C, Ebbo M, Perchet T, Petit M, Yessaad N, Touzot F, Bruneau J, Mahlaoui N, Zucchini N, Farnarier C, Michel G, Moshous D, Blanche S, Dujardin A, Spits H, Distler JHW, Ramming A, Picard C, Golub R, Fischer A, Vivier E. Evidence of innate lymphoid cell redundancy in humans. Nat Immunol 2016;17:1291–1299

Viant C, Rankin LC, Girard-Madoux MJH, Seillet C, Shi W, Smyth MJ, Bartholin L, Walzer T, Huntington ND, Vivier E, Belz GT. Transforming growth factor–β and Notch ligands act as opposing environmental cues in regulating the plasticity of type 3 innate lymphoid cells. Sci Signal 2016;9

Villanova F, Flutter B, Tosi I, Grys K, Sreeneebus H, Perera GK, Chapman A, Smith CH, Di Meglio P, Nestle FO. Characterization of Innate Lymphoid Cells in Human Skin and Blood Demonstrates Increase of NKp44+ ILC3 in Psoriasis. J Invest Dermatol 2014;134:984–91

Vivier E, Artis D, Colonna M, Diefenbach A, Di Santo JP, Eberl G, Koyasu S, Locksley RM, McKenzie ANJ, Mebius RE, Powrie F, Spits H. Innate Lymphoid Cells: 10 Years On. Cell 2018;174:1054–66

Wang H, Park O, Gao B. NKT cells in liver fibrosis: Controversies or complexities. J Hepatol 2011;55:1166

Wang L, Tang J, Yang X, Zanvit P, Cui K, Ku WL, Jin W, Zhang D, Goldberg N, Cain A, Ni B, Zhao K, Wu Y, Chen W. TGF-β induces ST2 and programs ILC2 development. Nat Commun 2020;11:35

Wang S, Li J, Wu S, Cheng L, Shen Y, Ma W, She W, Yang C, Wang J, Jiang W. Type 3 innate lymphoid cell: a new player in liver fibrosis progression. Clin Sci 2018;132:2565–2582

Wang Y, Zhang C. The Roles of Liver-Resident Lymphocytes in Liver Diseases. Front Immunol 2019;10:1582

Weiner J, Zuber J, Shonts B, Yang S, Fu J, Martinez M, Farber DL, Kato T, Sykes M. Long-term Persistence of Innate Lymphoid Cells in the Gut After Intestinal Transplantation. Transplantation 2017;101:2449–2454

Weng H-L, Liu Y, Chen J-L, Huang T, Xu L-J, Godoy P, Hu J-H, Zhou C, Stickel F, Marx A, Bohle RM, Zimmer V, Lammert F, Mueller S, Gigou M, Samuel D, Mertens PR, Singer MV, Seitz HK, Dooley S. The etiology of liver damage imparts cytokines transforming growth factor β1 or interleukin-13 as driving forces in fibrogenesis. Hepatology 2009;50:230–243

Weng H-L, Wang B-E, Jia J-D, Wu W-F, Xian J-Z, Mertens PR, Cai W-M, Dooley S. Effect of Interferon-Gamma on Hepatic Fibrosis in Chronic Hepatitis B Virus Infection: A Randomized Controlled Study. Clin Gastroenterol Hepatol 2005;3:819–828

Wynn TA. Fibrotic disease and the TH1/TH2 paradigm. Nat Rev Immunol 2004;4:583–594

Xu R, Zhang Z, Wang F-S. Liver fibrosis: mechanisms of immune-mediated liver injury. Cell Mol Immunol 2012;9:296–301

Yang Z, Tang T, Wei X, Yang S, Tian Z. Type 1 innate lymphoid cells contribute to the pathogenesis of chronic hepatitis B. Innate Immun 2015;21:665–673

Zang M, Li Y, He H, Ding H, Chen K, Du J, Chen T, Wu Z, Liu H, Wang D, Cai J, Qu C. IL-23 production of liver inflammatory macrophages to damaged hepatocytes promotes hepatocellular carcinoma development after chronic hepatitis B virus infection. Biochim Biophys Acta BBA - Mol Basis Dis 2018;1864:3759–3770

Zenewicz LA, Yancopoulos GD, Valenzuela DM, Murphy AJ, Karow M, Flavell RA. Interleukin-22 but Not Interleukin-17 Provides Protection to Hepatocytes during Acute Liver Inflammation. Immunity 2007;27:647–659

Zeng B, Shi S, Ashworth G, Dong C, Liu J, Xing F. ILC3 function as a double-edged sword in inflammatory bowel diseases. Cell Death Dis 2019;10:315

Zhang C-Y, Yuan W-G, He P, Lei J-H, Wang C-X. Liver fibrosis and hepatic stellate cells: Etiology, pathological hallmarks and therapeutic targets. World J Gastroenterol 2016;22:10512

Zhang K, Xu X, Pasha MA, Siebel CW, Costello A, Haczku A, MacNamara K, Liang T, Zhu J, Bhandoola A, Maillard I, Yang Q. Cutting Edge: Notch Signaling Promotes the Plasticity of Group-2 Innate Lymphoid Cells. J Immunol 2017;198:1798–1803

Zhang M, Zhang S. T Cells in Fibrosis and Fibrotic Diseases. Front Immunol 2020;11:1142

Zhang Y, Cobleigh MA, Lian J, Huang C, Booth CJ, Bai X, Robek MD. A Proinflammatory Role for Interleukin-22 in the Immune Response to Hepatitis B Virus. Gastroenterology 2011;141:1897–1906

Zhao J, Zhang Z, Luan Y, Zou Z, Sun Y, Li Y, Jin L, Zhou C, Fu J, Gao B, Fu Y, Wang F-S. Pathological functions of interleukin-22 in chronic liver inflammation and fibrosis with hepatitis B virus infection by promoting T helper 17 cell recruitment: Zhao, Zhang et al. Hepatology 2014;59:1331–1342

Zhu B, Lin N, Zhang M, Zhu Y, Cheng H, Chen S, Ling Y, Pan W, Xu R. Activated hepatic stellate cells promote angiogenesis via interleukin-8 in hepatocellular carcinoma. J Transl Med 2015;13:365

Zimmermann HW, Seidler S, Gassler N, Nattermann J, Luedde T, Trautwein C, Tacke F. Interleukin-8 Is Activated in Patients with Chronic Liver Diseases and Associated with Hepatic Macrophage Accumulation in Human Liver Fibrosis. PLoS ONE 2011;6:e21381

8.2 Publications

List of scientific publications and congress contributions included in this study:

Original Articles as first author:

Raabe J, Kaiser K, ToVinh M, Finnemann C, Lutz P, Hoffmeister C, Bischoff J, Goeser F, Kaczmarek DJ, Glowka TR, Manekeller S, Charpentier A, Langhans B, Nischalke HD, Toma M, Strassburg CP, Spengler U, Abdallah AT, Krämer B, Nattermann J. Identification and characterisation of a hepatic IL-13 producing ILC3-like population potentially involved in liver fibrosis. *Hepatology* (*under review*)

Conference Talks:

Raabe J. KLRG1+ ILCP as progenitors of IL-13-producing in the ILC3 Human Liver. Natural Killer Cell Symposium Berlin, Germany 2021

Raabe J. Role of human ILC3 in the modulation of hepatic fibrogenesis. Natural Killer Cell Symposium Hamburg, Germany 2018

Conference Posters:

Raabe J. TGF-beta drives conversion of ILC2 to an IL-13-producing ILC3 in the human liver. The 18th Meeting of the Society for Natural Immunity, Luxemburg 2019

Raabe J. Role of human ILC3 in the regulation of hepatic fibrogenesis. 35th Annual Meeting of the German Association of the Study of the Liver, Heidelberg 2019

Raabe J. The human liver contains an IL-13-producing ILC3-like cell that might be involved in the modulation of hepatic fibrogenesis. The 3rd International Conference on Innate Lymphoid Cells (ILC2018), Tokyo 2018

Raabe J. Role of human ILC3 in the regulation of hepatic fibrogenesis. 34th Annual Meeting of the German Association of the Study of the Liver, Hamburg 2018

List of scientific publications not included in this study:

Original Articles as shared first author:

Krämer B, Knoll R, Bonaguro L, ToVinh M, Raabe J, Astaburuaga-García R, Schulte-Schrepping J, Kaiser KM, Rieke GJ, Bischoff J, Monin MB, Hoffmeister C, Schlabe S, De Domenico E, Reusch N, Händler K, Reynolds G, Blüthgen N, Hack G, Finnemann C, Nischalke HD, Strassburg CP, Stephenson E, Su Y, Gardner L, Yuan D, Chen D, Goldman J, Rosenstiel Philipp, Schmidt SV, Latz E, Hrusovsky K, Ball AJ, Johnson JM, Koenig P-A, Schmidt FI, Haniffa M, Heath JR, Kümmerer BM, Keitel V, Jensen B, Stubbemann P, Kurth F, Sander Leif E., Sawitzki B, Aschenbrenner AC, Schultze JL, Nattermann J, Altmüller J, Angelov A, Aschenbrenner AC, Bals R, Bartholomäus A, Becker A, Becker M, Bezdan D, Bitzer M, Blumert C, Bonifacio E, Bork P, Boyke B, Blum H, Casadei N, Clavel T, Colome-Tatche M, Cornberg M, De La Rosa Velázquez IA, Diefenbach A, Dilthey A, Fischer N, Förstner K, Franzenburg S, Frick J-S, Gabernet G, Gagneur J, Ganzenmueller T, Gauder M, Geißert J, Goesmann A, Göpel S, Grundhoff A, Grundmann H, Hain T, Hanses F, Hehr U, Heimbach A, Hoeper M, Horn F, Hübschmann D, Hummel M, Iftner T, Iftner A, Illig T, Janssen S, Kalinowski J, Kallies R, Kehr B, Keller A, Keppler OT, Kim-Hellmuth S, Klein C, Knop M, Kohlbacher O, Köhrer K, Korbel J, Kremsner PG, Kühnert D, Kurth I, Landthaler M, Li Y, Ludwig KU, Makarewicz O, Marini F, Marz M, McHardy AC, Mertes C, Münchhoff M, Nahnsen S, Nöthen M, Ntoumi F, Nürnberg P, Ossowski S, Overmann J, Peter S, Pfeffer K, Pink I, Poetsch AR, Protzer U, Pühler A, Rajewsky N, Ralser M, Reiche K, Rieß O, Ripke S, Nunes da Rocha U, Rosenstiel Philip, Saliba A-E, Sander Leif Erik, Sawitzki B, Scheithauer S, Schiffer P, Schmid-Burgk J, Schneider W,

Schulte E-C, Schultze JL, Sczyrba A, Sharaf ML, Singh Y, Sonnabend M, Stegle O, Stoye J, Theis F, Ulas T, Vehreschild J, Velavan TP, Vogel J, Volland S, von Kleist M, Walker A, Walter J, Wieczorek D, Winkler S, Ziebuhr J. Early IFN-α signatures and persistent dysfunction are distinguishing features of NK cells in severe COVID-19. Immunity 2021;54:2650-2669.e14

Original Articles as contributing author:

German COVID-19 Omics Initiative (DeCOI), Aschenbrenner AC, Mouktaroudi M, Krämer B, Oestreich M, Antonakos N, Nuesch-Germano M, Gkizeli K, Bonaguro L, Reusch N, Baßler K, Saridaki M, Knoll R, Pecht T, Kapellos TS, Doulou S, Kröger C, Herbert M, Holsten L, Horne A, Gemünd ID, Rovina N, Agrawal S, Dahm K, van Uelft M, Drews A, Lenkeit L, Bruse N, Gerretsen J, Gierlich J, Becker M, Händler K, Kraut M, Theis H, Mengiste S, De Domenico E, Schulte-Schrepping J, Seep L, Raabe J, Hoffmeister C, ToVinh M, Keitel V, Rieke G, Talevi V, Skowasch D, Aziz NA, Pickkers P, van de Veerdonk FL, Netea MG, Schultze JL, Kox M, Breteler MMB, Nattermann J, Koutsoukou A, Giamarellos-Bourboulis EJ, Ulas T. Disease severity-specific neutrophil signatures in blood transcriptomes stratify COVID-19 patients. Genome Med 2021;13:7

Krämer B, Nalin AP, Ma F, Lutz P, Goeser F, Finnemann C, Raabe J, ToVinh M, Hoffmeiser C, Kaiser K, Manekeller S, Branchi V, Hüneburg R, Nischalke HD, Semaan A, Langhans B, Kaczmarek DJ, Hack G, Benner B, Lordo MR, Kowalski J, Gerhardt A, Timm J, Toma M, Mohr R, Türler A, Charpentier A, van Bremen T, Feldmann G, Sattler A, Kotsch K, Abdallah AT, Strassburg CP, Spengler U, Mundy-Bosse BL, Pellegrini M, O'Sullivan TE, Freud AG, Nattermann J. Single-cell RNA sequencing identifies a population of human liver-type ILC1. Cell Rep (*in revision*)

Schulte-Schrepping J, Reusch N, Paclik D, Baßler K, Schlickeiser S, Zhang B, Krämer B, Krammer T, Brumhard S, Bonaguro L, De Domenico E, Wendisch D, Grasshoff M, Kapellos TS, Beckstette M, Pecht T, Saglam A, Dietrich O, Mei HE, Schulz AR, Conrad C, Kunkel D, Vafadarnejad E, Xu C-J, Horne A, Herbert M, Drews A, Thibeault C, Pfeiffer M, Hippenstiel S, Hocke A, Müller-Redetzky H, Heim K-M, Machleidt F, Uhrig A, Bosquillon de Jarcy L, Jürgens L, Stegemann M, Glösenkamp CR, Volk H-D, Goffinet C,

Landthaler M, Wyler E, Georg P, Schneider M, Dang-Heine C, Neuwinger N, Kappert K, Tauber R, Corman V, Raabe J, Kaiser KM, Vinh MT, Rieke G, Meisel C, Ulas T, Becker M, Geffers R, Witzenrath M, Drosten C, Suttorp N, von Kalle C, Kurth F, Händler K, Schultze JL, Aschenbrenner AC, Li Y, Nattermann J, Sawitzki B, Saliba A-E, Sander LE, Angelov A, Bals R, Bartholomäus A, Becker A, Bezdan D, Bonifacio E, Bork P, Clavel T, Colome-Tatche M, Diefenbach A, Dilthey A, Fischer N, Förstner K, Frick J-S, Gagneur J, Goesmann A, Hain T, Hummel M, Janssen S, Kalinowski J, Kallies R, Kehr B, Keller A, Kim-Hellmuth S, Klein C, Kohlbacher O, Korbel JO, Kurth I, Landthaler M, Li Y, Ludwig K, Makarewicz O, Marz M, McHardy A, Mertes C, Nöthen M, Nürnberg P, Ohler U, Ossowski S, Overmann J, Peter S, Pfeffer K, Poetsch AR, Pühler A, Rajewsky N, Ralser M, Rieß O, Ripke S, Nunes da Rocha U, Rosenstiel P, Saliba A-E, Sander LE, Sawitzki B, Schiffer P, Schulte E-C, Schultze JL, Sczyrba A, Stegle O, Stoye J, Theis F, Vehreschild J, Vogel J, von Kleist M, Walker A, Walter J, Wieczorek D, Ziebuhr J. Severe COVID-19 Is Marked by a Dysregulated Myeloid Cell Compartment. Cell 2020;182:1419-1440.e233

9. Acknowledgments

Wenn mir eines nach diesen Jahren des Forschens klar geworden ist, dann, dass ich kaum etwas ohne die Unterstützung aus Nah und Fern geschafft hätte. Zeit, endlich einmal allen “Danke” zu sagen, nach fünf Jahren kommt schließlich einiges zusammen.

An erster Stelle geht mein Dank natürlich an Jacob Nattermann. Unter seiner Betreuung habe ich mich und meinen bescheidenen geistigen Input stets wertgeschätzt gefühlt und gelernt eigenständig und selbstbewusst meine wissenschaftliche Arbeitsweise zu reflektieren. Bei beruflichen wie persönlichen Anliegen konnte ich mich stets auf seine menschliche und entgegenkommende Art verlassen, wofür ich ihm vor allem im Hinblick auf meine Zeit als frischgebackener Vater dankbar bin.
Ebenso möchte Ulrich Spengler danken, der sich immer viel Zeit genommen hat, um den Schaffensprozess zu verfolgen und dem ich viel wertvolles Feedback zu verdanken habe.

Ganz entscheidend beigetragen zu meiner Zeit als PhD Student haben selbstverständlich auch meine Kolleg*innen auf dem Venusberg. Es war ein wirklich freundschaftliches Arbeitsumfeld, in das ich aufgenommen wurde, was ich jederzeit zu wertschätzen wusste und sicher auch vermissen werde! Mein Dank geht an Benni, Claudia, Kim, Christoph, Michael, Hans Dieter, Gudrun, Felix, Philipp, Jenny, Gereon (herrje das nimmt ja kein Ende mehr!) und all die anderen Kolleg*innen, die sich hier vielleicht nicht namentlich wiederfinden aber doch auf jeden Fall adressiert fühlen dürfen! Danke vor allem, dass ihr mich ertragen habt, wenn ich besonders gute Laune hatte, kam ja durchaus mal vor! Viele Dinge werden mir sicher lange in Erinnerung bleiben und mich gerne mal zurückblicken lassen, wie donnerstags stattfindende Mittwochstreffen, schlaflose Kongressnächte (ich habe überlebt!), nächtliche Ausflüge ins OP, Momente, in denen viel gelacht wurde, Momente, in denen es Kuchen gab… auch hier scheitere ich am Aufzählen!

Keine Frage, manchmal sah es auch trübe aus und der Nostalgiker in mir hätte sich am liebsten wieder in unbeschwerte Zeiten zurück geflüchtet. Gut, wenn man immer auf den Beistand von alten Freunden und Leidensgenossen zählen kann, von denen ich in diesem

Zusammenhang vor allem Stefan und Hardin hervorheben will. Kein Problem, das sich nicht wegphilosophieren lässt oder zumindest im Vergleich zu montenegrinischen Braunbären harmlos erscheint!

Und zu guter Letzt, geht meine allergrößte Dankbarkeit natürlich an meine Familie. Endlich, eeeendlich, liebe Mama, lieber Papa, liebe Nina: Ich glaub das war's jetzt. Zu Ende studiert! Ihr wart nun wirklich von Anfang an dabei, habt mich bei allem akademischen Unsinn unterstützt und wo wäre ich nur ohne euren familiären Beistand, ich will's nicht wissen!
Und dann wäre da natürlich noch der Dreh- und Angelpunkt in meinem Leben, der Grund, warum ich mich wahrhaft glücklich schätzen kann: meine eigene kleine Familie. An Lara und Matilda, mit euch an meiner Seite ist alles leicht, auch das Doktorandendasein. Danke, dass es euch gibt. Ich komm jetzt heim!